D_A_ DITMARS (28)

NBSIR 74-600

AFOSR SCIENTIFIC REPORT

AFOSR-TR-75-0596

Thermodynamics of Chemical Species Important to Rocket Technology

Various authors

Physical Chemistry Division
Institute for Materials Research
National Bureau of Standards
Washington, D. C. 20234

1 October 1974

Final Report for Agreement No.
AFOSR–ISSA–74–0001
July 1973 – June 1974

Approved for public release; distribution unlimited.

Prepared for

Air Force Office of Scientific Research
1400 Wilson Boulevard
n, Virginia 22209

Qualified requestors may obtain additional copies from the Defense Documentation Center, all others should apply to the National Technical Information Service.

Conditions for Reproduction

Previous reports describing related work have the NBS Report Nos. 6297, 6484, 6645, 6928, 7093, 7192, 7437, 7587, 7796, 8033, 8186, 8504, 8628, 8919, 9028, 9389, 9500, 9601, 9803, 9905, 10004, 10074, 10326, 10481, 10904, and NBSIR 73-280, 73-281.

NBSIR 74–600

AFOSR SCIENTIFIC REPORT
AFOSR–TR–75–0596

THERMODYNAMICS OF CHEMICAL SPECIES IMPORTANT TO ROCKET TECHNOLOGY

Various authors

Physical Chemistry Division
Institute for Materials Research
National Bureau of Standards
Washington, D. C. 20234

1 October 1974

Final Report for Agreement No.
AFOSR–ISSA–74–0001
July 1973 – June 1974

Approved for public release; distribution unlimited.

Prepared for
Air Force Office of Scientific Research
1400 Wilson Boulevard
Arlington, Virginia 22209

U. S. DEPARTMENT OF COMMERCE, Frederick B. Dent, Secretary
NATIONAL BUREAU OF STANDARDS, Richard W. Roberts, Director

REPORT DOCUMENTATION PAGE

READ INSTRUCTIONS
BEFORE COMPLETING FORM

1. REPORT NUMBER: AROSR-TR-75-0596
2. GOVT ACCESSION NO.:
3. RECIPIENT'S CATALOG NUMBER:
4. TITLE (and Subtitle): THERMODYNAMICS OF CHEMICAL SPECIES IMPORTANT TO ROCKET TECHNOLOGY
5. TYPE OF REPORT & PERIOD COVERED: FINAL 1 July 1973-30 June 1974
6. PERFORMING ORG. REPORT NUMBER:
7. AUTHOR(s): CHARLES W BECKETT
8. CONTRACT OR GRANT NUMBER(s): ISSA-74-0001
9. PERFORMING ORGANIZATION NAME AND ADDRESS:
NATIONAL BUREAU OF STANDARDS
INSTITUTE FOR MATERIALS RESEARCH
WASHINGTON, DC 20234
10. PROGRAM ELEMENT, PROJECT, TASK AREA & WORK UNIT NUMBERS:
681308
9750-01
61102F
11. CONTROLLING OFFICE NAME AND ADDRESS:
AIR FORCE OFFICE OF SCIENTIFIC RESEARCH/NA
1400 WILSON BOULEVARD
ARLINGTON, VIRGINIA 22209
12. REPORT DATE: Oct 1974
13. NUMBER OF PAGES: 200
14. MONITORING AGENCY NAME & ADDRESS(if different from Controlling Office):
15. SECURITY CLASS. (of this report): UNCLASSIFIED
15a. DECLASSIFICATION DOWNGRADING SCHEDULE:
16. DISTRIBUTION STATEMENT (of this Report): Approved for public release; distribution unlimited.
17. DISTRIBUTION STATEMENT (of the abstract entered in Block 20, if different from Report):
18. SUPPLEMENTARY NOTES:
19. KEY WORDS (Continue on reverse side if necessary and identify by block number)

graphite
vanadium
zirconium
melting point
electrical resistivity
radiance temperature
enthalpy of transition
specific heat
infrared matrix isolation spectroscopy
reaction of $Fe_{(g)}$ and oxygen
total emittance

20. ABSTRACT (Continue on reverse side if necessary and identify by block number)

Using a subsecond-duration transient technique the specific heat, electrical resistivity, and hemispherical total emittance were simultaneously measured over the temperature range 1500-3000 K for some grades of graphite. Similar measurements were made on vanadium, and zirconium in the temperature range of 1500-2100 K. Melting points and radiance temperature (at 650 nm) are reported for zirconium and molybdenum. The temperature of the (continued)

DD FORM 1 JAN 73 1473 EDITION OF 1 NOV 65 IS OBSOLETE

19. reaction of Ba(g) and excited ozone
scandium group and rare-earth gaseous monoxides
calculation of dissociation energies
review of literature on rate of effusion and mass-spectrometric data
bibliography on spectroscopy of fluorides and oxides of the lanthanide series

20. transition from the α-β phase of zirconium and the energy difference of these phases has also been measured using the subsecond duration transient technique.

The products of the reaction of Fe(g) and O_2 have been investigated and identified using the methods of infrared matrix isolation spectroscopy. A preliminary report on the study of the reaction of Ba(g) with vibrationally excited ozone is also presented.

The dissociation energies of the scandium group and rare-earth gaseous monoxides are evaluated by reviewing the literature available on Knudsen effusion rates and mass-spectrometric data. Criteria are discussed for choosing data for evaluation of dissociation energies. A bibliography of the available literature on the spectroscopy of fluorides, oxides, and oxyfluorides belonging to the lanthanide series is given.

FOREWORD

Structure, propulsion, and guidance of new or improved weapons delivery systems are dependent in crucial areas of design on the availability of accurate thermodynamic data. Data on high-temperature materials, new rocket propellant ingredients, and combustion products (including exhaust ions) are, in many cases, lacking or unreliable. A broad integrated research program at the National Bureau of Standards has supplied new or more reliable thermodynamic properties essential in several major phases of current propulsion development and application. Measured were compounds of those several chemical elements important in efficient propulsion fuels; those substances most affecting ion concentrations in such advanced propulsion concepts as ion propulsion; and the transition and other refractory metals (and their pertinent compounds) which may be suitable as construction materials for rocket motors, rocket nozzles, and nose cones that will be durable under extreme conditions of high temperature and corrosive environment. The properties determined extend in temperature up to 6000 degrees Kelvin. The principal research activities were experimental, and involved developing new measurement techniques and apparatus, as well as measuring heats of reaction, of fusion, and of vaporization; specific heats; equilibria involving gases; several properties from fast processes at very high temperatures; spectra of the infrared, matrix-isolation, microwave, and electronic types; and mass spectra. Some of these techniques, by relating thermodynamic properties to molecular or crystal structures, make it possible to tabulate reliably these properties over far wider ranges of temperature and pressure than those actually employed in the basic investigations. Additional research activities of the program have involved the critical review of published chemical-thermodynamic (and some chemical-kinetic) data, and the generation of new thermochemical tables important in current chemical-laser research.

ABSTRACT

This report (covering July 1973-June 1974) gives accounts on the determination of the thermophysical properties of conductors by high speed techniques, studies of reaction intermediates of possible interest to chemical laser systems by the methods of matrix isolation infrared spectroscopy, preliminary report on the reaction kinetics of Ba(g) with vibrationally excited ozone, a survey of the dissociation energies of the scandium group and rare-earth oxides, and a bibliography on spectroscopy of fluorides and oxides belonging to the lanthanide series.

Using a subsecond-duration transient technique the specific heat, electrical resistivity, and hemispherical total emittance were simultaneously measured over the temperature range 1500-3000 K for some grades of graphite. Similar measurements were made on vanadium, and zirconium in the temperature range of 1500-2100 K. Melting points and radiance temperatures (at 650 nm) are reported for zirconium and molybdenum. The temperature of the transition from the α-β phase of zirconium and the energy difference of these phases has also been measured using the subsecond duration transient technique.

The products of the reaction of Fe(g) and O_2 have been investigated and identified using the methods of infrared matrix isolation spectroscopy. A preliminary report on the study of the reaction of Ba(g) with vibrationally excited ozone is also presented.

The dissociation energies of the scandium group and rare-earth gaseous monoxides are evaluated by reviewing the literature available on Knudsen effusion rates and mass-spectrometric data. Criteria are discussed for choosing data for evaluation of dissociation energies. A bibliography of the available literature on the spectroscopy of fluorides, oxides, and oxyfluorides belonging to the lanthanide series is given.

Charles W. Beckett

TABLE OF CONTENTS

Foreword i
Abstract iii

Chap. 1. MEASUREMENTS OF HEAT CAPACITY, ELECTRICAL RESISTIVITY AND HEMISPHERICAL TOTAL EMITTANCE OF TWO GRADES OF GRAPHITE IN THE RANGE 1500 TO 3000 K BY A PULSE HEATING TECHNIQUE (by Ared Cezairliyan and F. Righini) 1

Abstract 1
1. Introduction 2
2. Method 3
3. Measurements 4
Table 1. Characteristics of the Graphite Specimens 5
4. Experimental Results 6
Heat Capacity 6
Table 2. Operational Characteristic of the Measurement System During Experiments of Graphite Specimens 7
Table 3. Heat Capacity of Poco and Pyrolytic Graphites 9
Figure 1. Deviation of Heat Capacity Results of Poco Graphite 10
Figure 2. Deviation of Heat Capacity Results of Pyrolytic Graphite 11
Electrical Resistivity 12
Table 4. Electrical Resistivity of Poco and Pyrolytic Graphites 14
Figure 3. Electrical Resistivity of Poco and Pyrolytic Graphites 15
Hemispherical Total Emittance 16
Table 5. Hemispherical Total Emittance of Poco and Pyrolytic Graphites . . 17
Figure 4. Hemispherical Total Emittance of Poco and Pyrolytic Graphites . 18
5. Estimate of Errors 19
6. Discussion 19
Heat capacity 19
Figure 5. Heat Capacity of Graphite Reported in the Literature 20
Electrical Resistivity 23
Figure 6. Electrical Resistivity of Poco and Pyrolytic Graphite 24
Hemispherical Total Emittance 25
Acknowledgement 26
7. References 27

Chap. 2. SIMULTANEOUS MEASUREMENTS OF HEAT CAPACITY, ELECTRICAL RESISTIVITY AND HEMISPHERICAL TOTAL EMITTANCE BY A PULSE HEATING TECHNIQUE: VANADIUM, 1500 TO 2100 K (by A. Cezairliyan, F. Righini and J. L. McClure) 30

Abstract 30
1. Introduction 31
    Table 1. Specimen Information 32
2. Measurements 33
    Table 1a. 33
    Table 2. Measurement Technique and System Characteristics 34
    Table 3. Functional Representation of Results on Vanadium 35
    Table 4. Results on Properties of Vanadium 35
    Table 5. Error Analysis 36
3. Discussion 37
    Figure 1. Heat Capacity of Vanadium Reported in the Literature 38
    Figure 2. Electrical Resistivity of Vanadium Reported in the Literature 39
    Figure 3. Hemispherical Total Emittance of Vanadium Reported in the Literature 40
Acknowledgement 42
4. Appendix 43
    Table A-1 Experimental Results on Heat Capacity and Electrical Resistivity of Vanadium 43
    Table A-2 Experimental Results on Hemispherical Total Emittance of Vanadium . . . 44
5. References 45

Chap. 3. SIMULTANEOUS MEASUREMENTS OF HEAT CAPACITY, ELECTRICAL RESISTIVITY AND HEMISPHERICAL TOTAL EMITTANCE BY A PULSE HEATING TECHNIQUE (A. Cezairliyan and F. Righini) 47

Abstract 47
1. Introduction 48
    Table 1. Specimen Information 49
2. Measurements 50
    Table 1a Impurities in the Specimen 50
    Table 2. Measurement Technique and System Characteristics 51
    Table 3. Functional Representation of Results on Zirconium 52
    Table 4. Results on Properties of Zirconium 52
    Table 5. Error Analysis 53
3. Discussion 54
Acknowledgement 55

Figure 1. Heat Capacity of Zirconium Reported in the Literature . . . 56
Figure 2. Electrical Resistivity of Zirconium Reported in the Literature 57
Figure 3. Hemispherical Total Emittance of Zirconium Reported in the Literature 58
4. Appendix 59
Table A-1 Experimental Results on Heat Capacity of Zirconium 59
Table A-2 Experimental Results on Resistivity of Zirconium 60
Table A-3 Experimental Results on Hemispherical Total Emittance of Zirconium 61
5. References 62

Chap. 4. MEASUREMENT OF MELTING POINTS, RADIANCE TEMPERATURE (AT MELTING POINT), AND ELECTRICAL RESISTIVITY OF ZIRCONIUM BY A PULSE HEATING METHOD (A. Cezairliyan and F. Righini) 64

Abstract 64
1. Introduction 65
2. Measurements 66
3. Experimentsl Results 67
Melting Point 67
Figure 1. Variation of Temperature of Zirzonium as a Function of Time Near and at the Melting Point. . 68
Table 1. Experimental Results of the Melting Point of Tubular Zirconium Samples 69
Radiance Temperature at the Melting Point . . . 70
Figure 2. Variation of Radiance Temperature (at 650 nm) of Zirconium as a function of time near and at its melting point for three typical experiments 71
Table 2. Summary of Experiments for the Measurement of Radiance Temperature of Zirconium During Melting 72
Electrical Resistivity 74
Figure 3. Difference of Radiance Temperature (at the melting point of zirconium, at 650 nm) for Individual Experiments from their Average Value of 1940.5 K. . . . 75
Figure 4. Typical Variation of Radiance Temperature (at 650 nm) of Zirconium (with oxide coating) as a Function of Time near and at its Mleting Point 76

4. Estimate of Errors 77
Figure 5. Variation of Electrical Resistivity of Zirconium (Specimen II) as a Function of Temperature Near and at its Melting Point 78
5. Discussion 79
Table 3. Imprecision and Inaccuracy of Measured and Computed Quantities 80
Table 4. Values of the Melting Points of Zirconium Reported in the Literature 81
Acknowledgement 83
6. References 84

Chap. 5. THERMODYNAMIC STUDIES OF THE $\alpha \rightarrow \beta$ PHASE TRANSFORMATION IN ZIRCONIUM USING A SUBSECOND PULSE HEATING TECHNIQUE (A. Cezairliyan and F. Righini) 88

Abstract 88
1. Introduction 89
2. Measurements 90
3. Experimental Results 91
Table 1. Results for the $\alpha \rightarrow \beta$ Transformation Temperature and Transformation Energy of Zirconium 92
Figure 1. Variation of Temperature as a Function of Time, Near and at the Transformation Point of Zirconium 94
Figure 2. Variation of Resistivity as a Function of Time Near and at the Transformation Point of Zirconium 95
Figure 3. Variation of Resistivity as a Function of Temperature Near and at the Transformation Point of Zirconium 96
4. Discussion 97
Table 2. Values of the $\alpha \rightarrow \beta$ Transformation Temperature of Zirconium Reported in the Literature 99
Acknowledgement 100
Table 3. Change of the Electrical Resistivity of Zirconium During the α-β Transformation Reported in the Literature 101
5. References 102

Chap. 6. RADIANCE TEMPERATURE (AT 650 nm) OF MOLYBDENUM AT ITS MELTING POINT
(A. Cezairliyan) 105

Figure 1. Variation of Radiance Temperature (at 650 nm) of Molybdenum as a Function of Time Near and at its Melting Point for Three Typical Experiments 107
Table 1. Symmary of Experiments for the Measurement of Radiance Temperature (at 650 nm) of Molybdenum during Melting 108
Figure 2. Difference of Radiance Temperature (at the Melting Point) of Molybdenum at 650 nm) for Individual Experiments from their Average Value of 2530.4 K 110
1. References 112

Chap. 7. MATRIX ISOLATION STUDIES ON THE REACTION OF IRON VAPOR WITH OXYGEN
(S. Abramowitz and N. Acquista) 113

1. Introduction 113
2. Experimental 113
3. Reeults 114
4. Discussion 115
5. Conclusion. 118
Table 1. Observed Fundamental Modes for FeO_2. 118
Figure 1. The Infrared Spectrum of Matrix Isolated FeO_2 119
6. References 120

Chap. 8. STUDIES OF THE REACTIONS OF Ba(g) WITH $O_3^{\neq}$
(W. Braun, M. Kurylo, S. Abramowitz) 122

Capt. 9. DISSOCIATION ENERGIES OF THE SCANDIUM GROUP AND RARE-EARTH GASEOUS MONOXIDES
(Ralph F. Krause, Jr.) 123

Abstract 123
I. Introduction 124
Table 1. Compilations of Dissociation Energies for the Gaseous Monoxides 125
II. Weight-Loss Vaporization of Sesquioxides . . . 126
Table 2. Some Equilibria Involved with the Vaporization of Sesquioxides 128
Table 3. Ratio of Mass-Spectrometric Ion Intensities from Vaporization of the Sesquioxides 128
III. Auxiliary Data 130
Table 4. Selected Values of Chemical Thermodynamic Properties for the Solid Sesquioxides 131

Table 5. Selected Values of Chemical Thermodynamic Properties of the Atomic Metals and Atomic Oxygen 132
Table 6. Values of the Gibbs Free Energy Functions for the Gaseous Monoxides 134
Table 7. Differences in Dissociation Energies from Different Values of the Gibbs Free Energy Functions for the Gaseous Monoxides 134
IV. Errors in Vapor Composition 135
Table 8. Effect of the Uncertainty of Forming Neodynium Dioxide Gas on Calculations Using Sesquioxide Rate of Effusion Data 136
Table 9. Effects of Correcting for Gaseous Tantalum Oxides on Calculations Using Sesquioxide Rate of Effusion Data 136
Table 10. Effects of Other Assumptions on Calculations Using Sesquioxide Rate of Effusion Data 138
V. Equilibria Data by Mass Spectroscopy 139
Table 11. Mass-Spectrometrically Determined Enthalpy Changes of Isomolecular Exchange Reactions 140
VI. Recalculated Results 141
Table 12. Dissociation Energies Recalculated from Published Weight-Loss and Mass Spectrometric Data . . . 142
VII. References 144
Acknowledgement 147

Chap. 10. BIBLIOGRAPHY ON SPECTROSCOPY OF FLUORIDES AND OXIDES BELONGING TO LANTHANIDE SERIES
(Francis Westley) 148

I. Cerium 151
II. Dysprosium 153
III. Erbium 155
IV. Europium 158
V. Gadolinium 162
VI. Holmium 165
VII. Lanthanum 167
VIII. Lutetium 171
IX. Neodymium 173
X. Promethium 176
XI. Praseodymium 176
XII. Samarium 179
XIII. Terbium 182
XIV. Thulium 184
XV. Ytterbium 186

MEASUREMENTS OF HEAT CAPACITY, ELECTRICAL RESISTIVITY AND HEMISPHERICAL TOTAL EMITTANCE OF TWO GRADES OF GRAPHITE IN THE RANGE 1500 TO 3000 K BY A PULSE HEATING TECHNIQUE*

A. Cezairliyan and F. Righini**
National Bureau of Standards
Washington, D. C. 20234, U.S.A.

Abstract

Measurements of heat capacity, electrical resistivity and hemispherical total emittance of Poco and pyrolytic graphites in the temperature range 1500 to 3000 K by a subsecond duration pulse heating technique are described. For a given graphite grade, heat capacities of different specimens were in agreement within 0.5%. The difference between the results for the two different grades was about 1.8%; the results of Poco being higher than those of pyrolytic. Electrical resistivity of the Poco graphite was about four times greater than that of pyrolytic graphite (parallel to basal planes). Hemispherical total emittance of Poco graphite was almost twice that of pyrolytic graphite.

---

*This work was supported in part by the U. S. Air Force Office of Scientific Research.

**Guest scientist from the Istituto di Metrologia "G. Colonnetti" in Torino, under a fellowship from the Consiglio Nazionale delle Ricerche of Italy.

1. Introduction

Disagreements exist between the limited number of experimental results for the properties of graphite above 1500 K reported in the literature. Most of the reported measurements were performed on different grades of graphite, which complicates their evaluation and poses the question whether the differences were due to measurement errors or were really indicative of differences in the graphite grades.

As an attempt to elucidate this, a program was initiated for the systematic and accurate measurement of selected properties of various grades of graphite at high temperatures. The results of the first phase, namely the measurement of heat capacity of a grade of graphite (Poco, AXM-5Q)[1] in the temperature range 1500 to 3000 K, were presented in an earlier publication [1]. The objective of this paper is to report the results of the measurements of heat capacity, electrical resistivity and hemispherical total emittance of two grades of graphite (Poco and pyrolytic) in the range 1500 to 3000 K. The Poco graphite used in this work (Poco, DFP-2) is different from the one used in the earlier study. For completeness and for ease of comparison, the results of the earlier study on Poco graphite are also included in this paper.

---

[1] Commercial identification of graphites is made in this paper in order to specify adequately the grade of the graphite specimens whose properties were determined experimentally. In no case does such identification imply recommendation or endorsement by the National Bureau of Standards.

2. Method

The method is based on rapid resistive self-heating of the tubular specimen from room temperature to high temperatures (above 1500 K) in less than one second by the passage of an electrical current pulse through it; and on measuring, with millisecond resolution, such experimental quantities as current through the specimen, potential drop across the specimen, and specimen temperature.

The current through the specimen is determined from the measurement of the potential difference across a standard resistance placed in series with the specimen. The potential difference across the middle one third of the specimen is measured between spring-loaded, knife-edge probes. The specimen temperature is measured at the rate of 1200 times per second with a high-speed photoelectric pyrometer [2]. The small hole in the wall at the middle of the tubular specimen provides an approximation to blackbody conditions for optical temperature measurements. All these data are recorded with a digital data acquisition system, which has a time resolution of 0.4 millisecond and a full-scale signal resolution of one part in 8000.

Details regarding the construction and operation of the measurement system, the methods of measuring experimental quantities, and other pertinent information, such as the formulation of relations for properties, etc. are given in earlier publications [3, 4].

3. Measurements

The new measurements reported in this paper were performed on one Poco graphite (DFP-2) specimen and two pyrolytic graphite specimens. The characteristics of these specimens, as well as those of the Poco graphite (AXM-5Q) specimen used in the earlier study, are given in Table 1. In the rest of this paper, the specimens are referred to by their designated numbers as listed in Table 1. The pyrolytic graphite specimens were fabricated in a way to allow the pulse current to flow in the direction parallel to the basal planes. Before the start of the measurements, the specimens were heat treated by subjecting them to 15-20 heating pulses (up to 2800 K). All the experiments were conducted with the specimen in a vacuum environment at approximately 10^{-5} torr.

To study possible effects that might be attributable to the rate with which the specimen heats, two ranges of heating rates, designated as "fast" and "slow", were used in the experiments on specimens-1, 2 and 3. To optimize the operation of the high-speed pyrometer, the temperature interval (1500 to 3000 K) was divided into six ranges. A "fast" and a "slow" experiment were performed in each temperature range. These yielded a total of 12 experiments for each of the specimens-1, 2 and 3. In the case of specimen-4, only a "slow" heating rate was used yielding a total of 6 experiments for the specimen.

Table 1

Characteristics of the Graphite Specimens

Specimen Designation	Graphite Grade	Purity %	Density g.cm^{-3}	Nominal Dimensions, mm		
				length	O.D.	thickness
Specimen-1	Poco (AXM-5Q)*	99.9^+	1.755	76	6.3	0.5
Specimen-2	Poco (DFP-2)**	99.99^+	1.791	76	6.3	0.5
Specimen-3	Pyrolytic***	99.99^+	2.19	76	7.2	0.5
Specimen-4	Pyrolytic***	99.99^+	2.19	76	7.2	0.5

*The graphite block was kindly furnished by the U.S. Air Force Materials Laboratory, Wright-Patterson Air Force Base, Ohio.

**The graphite block was purchased from the Poco Graphite, Inc.

***The graphite in the form of tubes was kindly furnished by the Union Carbide Corporation through Dr. A. W. Moore. Deposition temperature: 2400 K.

To optimize the operation of the measurement system, the heating rate of the specimen (in both "fast" and "slow" experiments) was varied depending on the desired temperature range by adjusting the value of the resistance in series with the specimen. Duration of the current pulses ranged from 210 to 330 ms for the "fast" experiments, and 280 to 520 ms for the "slow" experiments. Other typical operational characteristics of the measurement system during the experiments on the two different-grade graphite specimens, such as specimen heating rate, and heat loss from specimen by thermal radiation, are summarized in Table 2.

Optical checks performed on the experiment chamber window after the pulse experiments did not indicate any graphite deposition. Also, weight measurements before and after the entire set of pulse experiments did not show any change in specimen weight.

4. Experimental Results

This section presents the properties determined from the measured quantities. All values are based on the International Practical Temperature Scale of 1968 [5]. In all computations, the geometrical quantities are based on their room temperature (298 K) dimensions.

4.1. Heat Capacity

The heat capacity data were determined from the measurements of current, voltage, and temperature obtained during the heating period. A correction for heat loss due to thermal radiation was made using the results on hemispherical total emittance.

Table 2

Operational Characteristics of the Measurement System During Experiments on Graphite Specimens

Graphite Grade	Temperature K	Specimen Heating Rate $K \cdot s^{-1}$		Radiative Heat Loss from Specimen % of input power	
		"Fast"	"Slow"	"Fast"	"Slow"
Poco (Specimen-1) 2?	1500	6000	4400	2	3
	2000	6000	4000	7	10
	2500	6900	3800	13	22
	3000	6200	2700	26	45
Pyrolytic (Specimen-3)	1500	3800	2900	2	3
	2000	5100	3600	4	6
	2500	6600	5200	7	9
	3000	7500	5700	12	15

The heat capacity results obtained for the "fast" and "slow" experiments were fitted separately for each specimen by polynomial functions of temperature using the least squares method. The best fits were quadratic for Poco graphite and linear for pyrolytic graphite, with standard deviations (of an individual point) in the range 0.4 to 0.6%. A study of the results indicated the following: (a) the difference in the results corresponding to "fast" and slow experiments for a given specimen (in the range 0.2 to 0.6%) is less than or comparable to the measurement resolution, and (b) the difference in the results corresponding to the two specimens of the same graphite grade (0.3% for Poco and 0.5% for pyrolytic) is less than or comparable to the measurement resolution. It may be concluded that for a given graphite grade, two different specimens and two different heating rates yielded the same value for heat capacity. However, the average absolute difference between the results of Poco and pyrolytic graphites was 1.8%; the results of Poco being higher than those of pyrolytic.

The functions for heat capacity that represent the combined results of the two specimens and the two heating rates for each graphite grade in the range 1500 to 3000 K are:

For Poco graphite (standard deviation, 0.5%)

$$C_p = 19.84 + 3.490 \times 10^{-3} T - 4.119 \times 10^{-7} T^2 \qquad (1)$$

For pyrolytic graphite (standard deviation, 0.6%)

$$C_p = 21.60 + 1.534 \times 10^{-3} T \qquad (2)$$

where T is in K and C_p is in $J \cdot mol^{-1} \cdot K^{-1}$. In the computations of heat capacity, the atomic weight of graphite was taken as 12.011. The heat

Table 3

Heat Capacity of Poco and Pyrolytic Graphites According to Equations (1) and (2)

Temperature K	Heat Capacity, $J \cdot mol^{-1} \cdot K^{-1}$	
	Poco	Pyrolytic
1500	24.15	23.90
1600	24.37	24.05
1700	24.58	24.21
1800	24.79	24.36
1900	24.98	24.51
2000	25.17	24.67
2100	25.35	24.82
2200	25.52	24.97
2300	25.69	25.13
2400	25.84	25.28
2500	25.99	25.44
2600	26.13	25.59
2700	26.26	25.74
2800	26.38	25.90
2900	26.50	26.05
3000	26.60	26.20

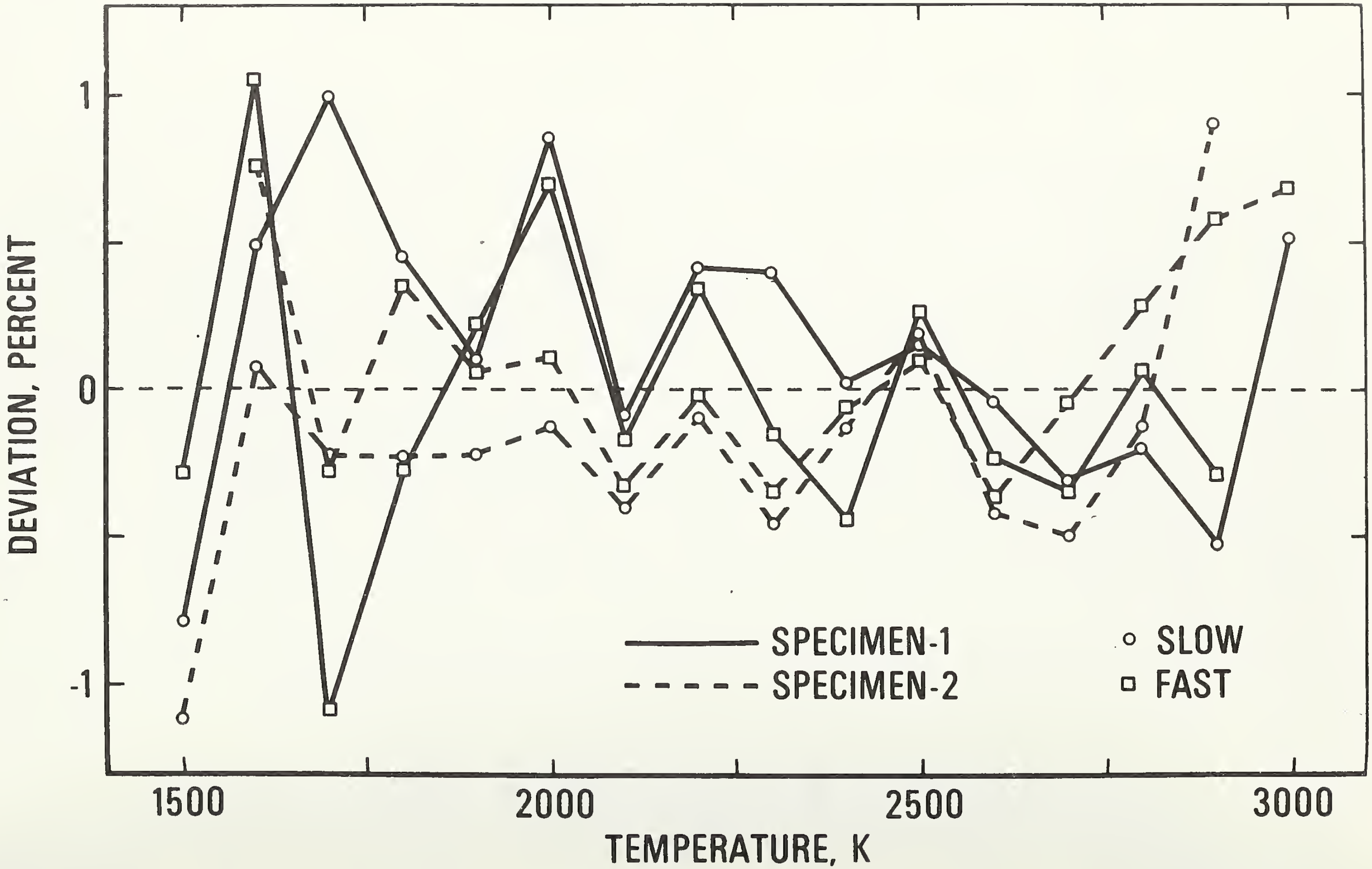

Figure 1. Deviation of heat capacity results of Poco graphite from Equation (1).

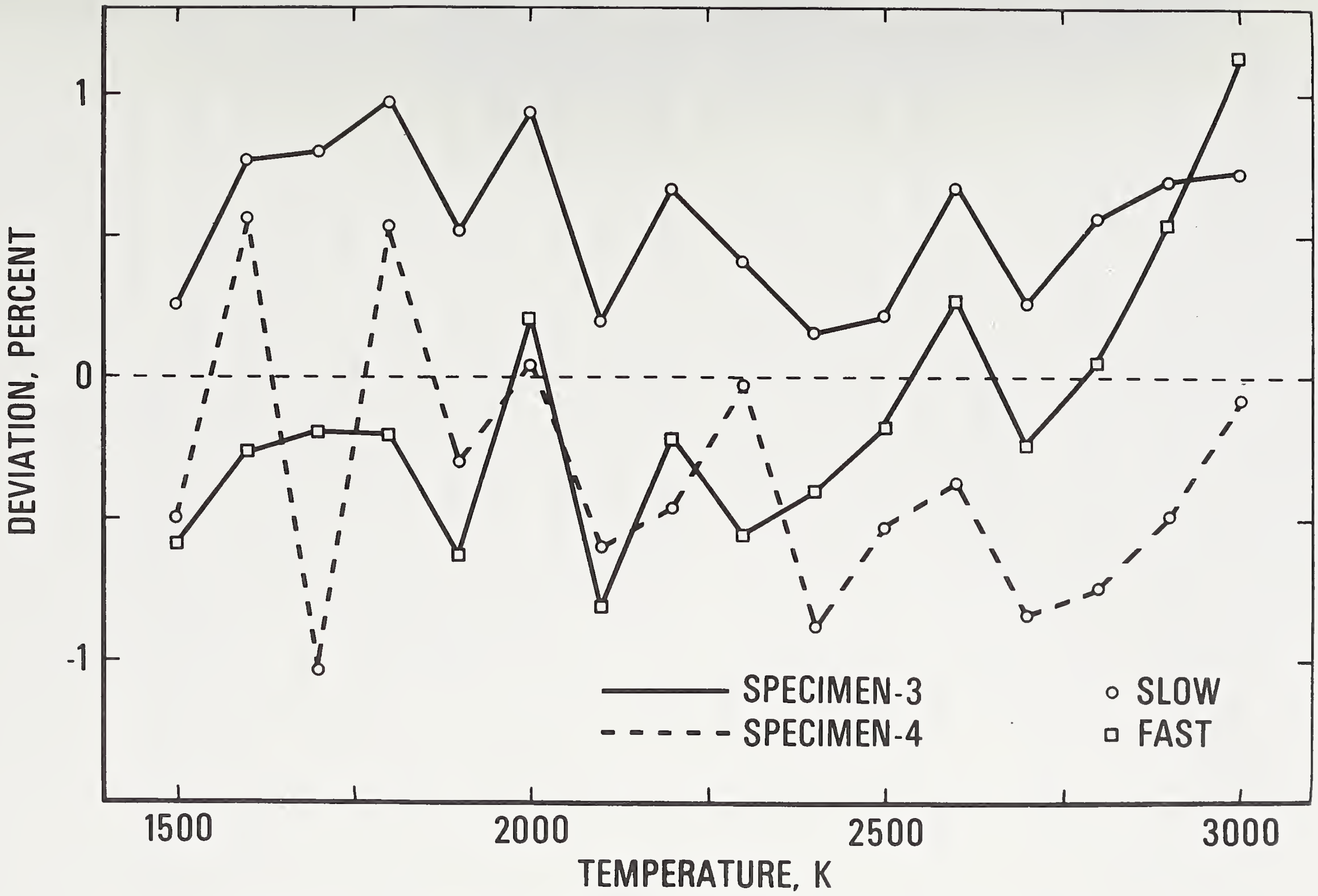

Figure 2. Deviation of heat capacity results of pyrolytic graphite from Equation (2).

capacity for the two grades of graphite computed using the Equations (1) and (2) is presented in Table 3. Figures 1 and 2 show the deviation of the measured heat capacity values of Poco and pyrolytic graphite specimens from the values calculated from Equations (1) and (2), respectively.

4.2. Electrical Resistivity

Electrical resistivity of the graphite specimens was determined from the same experiments that were used to calculate heat capacity. In the case of pyrolytic graphite, the results correspond to the measurements in the direction parallel to the basal planes. The differences in the results between "fast" and "slow" experiments for a given specimen were within the measurement resolution. However, unlike heat capacity, there were differences in the electrical resistivity of the two specimens belonging to the same graphite grade. The average absolute difference between the two specimens was about 7% for Poco graphite and 1.5% for pyrolytic graphite. It should be noted, however, that the Poco graphite specimens represented two different types, therefore, a difference in their electrical resistivity may be expected. The difference in the case of pyrolytic graphite may largely be attributed to the differences in the fabrication of the specimens. The electrical resistivity of Poco graphite at temperatures above 1500 K was about four times greater than that of pyrolytic graphite.

The functions for electrical resistivity that represent the average of the results corresponding to two different heating rates for the two types of Poco graphite specimens in the range 1500 to 3000 K are:

Poco (AXM-5Q) graphite (standard deviation, 0.07%)

$$\rho = 908.56-1.4324 \times 10^{-1}T + 1.4766 \times 10^{-4}T^{2}-2.2603 \times 10^{-8}T^{3} \qquad (3)$$

Poco (DFP-2) graphite (standard deviation, 0.05%)

$$\rho = 808.97-1.0082 \times 10^{-1}T + 1.2824 \times 10^{-4}T^{2}-1.9763 \times 10^{-8}T^{3} \qquad (4)$$

The function for electrical resistivity that represents the average of the results for the two pyrolytic graphite specimens corresponding to two different heating rates in the range 1500 to 3000 K is:

Pyrolytic graphite (standard deviation, 0.9%)

$$\rho = 190.21-1.3574 \times 10^{-3}T + 1.6492 \times 10^{-5}T^{2} \qquad (5)$$

where T is in K and ρ is in 10^{-8} $\Omega\cdot$m. The electrical resistivity of the graphites computed using Equations (3), (4) and (5) is presented in Table 4. The measured electrical resistivity values of the graphite specimens are shown in Figure 3. The data on both Poco graphite specimens indicate the presence of an inflection point in the function of electrical resistivity versus temperature in the vicinity of 2170 K (2178 K for specimen-1 and 2163 K for specimen-2). The data on pyrolytic graphite do not indicate any inflection point in the present temperature range.

Electrical resistance measurements at 283 K with a Kelvin bridge before and after the pulse experiments were in agreement within 0.1% for the Poco graphite specimens and 0.5% for the pyrolytic graphite specimens. This indicates that no significant irreversible structural or chemical changes had taken place in the specimens as the result of

Table 4

Electrical Resistivity of Poco and Pyrolytic Graphites According to Equations (3), (4) and (5)

Temperature K	Electrical Resistivity, 10^{-8} $\Omega \cdot$m		
	Poco		Pyrolytic
	AXM-5Q (Specimen-1)	DFP-2 (Specimen-2)	Specimens 3 and 4
1500	949.7	879.6	225.3
1600	964.8	895.0	230.3
1700	980.7	911.1	235.6
1800	997.3	927.7	241.2
1900	1014.4	944.8	247.2
2000	1031.9	962.2	253.5
2100	1049.6	979.8	260.1
2200	1067.4	997.4	267.0
2300	1085.2	1015.0	274.3
2400	1102.8	1032.5	281.9
2500	1120.2	1049.6	289.9
2600	1137.1	1066.4	298.2
2700	1153.4	1082.6	306.8
2800	1169.0	1098.2	315.7
2900	1183.7	1113.1	325.0
3000	1197.5	1127.1	334.6

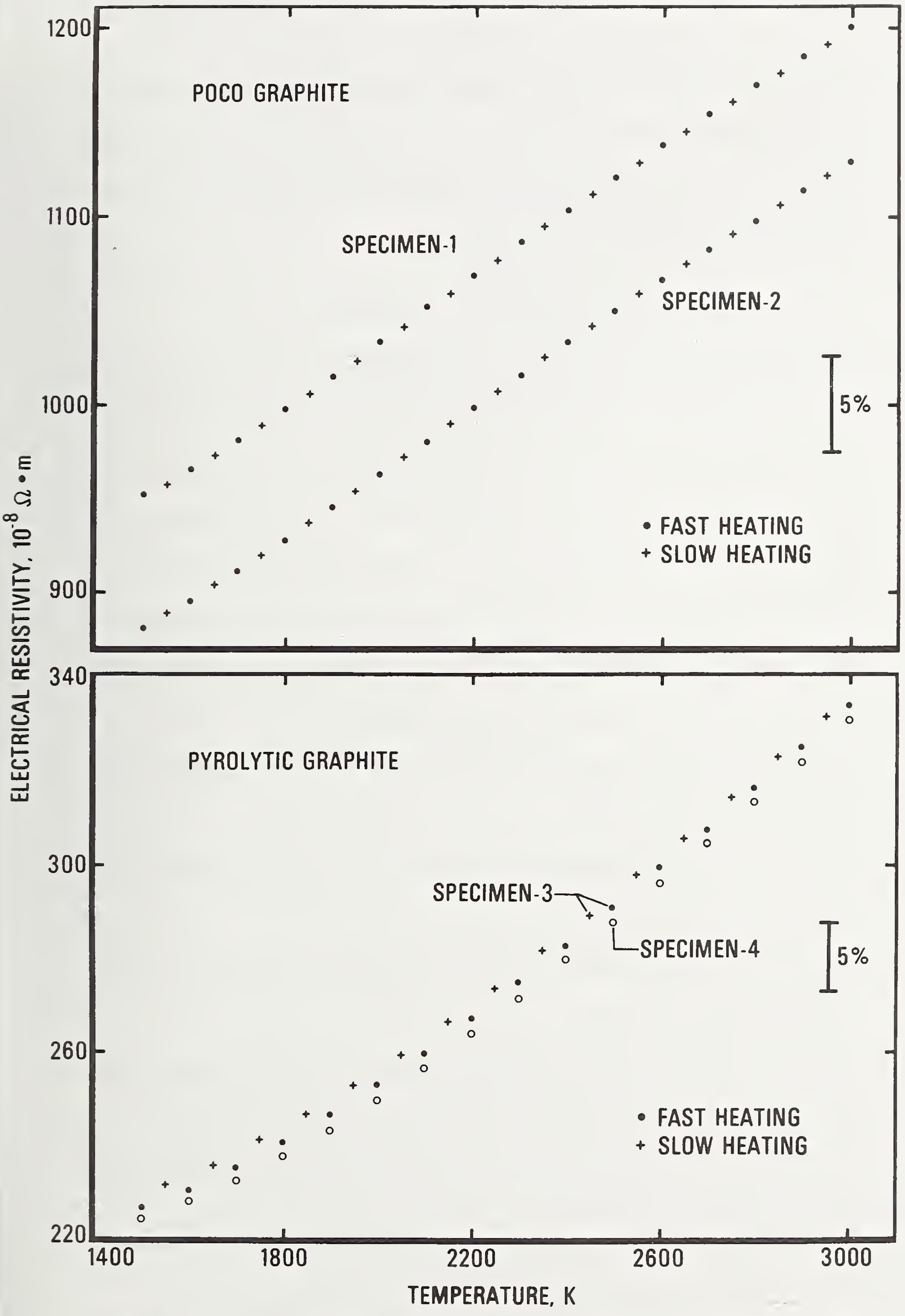

Figure 3. Electrical resistivity of Poco and pyrolytic graphites.

their having been heated to high temperatures. The average values of the electrical resistivity (in 10^{-8} $\Omega \cdot m$) for the graphites at 283 K were as follows: 1475 for Poco (AXM-5Q), 1338 for Poco (DFP-2) and 511 for pyrolytic graphite.

4.3. Hemispherical Total Emittance

Hemispherical total emittance was computed for each specimen using data taken during both heating and cooling periods. In the case of pyrolytic graphite, the results correspond to radiation emitted from the surface parallel to the basal planes. The differences between the "fast" and "slow" experiments for a given specimen were within the measurement resolution. However, the results were different for different specimens. The functions for hemispherical total emittance that represent the results of the graphites are:

Poco (AXM-5Q) graphite, 1800 to 2900 K (standard deviation, 0.7%)

$$\epsilon = 0.679 + 6.00 \times 10^{-5}\ T \qquad (6)$$

Poco (DFP - 2) graphite, 1700 to 2900 K (standard deviation, 0.7%)

$$\epsilon = 0.794 + 2.28 \times 10^{-5}\ T \qquad (7)$$

Pyrolytic graphite, 2300 to 3000 K (standard deviation, 1.2%)

$$\epsilon = 0.641 - 5.70 \times 10^{-5}\ T \qquad (8)$$

where T is in K. The hemispherical total emittance of the graphites computed using Equations (6), (7) and (8) is presented in Table 5. The measured values of the hemispherical total emittance of the graphite specimens are shown in Figure 4.

Table 5

Hemispherical Total Emittance of Poco and Pyrolytic Graphites According to Equations (6), (7) and (8)

Temperature K	Hemispherical Total Emittance		
	Poco		Pyrolytic
	AXM-5Q (Specimen-1)	DFP- 2 (Specimen-2)	(Specimen-3)
1700	---	0.833	---
1800	0.787	0.835	---
1900	0.793	0.837	---
2000	0.799	0.840	---
2100	0.805	0.842	---
2200	0.811	0.844	---
2300	0.817	0.846	0.510
2400	0.823	0.849	0.504
2500	0.829	0.851	0.499
2600	0.835	0.853	0.493
2700	0.841	0.856	0.487
2800	0.847	0.858	0.481
2900	0.853	0.860	0.476
3000	---	---	0.470

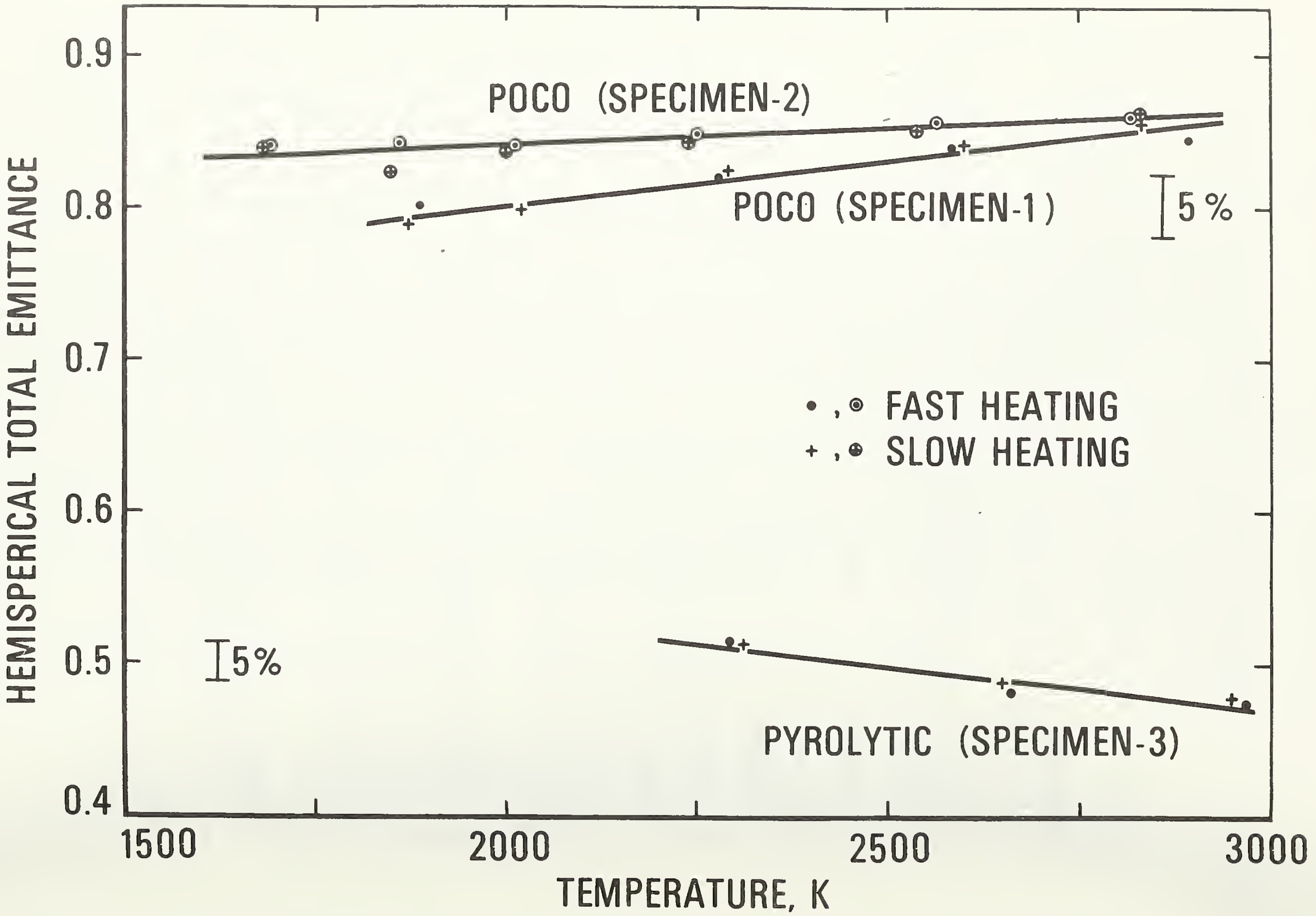

Figure 4. Hemispherical total emittance of Poco and pyrolytic graphites.

5. Estimate of Errors

Estimates of errors in measured and computed quantities lead to the following estimates of errors in the properties: heat capacity, 3%; electrical resistivity, 1% (Poco) and 3% (pyrolytic); hemispherical total emittance, 5%. Details regarding the estimates of errors and their combination in experiments using the present measurement system are given in a previous publication [4]. Specific items in the error analyses were recomputed whenever the present conditions differed from those in the earlier publication.

Because of the high value of the hemispherical total emittance of graphite (especially Poco grades), heat loss from the specimen due to thermal radiation constitutes a substantial fraction of the input power, especially at temperatures above 2500 K (Table 2). However, as a result of data taken during the cooling period, an accurate account of its magnitude in correcting heat capacity was possible. This is demonstrated by the rather closely agreeing results (within measurement resolution) of the two sets of experiments performed on the same specimen at two different heating rates.

6. Discussion

6.1. Heat Capacity

Only a limited number of experimental heat capacity results for graphite at temperatures above 1500 K was found in the literature. Since most of them are for different grades of graphite, it is questionable whether one has a common ground for comparison. As it may be seen in Figure 5, considerable differences exist between the results of various investigators.

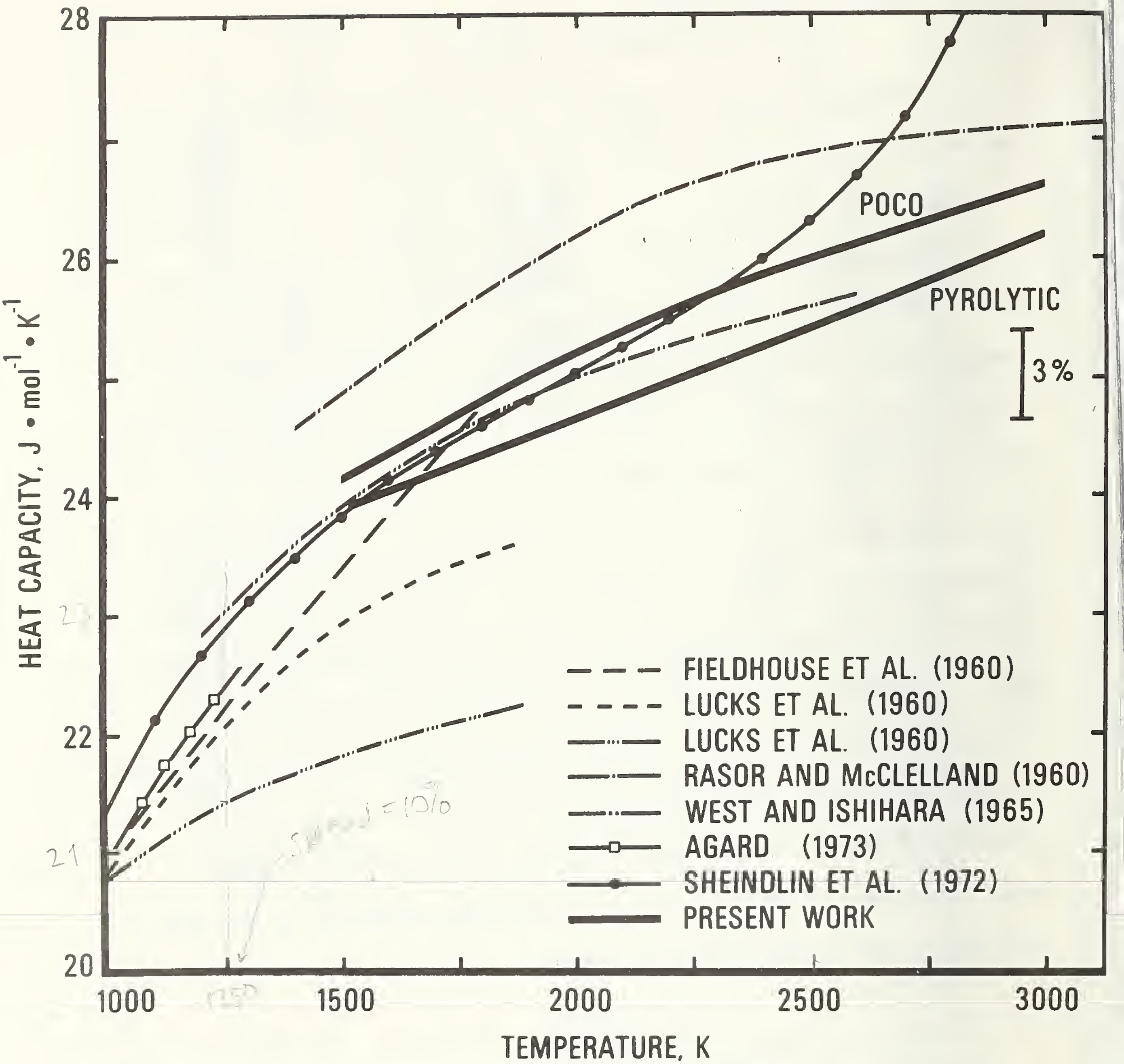

Figure 5. Heat capacity of graphite reported in the literature. The measurements, with the exception of those of Rasor and McClelland and the present work, were performed using drop calorimetric techniques.

The heat capacity results of the present work agree best with those reported by West and Ishihara [6] on grade CCH graphite. In the overlapping temperature region (1500 to 2600 K), the results of West and Ishihara are, on the average, about 0.6% lower than the Poco graphite results and about 1.2% higher than the pyrolytic graphite results. This rather close agreement is even more significant if one considers that different measurement techniques (drop and pulse) were employed in the two cases.

The smoothed results of Rasor and McClelland [7] are average values, as given by the authors, representing data on four grades of graphite (3474D, 7087, GBH, and GBE). Their actual data have a scatter of approximately 5% about their smooth curve. The difference between the results of Rasor and McClelland and those of the present work is, on the average, about 3% (Poco) and 5% (pyrolytic).

Lucks et al. [8] have reported results for two grades of graphite. The upper and lower curves (in Figure 5) represent the results for the grades 7087 and GBH, respectively. The disagreement between the results of Lucks et al. and Rasor and McClelland for the same grades of graphite is more than 10%, suggesting serious experimental errors.

In the temperature region of overlap with the present work (1500 to 1800 K), the results for ATJ graphite reported by Fieldhouse et al. [9] agree, within 3%, with those of the present work. However, the slope of the curve representing the results of Fieldhouse et al. is considerably greater than the slopes of the curves representing the present work.

The results reported recently by Sheindlin et al. [10] on a number of different graphites fall between the present work results on the two graphite grades in the range 1500 to 2300 K. However, above 2300 K, their results indicate a sharp increase in heat capacity which reaches a value of 29.55 $J \cdot mol^{-1} \cdot K^{-1}$ at 3000 K, which is 11% higher than the present work result on Poco graphite.

In addition to the present measurements, the only other known measurements on Poco (AXM-5Q) graphite were those reported in the AGARD Report [11] covering the temperature range 373 to 1273 K. Since these data have no overlapping region with the present results it is difficult to estimate the differences in the two results. However, from Figure 5 it may be seen that an extrapolation of the literature results to 1500 K is likely to yield a value approximately 2% lower than that of the present work on Poco graphite.

The rather closely agreeing results of West and Ishihara [6] and those of the present work were obtained on different grades of graphite using different measurement techniques indicating that the heat capacity of graphite may not be very sensitive to differences in certain grades. Therefore, the differences in the literature results should not be entirely attributed to grade differences, and the foregoing observation suggests that these differences might have been partly due to experimental errors. In addition, the state of the specimen (purity, degree of graphitization and annealing) have undoubtedly played an important role in the results. Sheindlin et al. [10] have also arrived to a similar conclusion as a result of their measurements on several graphites. They have observed that the values obtained for different graphites did not differ by more than their experimental error (1.5 to 2.5% in enthalpy).

It may be seen that heat capacity of graphite reaches the Dulong and Petit value of 3R at a temperature in the vicinity of 2000 K, and continues to increase above that temperature.

The next challange in heat capacity measurements is likely to be at temperatures above 3000 K where measurements will yield information of practical and theoretical significance. It is important to resolve the questions of whether the heat capacity of graphite reaches a constant value at high temperatures, or increases sharply, as was reported by Rasor and McClelland [7] and Sheindlin et al. [10].

6.2. Electrical Resistivity

A comparison of the present work and literature results on the electrical resistivity of the two graphite grades is presented in Figure 6.

In addition to the present measurements, the only other known measurements of the electrical resistivity of Poco graphite above 1500 K are those reported in the AGARD Report [11]. A comparison of the present work results with the two different measurements indicates that in one case the present work values are 8% lower (at 1500 K) and 1% higher (at 2500 K) than the literature values; in the other case, an extrapolation over 200 K indicates that at 1500 K the present work value is about 5% higher than the literature value.

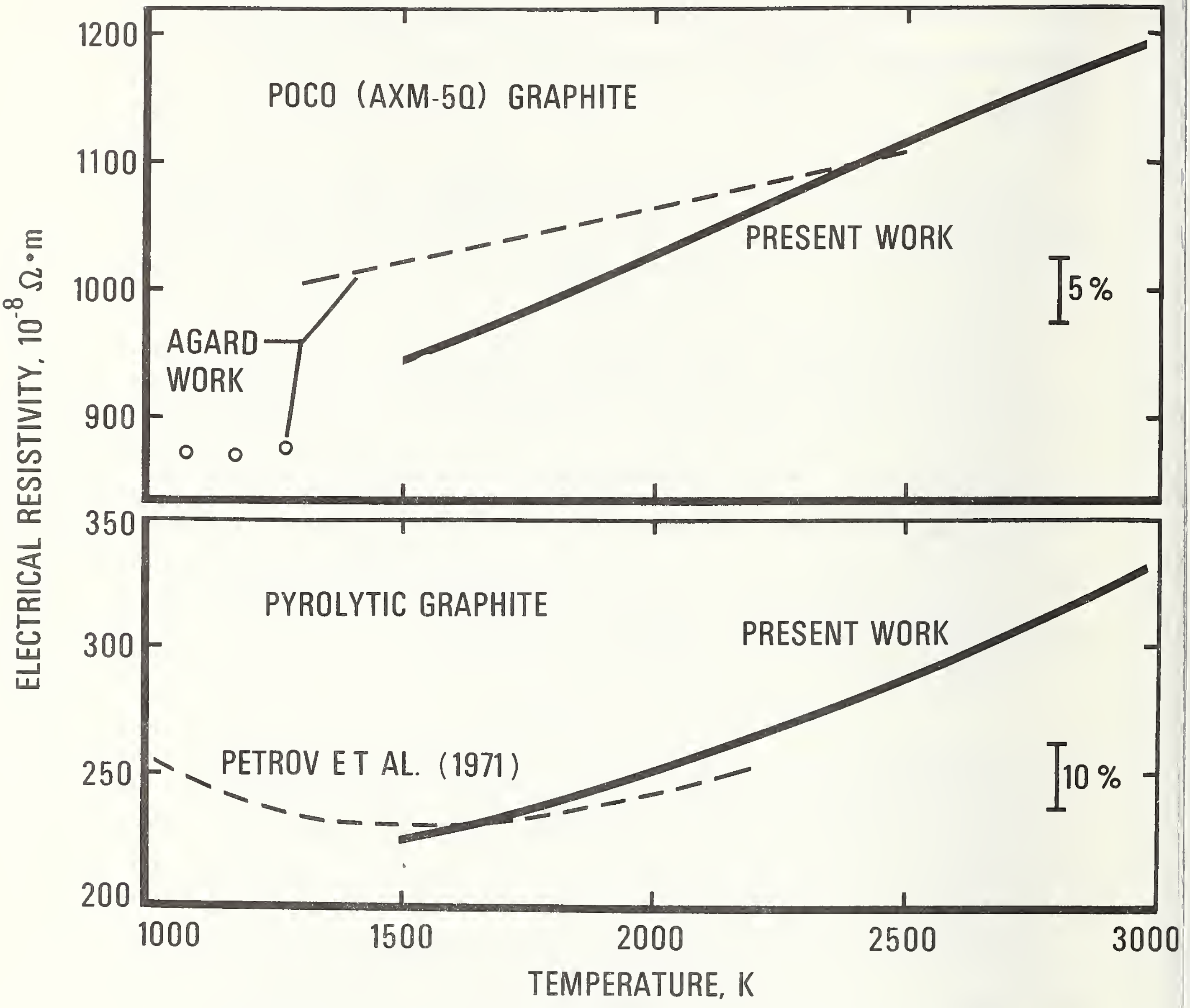

Figure 6. Electrical resistivity of Poco (AXM-5Q) and pyrolytic graphite reported in the literature. The "AGARD Work" corresponds to measurements by two different participants reported in Reference [11].

Electrical resistivity of pyrolytic graphite was reported by Pappis and Blum [12] up to 1700 K and by Petrov et al. [13] up to 2200 K. At 1500 K the present work result is 2 and 3% lower than the values reported by Pappis and Blum, and Petrov et al., respectively; at 1700 K it is 7% lower than that of Pappis and Blum; at 2200 K it is 5% higher than that of Petrov et al.

6.3. Hemispherical Total Emittance

No other measurements of the hemispherical total emittance of Poco graphite have been located in the literature. The results for other graphites such as Acheson graphite reported by Jain and Krishnan [14] yield 0.81 at 1700 K and 0.83 at 2100 K which are within 3% of the results of the present work.

Because of differences in the methods of fabrication for the specimens and the anisotropic properties of pyrolytic graphite, considerable differences in hemispherical total emittance measurements by different investigators may be expected. As presented by Petrov et al. [15], the values for emittance reported in the literature at temperatures above 1200 K range from 0.5 to 0.9. In addition to the large differences, the trends (emittance versus temperature) are also considerably different, in some cases emittance is reported to increase with increasing temperature and in others to decrease with temperature. The results of the present work indicate a decrease of emittance with temperature and their closest agreement is with those of Petrov et al. [15]. The measurements by Petrov et al. show a decrease in emittance up to about 2000 K and a small increase above 2000 K. Extrapolation of the present work results to 2000 K yields a value of 0.53 which is about 5% lower than the value given by Petrov et al.

Acknowledgement

The authors express their gratitude to Dr. C. W. Beckett for his encouragement of research in high-speed thermophysical measurements and to Mr. M. S. Morse for his help with the electronic instrumentation.

7. References

1. A. Cezairliyan. - Measurement of the heat capacity of graphite in the range 1500 to 3000 K by a pulse heating method, in Proceedings of the Sixth Symposium on Thermophysical Properties, P. E. Liley, ed. Am. Soc. Mech. Eng., New York, 1973, 279-285.
2. G. M. Foley. - High-speed optical pyrometer. Rev. Sci. Instr., 1970, 41, 827-834.
3. A. Cezairliyan. - Design and operational characteristics of a high-speed (millisecond) system for the measurement of thermophysical properties at high temperatures. J. Res. Nat. Bur. Stand. (U.S.), 1971, 75C (Eng. and Instrum.), 7-18.
4. A. Cezairliyan, M. S. Morse, H. A. Berman and C. W. Beckett. - High speed (subsecond) measurement of heat capacity, electrical resistivity, and thermal radiation properties of molybdenum in the range 1900-2800 K. J. Res. Nat. Bur. Stand. (U.S.), 1970, 74A (Phys. and Chem.), 65-92.
5. International Committee for Weights and Measures. - The International Practical Temperature Scale of 1968. Metrologia, 1969, 5, 35-44.
6. E. D. West and S. Ishihara. - A calorimetric determination of the enthalpy of graphite from 1200 to 2600 K, in Advances in Thermophysical Properties at Extreme Temperatures and Pressures, S. Gratch, ed. Am. Soc. Mech. Eng., New York, 1965, 146-151.

7. N. S. Rasor and J. D. McClelland. - Thermal properties of graphites, molybdenum, and tantalum to their destruction temperatures. J. Phys. Chem. Solids, 1960, 15, 17-26.

8. C. F. Lucks, H. W. Deem and W. D. Wood. - Thermal properties of six glasses and two graphites. Am. Cer. Soc. Bull., 1960, 39, 313-319.

9. I. B. Fieldhouse, J. I. Land and H. H. Blau. WADC TR 59-744, 1960, 1-78 [AD 249 166].

10. A. E. Sheindlin, I. S. Belevich and I. G. Kozhevnikov. - Enthalpy and specific heat of graphite in the temperature range 273-3650 K. High Temperature, 1972, 10, 897-900.

11. E. Fitzer. - Thermophysical properties of solid materials - Project section II - Cooperative measurements on heat transport phenomena of solid materials at high temperatures. AGARD Report 606, 1973.

12. J. Pappis and S. L. Blum. - Properties of pyrolytic graphite. J. Am. Cer. Soc., 1961, 44, 592-597.

13. V. A. Petrov, I. I. Petrova, V. Ya. Chekhovskoi and E. N. Lyukshin. - Specific electrical resistivity of pyrographite. High Temperature, 1971, 9, 271-274.

14. S. C. Jain and K. S. Krishnan. - The distribution of temperature along a thin rod electrically heated in vacuo. Proc. Roy. Soc. (London), 1954, <u>225</u>, 7-18.

15. V. A. Petrov, I. I. Petrova, V. Ya. Chekhovskoi and A. E. Sheindlin. - Experimental determination of the emissivity, electrical resistivity, and thermal conductivity of pyrolytic carbon. High Temperatures-High Pressures, 1970, <u>2</u>, 155-160.

Chapter 2

SIMULTANEOUS MEASUREMENTS OF HEAT CAPACITY, ELECTRICAL RESISTIVITY AND HEMISPHERICAL TOTAL EMITTANCE BY A PULSE HEATING TECHNIQUE: VANADIUM, 1500 TO 2100 K*

A. Cezairliyan, F. Righini** and J. L. McClure
Institute for Materials Research
National Bureau of Standards
Washington, D. C. 20234

Abstract

Simultaneous measurements of heat capacity, electrical resistivity and hemispherical total emittance of vanadium in the temperature range 1500 to 2100 K by a subsecond duration, pulse heating technique are described. The results are expressed by the relations:

$$c_p = 56.34 - 3.839 \times 10^{-2}T + 1.563 \times 10^{-5}T^2$$
$$\rho = 8.794 + 6.282 \times 10^{-2}T - 6.804 \times 10^{-6}T^2$$

where c_p is in $J \cdot mol^{-1} \cdot K^{-1}$, ρ is in $10^{-8}\ \Omega \cdot m$, and T is in K. The values for the hemispherical total emittance are: 0.313 at 1900 K and 0.332 at 2000 K. Estimated inaccuracies of the measured properties are: 3% for heat capacity, 0.5% for electrical resistivity and 5% for hemispherical total emittance.

---

*This work was supported in part by the U. S. Air Force Office of Scientific Research.

**Guest scientist from the Istituto di Metrologia "G. Colonnetti" in Torino, under a fellowship from the Consiglio Nazionale delle Ricerche of Italy.

1. Introduction

In this paper, application of a pulse heating technique to the simultaneous measurements of heat capacity, electrical resistivity and hemispherical total emittance of vanadium in the temperature range 1500 to 2100 K is described.

The method is based on rapid resistive self-heating of the specimen from room temperature to high temperatures (above 1500 K) in less than one second by the passage of an electrical current pulse through it; and on measuring, with millisecond resolution, such experimental quantities as current through the specimen, potential drop across the specimen, and specimen temperature. Details regarding the construction and operation of the measurement system, the methods of measuring experimental quantities, and other pertinent information, such as the formulation of relations for properties, error analysis, etc. are given in earlier publications [1, 2][1].

In the following sections of this paper a new approach - tabular format - is adopted in presenting information on the specimen, measurements, system characteristics, results, and errors.

The reasons for adopting this format are: (1) to facilitate the preparation of manuscripts, (2) to standardize the contents of the papers on measurements using the present or similar systems in other laboratories, (3) to facilitate information retrieval by the reader, (4) to provide a means for efficient and accurate identification,

---

[1] Figures in brackets indicate the literature references at the end of this paper.

TABLE 1

Specimen information

No.	Item	Unit	Explanation
1	Substance		Vanadium (polycrystalline)
2	Source[*]		Materials Research Corporation
3	Purity		99.9^{+} %
4	Impurities		Listed in table 1a
5	Geometry		Tube made from rod by electro-erosion
6	Dimensions		
	total length	mm	76.26
	effective[**] length	mm	25.53
	outside diameter	mm	6.3
	wall thickness	mm	0.5
	blackbody hole	mm	0.5 x 1
7	Weight		
	total weight	g	4.319
	effective[**] weight	g	1.438
8	Characteristics		
	atomic weight		50.942
	density	$g \cdot cm^{-3}$	6.1
	resistivity at 293 K	$10^{-8}\Omega \cdot m$	21.72
9	Special treatment		Heat treated by pulse heating before the experiments - 30 pulses to 1900 K

---

[*] The supplier is identified in this paper in order to adequately characterize the specimen - Such an identification does not imply recommendation or endorsement by the National Bureau of Standards.

[**] Effective refers to the portion of the specimen between the voltage probes.

coding, characterization and data reduction by scientific and technical information centers, and (5) to ultimately lead to the computerized preparation of papers.

2. Measurements

The details regarding the vanadium specimen used in the present measurements are given in table 1. A summary of the measurement technique and the operational characteristics of the system is given in table 2. The polynomial functions (obtained by the least squares method) that represent the experimental results are given in table 3. The final values on properties at 100 degree temperature intervals computed using the functions are given in table 4. The experimental results are presented in the Appendix. Each number tabulated in the Appendix represents results from over fifty original data points. An estimate of errors in the measured and computed quantities is given in table 5. All values reported in this paper are based on the International Practical Temperature Scale of 1968 [3]. In all computations, the geometrical quantities are based on their room temperature (298 K) dimensions.

Table 1[a]

Element	C	Fe	Nb	N	O	P
ppm	120	20	60	10	15	15
Element	Si	Ta	Ti	W	Zr	
ppm	50	70	10	30	15	

[a] The total amount of all other detected elements is less than 50 ppm, each element being below 10 ppm limit.

TABLE 2

Measurement technique and system characteristics

No.	Item	Unit	Explanation and Data
1	General technique		Pulse heating (subsecond) [1, 2]
2	Voltage measurement		Across tungsten knife-edge probes
3	Current measurement		Across standard resistor (0.001 Ω) in series with the specimen
4	Temperature measurement		High-speed photoelectric pyrometer [4]
5	Specimen environment		Vacuum ~ 1.3×10^{-3} $N \cdot m^{-2}$ (~ 10^{-5} torr)
6	Power source		Battery bank (14 series-connected 2V batteries, capacity 1100 Ah each)
7	Recording		Digital data acquisition system
8	Signal resolution		~ 0.01% (at full scale)
9	Time resolution	ms	0.4
10	Data processing		Time-sharing computer
11	Date of measurements		August 1973
12	Number of experiments		4
13	Temperature range	K	1500 - 2100
14	Temperature subranges	K	I (1480 - 1710) II (1690 - 1890) III (1810 - 2050) IV (2000 - 2130)
15	Experiment duration	ms	600 - 620
16	Current pulse length	ms	400 - 420
17	Imparted power	W	4000 - 5200
18	Current	A	1300 - 1600
19	Rate of current change	$A \cdot ms^{-1}$	0.3 - 0.6
20	Heating rate	$K \cdot ms^{-1}$	3.9 - 4.5
21	Cooling rate	$K \cdot ms^{-1}$	0.04 - 0.15
22	Radiative heat loss (% of input power)		1% at 1500 K 4% at 2100 K

TABLE 3

Functional representation of results on vanadium

Heat capacity ($J \cdot mol^{-1} K^{-1}$)	Resistivity ($10^{-8} \Omega \cdot m$)	Hemispherical total emittance
$c_p = A + BT + CT^2$	$\rho = A + BT + CT^2$	$\epsilon = A + BT$
$A = 56.34$	$A = 8.794$	$A = -5.413 \times 10^{-2}$
$B = -3.839 \times 10^{-2}$	$B = 6.282 \times 10^{-2}$	$B = 1.930 \times 10^{-4}$
$C = 1.563 \times 10^{-5}$	$C = -6.804 \times 10^{-6}$	
$1500 \text{ K} < T < 2100 \text{ K}$	$1500 \text{ K} < T < 2100 \text{ K}$	$1880 \text{ K} < T < 2050 \text{ K}$
$\sigma^* = 1.1\%$	$\sigma^* = 0.06\%$	$\sigma^* = 0.05\%$

*Standard deviation of an "individual point".

TABLE 4

Results on properties of vanadium

T (K)	c_p ($J \cdot mol^{-1} \cdot K^{-1}$)	ρ ($10^{-8} \Omega \cdot m$)	ϵ
1500	33.92	87.72	-
1600	34.93	91.89	-
1700	36.25	95.92	-
1800	37.88	99.83	-
1900	39.82	103.59	0.313
2000	42.08	107.22	0.332
2100	44.65	110.71	-

TABLE 5

Error analysis (at 2000 K)

Quantity	Imprecision*	Inaccuracy**
Temperature	0.5 K	4 K
Voltage	0.03%	0.1%
Current	0.03%	0.1%
Heat capacity	1%	3%
Electrical resistivity	0.1%	0.5%
Hemispherical total emittance	0.1%	5%

*Imprecision refers to the standard deviation of an individual point as computed from the difference between measured value and that from the smooth function obtained by the least squares method.

**Inaccuracy refers to the estimated total error (random and systematic).

3. Discussion

The heat capacity, electrical resistivity and hemispherical total emittance of vanadium measured in this work are presented and compared graphically with those reported in the literature in figures 1, 2 and 3, respectively.

The heat capacity results of this work are approximately 6-8% lower than those of Jaeger and Veenstra [5] and Fieldhouse and Lang [6], and are approximately 8% higher than those of Peletskii et al. [7] over the respective overlapping regions. The results reported in the literature were for temperatures below 1900 K. In this work, the measurements are extended to 2100 K, which is approximately 90 K below the melting point of vanadium.

The electrical resistivity results are in reasonably good agreement (maximum differences about 2%) with those reported by Hörz et al. [8] and Peletskii et al. [7]. At 293 K, the electrical resistivity of this work is approximately 3% higher than the value ($21.02 \times 10^{-8}\ \Omega\cdot m$) reported by Peletskii et al. [7]. In the range of the present measurements, vanadium showed a negative departure from linearity in the temperature dependence of electrical resistivity. A similar behavior was previously noted for niobium [9] and tantalum [10], which belong to the same group (V) on the periodic table.

Considerable differences in hemispherical total emittance results of various investigators may be expected due to the differences in specimen surface conditions. The difference between the present results and the extrapolated values of Hörz et al. [8] is approximately 6%.

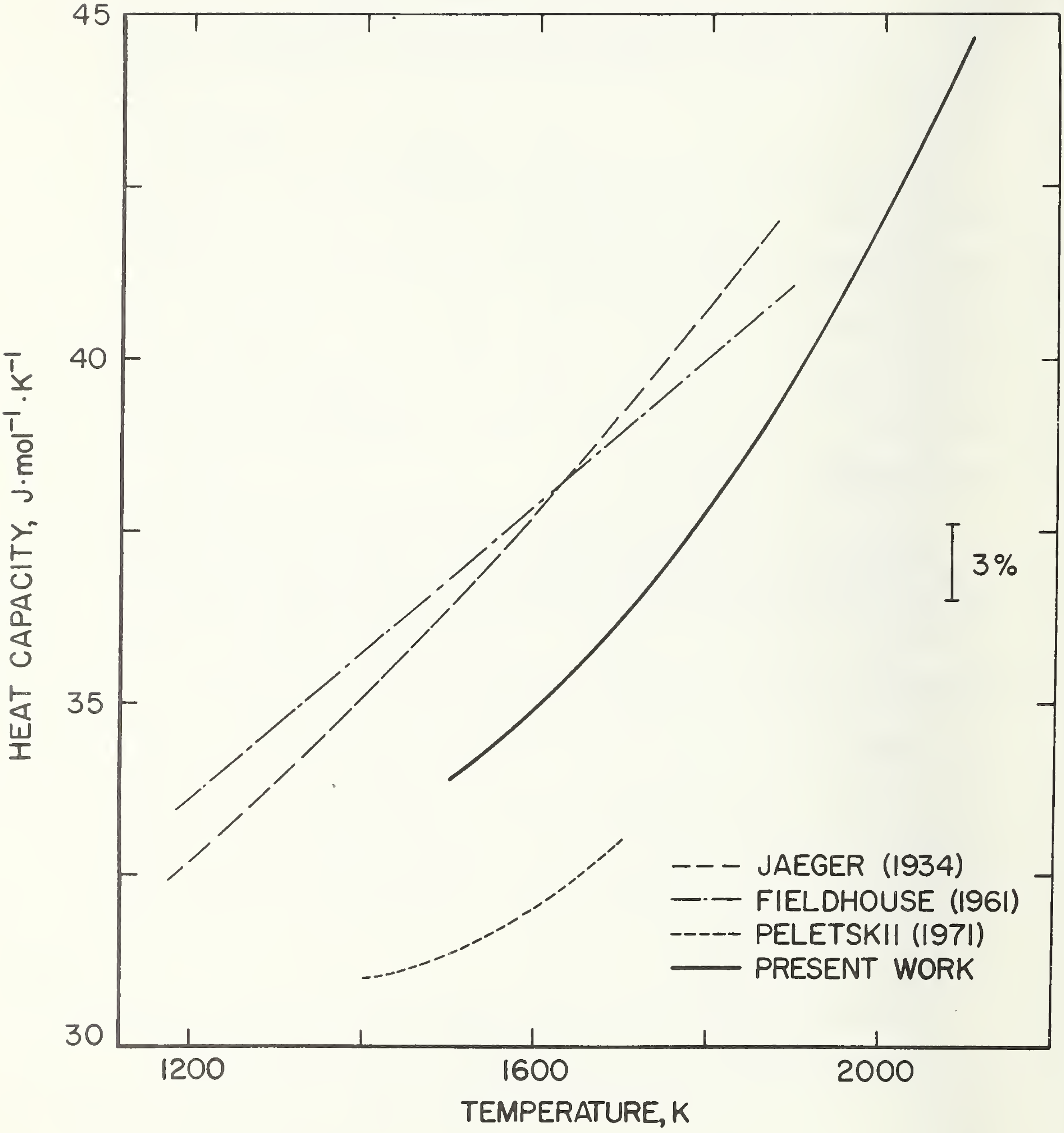

FIGURE 1. Heat capacity of vanadium as reported in the literature.

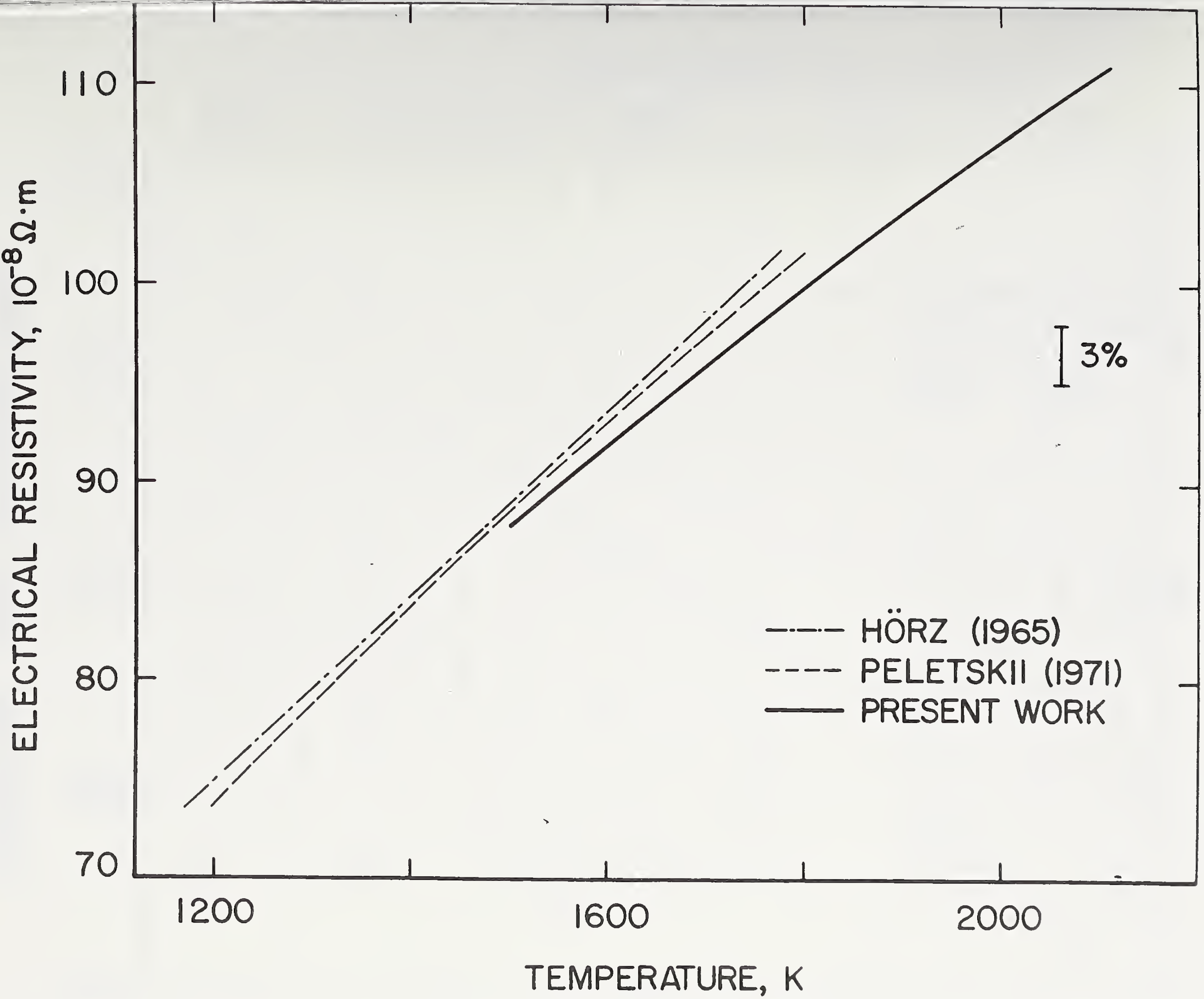

FIGURE 2. Electrical resistivity of vanadium as reported in the literature.

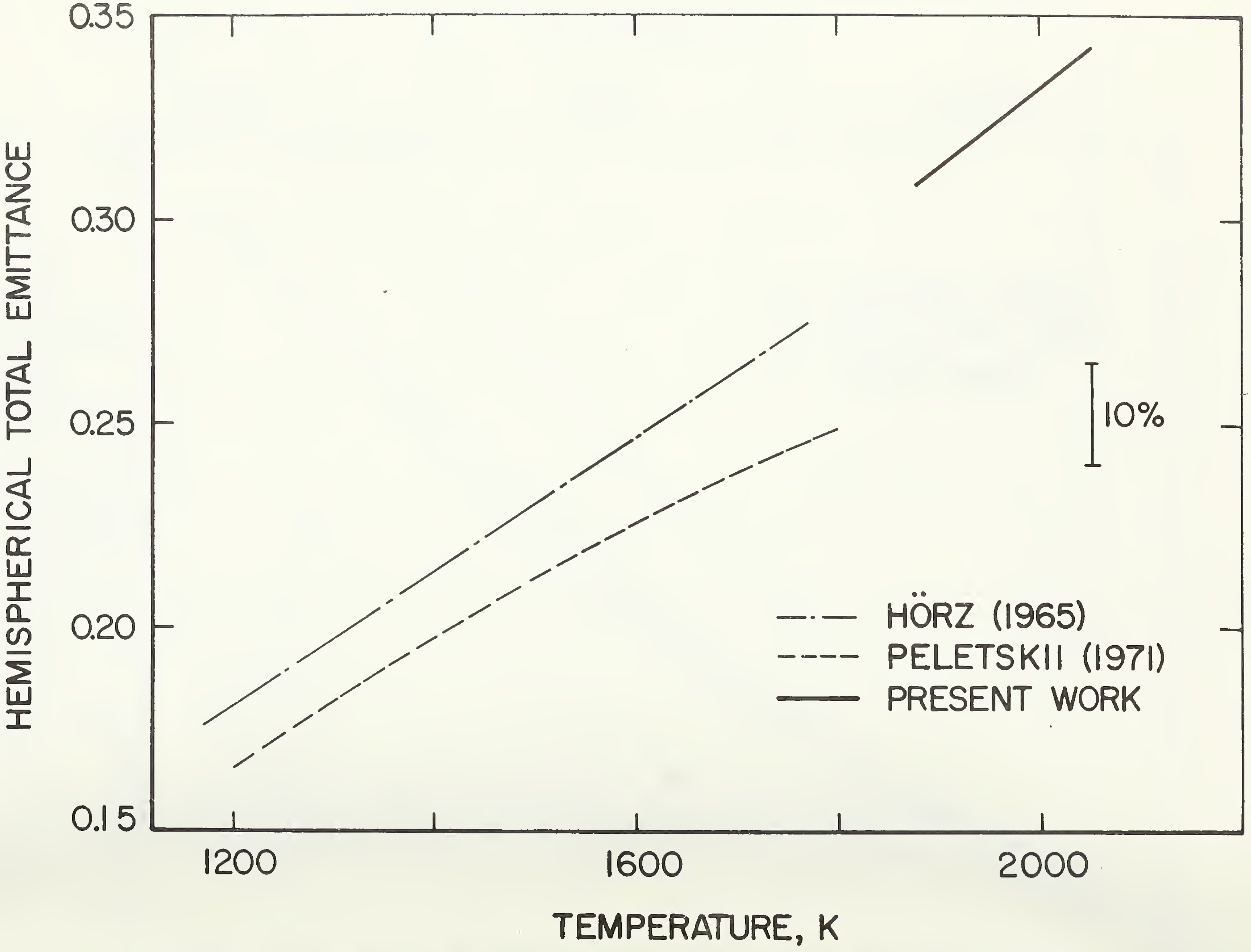

FIGURE 3. Hemispherical total emittance of vanadium as reported in the literature.

As was the case with the earlier results on other refractory metals [2, 9, 10, 11] obtained with the present measurement system, heat capacity of vanadium at high temperatures is considerably higher than the Dulong and Petit value of 3R. Some of this departure is due to c_p-c_v and the electronic terms. However, they do not account for the entire difference. Heat capacity above the Debye temperature may be expressed by

$$c_p = A - \frac{B}{T^2} + CT + \Delta c$$

where the constant term is 3R (24.943 J·mol^{-1}·K^{-1}), the term in T^{-2} is the first term in the expansion of the Debye function, the term in T represents c_p-c_v and electronic contributions, and the quantity Δc represents excess in measured heat capacity at high temperatures, which is not accounted for by the first three terms. The coefficients B (1.50 x 10^5) and C (4.86 x 10^{-3}) were obtained from heat capacity values at 270 K [12, 13] and at 1000 K. The value at 1000 K was estimated based on the extrapolation of the present work results and the low temperature results reported in the literature [12, 13].

Using the above equation and the heat capacity results of this work, the quantity Δc was computed for temperatures above 1500 K. The results for Δc in J·mol^{-1}·K^{-1} are: 1.8 at 1500 K, 4.2 at 1800 K, and 9.5 at 2100 K.

Although the mechanisms of vacancy generation become important at high temperatures, it was not possible to attribute the high heat capacity values entirely to vacancies. To demonstrate this, a crude estimate of the contribution of vacancies to heat capacity was made using the method described in a previous publication [2]. The results indicate that vacancy contribution would be small, approximately 0.03 $J \cdot mol^{-1} \cdot K^{-1}$ at 1500 K and 0.5 $J \cdot mol^{-1} \cdot K^{-1}$ at 2100 K, and would not account for the high heat capacity values. If the entire difference between measured and computed (using the first three terms in the above equation) heat capacities is attributed to vacancies, values of 1.1 eV for vacancy formation energy and 3.8% for vacancy concentration at the melting point are obtained. Both of these values, especially the concentration, seem to be unrealistic for vanadium.

The new format adopted in this paper has demonstrated the feasibility of concise yet complete and systematic documentation of measurements performed with the present system. For reasons enumerated in the Introduction, it is hoped that the approach of a standardized quasi-tabular presentation will find wide acceptance among the experimenters in the same and related fields.

Acknowledgement

The authors express their gratitude to C. W. Beckett for his encouragement of research in high-speed thermophysical measurements and to M. S. Morse for his help with the electronic instrumentation.

4. Appendix

TABLE A-1

Experimental results on heat capacity and electrical resistivity of vanadium

Temperature (K)	c_p (J $mol^{-1}K^{-1}$)	Δc_p* (%)	ρ ($10^{-8}\Omega\cdot m$)	$\Delta\rho$* (%)
1500	33.48	- 1.32	87.66	- 0.06
1550	34.50	+ 0.33	89.81	- 0.01
1600	35.32	+ 1.10	91.93	+ 0.05
1650	35.88	+ 0.92	94.03	+ 0.12
1700	35.81	- 1.23	95.83	- 0.09
1750	37.20	+ 0.46	97.86	- 0.03
1800	38.26	+ 0.99	99.87	+ 0.05
1850	38.61	- 0.53	101.69	- 0.03
1900	39.71	- 0.30	103.56	- 0.02
1950	40.80	- 0.29	105.40	- 0.02
2000	41.96	- 0.30	107.20	- 0.01
2050	42.72	- 1.43	109.01	+ 0.03
2100	45.34	+ 1.51	110.70	0.00

*The quantities Δc_p and $\Delta\rho$ are percentage deviations of the individual results from the smooth functions represented by the pertinent equations in table 3.

TABLE A-2

Experimental results on hemispherical total emittance of vanadium

Temperature (K)	ϵ	$\Delta\epsilon^*$ (%)	Temperature (K)	ϵ	$\Delta\epsilon^*$ (%)
1874.5	0.307	- 0.12	2022.6	0.336	- 0.06
1878.4	0.308	- 0.03	2028.0	0.337	- 0.02
1882.4	0.309	+ 0.03	2033.4	0.338	+ 0.01
1886.4	0.310	+ 0.06	2038.9	0.339	+ 0.02
1890.5	0.311	+ 0.06	2044.5	0.341	+ 0.02
1894.7	0.312	+ 0.03	2050.1	0.342	+ 0.01

*The quantity $\Delta\epsilon$ is percentage deviation of the individual results from the smooth function represented by the pertinent equation in table 3.

5. References

[1] Cezairliyan, A., Design and operational characteristics of a high-speed (millisecond) system for the measurement of thermophysical properties at high temperatures. J. Res. Nat. Bur. Stand. (U. S.) 75C (Eng. and Instr.), 7 (1971).

[2] Cezairliyan, A., Morse, M. S., Berman, H. A., and Beckett, C. W., High-speed (subsecond) measurement of heat capacity, electrical resistivity, and thermal radiation properties of molybdenum in the range 1900 to 2800 K. J. Res. Nat. Bur. Stand. (U. S.) 74A (Phys. and Chem.), 65 (1970).

[3] International Practical Temperature Scale of 1968. Metrologia 5, 35 (1969).

[4] Foley, G. M., High-speed optical pyrometer, Rev. Sci. Instr. 41, 827 (1970).

[5] Jaeger, F. M., and Veenstra, W. A., The exact measurement of the specific heats of solid substances at high temperatures. VI. The specific heats of vanadium, niobium, tantalum and molybdenum. Rec. Trav. Chim. 53, 677 (1934).

[6] Fieldhouse, I. B., and Lang, J. I., Measurement of thermal properties. Report WADD TR 60-904 (1961).

[7] Peletskii, V. E., Druzhinin, V. P., and Sobel', Ya. G., Thermophysical properties of vanadium at high temperatures. High Temp. - High Press. 3, 153 (1971).

[8] Hörz, G., Gebhardt, E., and Dürrschnabel, W., Emissionvermögen und elektrischer widerstand von vanadium, vanadiumstickstoff- und vanadium-sauerstoff- mischkristallen. Z. Metallkunde 56, 554 (1965).

[9] Cezairliyan, A., High-speed (subsecond) measurement of heat capacity, electrical resistivity, and thermal radiation properties of niobium in the range 1500 to 2700 K. J. Res. Nat. Bur. Stand. (U. S.) 75A (Phys. and Chem.), 565 (1971).

[10] Cezairliyan, A., McClure, J. L., and Beckett, C. W., High-speed (subsecond) measurement of heat capacity, electrical resistivity, and thermal radiation properties of tantalum in the range 1900 to 3200 K, J. Res. Nat. Bur. Stand. (U. S.) 75A (Phys. and Chem.), 1 (1971).

[11] Cezairliyan, A., and McClure, J. L., "High-speed (subsecond) measurement of heat capacity, electrical resistivity, and thermal radiation properties of tungsten in the range 2000 to 3600 K", J. Res. Nat. Bur. Stand. (U. S.) 75A (Phys. and Chem.), 283 (1971).

[12] Bieganski, Z., and Stalinski, B., Heat capacities and thermodynamic functions of vanadium and vanadium hydride within the range 24 to 340 K. The hydrogen contribution to the heat capacity of transition metal hydrides. Bull. Acad. Polon. Sci. Ser. Sci. Chim. 9, 367 (1961).

[13] Anderson, C. T., The heat capacities of vanadium, vanadium trioxide, vanadium tetroxide and vanadium pentoxide at low temperatures. J. Am. Chem. Soc. 58, 564 (1936).

Chapter 3

SIMULTANEOUS MEASUREMENTS OF HEAT CAPACITY, ELECTRICAL RESISTIVITY AND HEMISPHERICAL TOTAL EMITTANCE BY A PULSE HEATING TECHNIQUE: ZIRCONIUM, 1500 TO 2100 K*

A. Cezairliyan and F. Righini**
Institute for Materials Research
National Bureau of Standards
Washington, D. C. 20234

Abstract

Simultaneous measurements of heat capacity, electrical resistivity and hemispherical total emittance of zirconium in the temperature range 1500 to 2100 K by a subsecond duration, pulse heating technique are described. The results are expressed by the relations:

$$C_p = 36.65 - 1.435 \times 10^{-2}\,T + 6.624 \times 10^{-6}T^2$$

$$\rho = 87.95 + 1.946 \times 10^{-2}T$$

$$\epsilon = 0.2031 + 6.362 \times 10^{-5}T$$

where C_p is in $J{\cdot}mol^{-1}{\cdot}K^{-1}$, ρ is in $10^{-8}\Omega{\cdot}m$, and T is in K. Estimated inaccuracies of the measured properties are: 3% for heat capacity, 2% for electrical resistivity and 5% for hemispherical total emittance.

---

*This work was supported in part by the U. S. Air Force Office of Scientific Research.

**Guest scientist from the Istituto di Metrologia "G. Colonnetti" in Torino, under a fellowship from the Consiglio Nazionale delle Ricerche of Italy.

1. Introduction

In this paper, application of a pulse heating technique to the simultaneous measurements of heat capacity, electrical resistivity and hemispherical total emittance of zirconium in the temperature range 1500 to 2100 K is described.

The method is based on rapid resistive self-heating of the specimen from room temperature to high temperatures (above 1500 K) in less than one second by the passage of an electrical current pulse through it; and on measuring, with millisecond resolution, such experimental quantities as current through the specimen, potential drop across the specimen, and specimen temperature. Details regarding the construction and operation of the measurement system, the methods of measuring experimental quantities, and other pertinent information, such as the formulation of relations for properties, error analysis, etc. are given in earlier publications [1, 2][1].

In the following sections of this paper a tabular format is adopted in presenting information on the specimen, measurements, system characteristics, results and errors.

---

[1] Figures in brackets indicate the literature references at the end of this paper.

TABLE 1

Specimen information

No.	Item	Unit	Explanation
1	Substance		Zirconium (polycrystalline)
2	Source[*]		Materials Research Corporation
3	Purity		99.98%
4	Impurities		Listed in table 1a
5	Geometry		Tube made from rod by electro-erosion
6	Dimensions (nominal)		
	total length	mm	76.2
	effective[**] length	mm	25.4
	outside diameter	mm	6.3
	wall thickness	mm	0.5
	blackbody hole	mm	0.5 x 1 (rectangular)
7	Weight		
	total weight	g	4.312
	effective[**] weight	g	1.425
8	Characteristics		
	atomic weight [4]		91.22
	density[***]	$g \cdot cm^{-3}$	6.53
	resistivity at 293 K	$10^{-8}\Omega \cdot m$	42.8

---

[*] The supplier is identified in this paper in order to adequately characterize the specimen - Such an identification does not imply recommendation or endorsement by the National Bureau of Standards.

[**] Effective refers to the portion of the specimen between the voltage probes.

[***] Value measured in the present work.

2. Measurements

The details regarding the zirconium specimens used in the present measurements are given in table 1. A summary of the measurement technique and the operational characteristics of the system is given in table 2. The polynomial functions (obtained by the least squares method) that represent the experimental results are given in table 3. The values of properties at 100 degree temperature intervals computed using the functions are given in table 4. The experimental results are presented in the Appendix. Each number tabulated in the Appendix represents results from over fifty original data points. An estimate of errors in the measured and computed quantities is given in table 5. All values reported in this paper are based on the International Practical Temperature Scale of 1968 [3]. In all computations, the geometrical quantities are based on their room temperature (298 K) dimensions.

Table 1a

Impurities in the specimen*

(according to the manufacturer's analysis)

Element	C	H	O	N	Al	Fe	Hf	Ni	Si	Ti
ppm	6	3.3	125	2.1	3	30	40	1.5	1.5	1

* The total amount of all other detected elements is less than 6 ppm, each element being below 1 ppm limit.

TABLE 2

Measurement technique and system characteristics

No.	Item	Unit	Explanation and Data
1	General technique		Pulse heating (subsecond)
2	Voltage measurement		Across tungsten knife-edge probes
3	Current measurement		Across standard resistor (0.001 Ω) in series with the specimen
4	Temperature measurement		High-speed photoelectric pyrometer[5]
5	Specimen environment		Vacuum $\sim 1.3 \times 10^{-3}$ $N \cdot m^{-2}$ ($\sim 10^{-5}$ torr)
6	Power source		Battery bank (14 series-connected 2V batteries, capacity 1100 A·h each)
7	Recording		Digital data acquisition system
8	Signal resolution		~ 0.01% (at full scale)
9	Time resolution	ms	0.4
10	Data processing		Time-sharing computer
11	Number of specimens		3
12	Number of experiments		12
13	Temperature range	K	1500 - 2100
14	Temperature subranges	K	I (1450 - 1680) II (1680 - 1900) III (1810 - 2050) IV (1840 - 2110)
15	Experiment duration	ms	550 - 680
16	Current pulse length	ms	350 - 480
17	Imparted power	W	1700 - 3100
18	Current	A	730 - 840
19	Rate of current change	$A \cdot ms^{-1}$	0.08 - 0.13
20	Heating rate	$K \cdot ms^{-1}$	2.9 - 4.8
21	Cooling rate	$K \cdot ms^{-1}$	0.08 - 0.3
22	Radiative heat loss (% of input power)		2% at 1500 K 10% at 2100 K

TABLE 3

Functional representation of results on zirconium

Heat capacity ($J \cdot mol^{-1} \cdot K^{-1}$)	Resistivity ($10^{-8} \Omega \cdot m$)	Hemispherical total emittance
$C_p = a + bT + cT^2$	$\rho = a + bT$	$\epsilon = a + bT$
$a = 36.65$	$a = 87.95$	$a = 0.2031$
$b = -1.435 \times 10^{-2}$	$b = 1.946 \times 10^{-2}$	$b = 6.362 \times 10^{-5}$
$c = 6.624 \times 10^{-6}$		
$1500 \text{ K} < T < 2100 \text{ K}$	$1500 \text{ K} < T < 2100 \text{ K}$	$1650 \text{ K} < T < 2050 \text{ K}$
$\sigma^* = 0.7\%$	$\sigma^* = 0.6\%$	$\sigma^* = 0.9\%$

[*] Standard deviation as computed from the difference between the value of an experimental result (as tabulated in the Appendix) and that from the smooth functions reported above.

TABLE 4

Results on properties of zirconium

T (K)	C_p ($J \cdot mol^{-1} \cdot K^{-1}$)	ρ ($10^{-8} \Omega \cdot m$)	ϵ
1500	30.03	117.14	0.299*
1600	30.65	119.09	0.305*
1700	31.40	121.03	0.311
1800	32.28	122.98	0.318
1900	33.30	124.92	0.324
2000	34.45	126.87	0.330
2100	35.73	128.82	0.337*

[*] Extrapolated values

TABLE 5

Error analysis (at 2000 K)

Quantity	Imprecision*	Inaccuracy**
Temperature	0.5 K	4 K
Voltage	0.03%	0.1%
Current	0.03%	0.1%
Heat capacity	0.7%	3%
Electrical resistivity	0.6%	2%
Hemispherical total emittance	0.9%	5%

*Imprecision refers to the standard deviation of a quantity as computed from the difference between the value of the quantity and that from the smooth function obtained by the least squares method. The quantities in the case of temperature, voltage, and current are the individual points measured in a single experiment, and in the case of heat capacity, electrical resistivity, and hemispherical total emittance are the results from all experiments as tabulated in the Appendix.

**Inaccuracy refers to the estimated total error (random and systematic).

3. Discussion

The differences in the measured properties for the three specimens were within the measurement resolution for the properties, and the final smoothed results (represented by the equations in Table 3 and tabulations in Table 4) were obtained from the combined data for the three specimens. The heat capacity, electrical resistivity and hemispherical total emittance of zirconium measured in this work are presented and compared graphically with those reported in the literature in figures 1, 2 and 3, respectively. The present results are for temperatures up to 2100 K, which is approximately 30 K below the melting point of zirconium.

The heat capacity results of this work are approximately 1% lower than those of Skinner [6] in the overlapping temperature region. Extrapolation of the results of this work to lower temperatures (1200-1400 K) yields values which are 3-6% lower than those reported by Coughlin and King [7]. However, too much significance should not be attached to the latter since: (a) the comparison is based on an extrapolation of 100-300 K and (b) the constant heat capacity reported by Coughlin and King [7] is not realistic.

The electrical resistivity results are in reasonably good agreement (maximum difference less than 1%) with those of Zhorov [8], and are approximately 2-4% lower than those of Peletskii et al. [9] in the overlapping temperature regions.

Zirconium undergoes a solid-solid phase transformation around 1150 K. The measurements of the geometrical quantities of the specimen after a number of experiments indicated permanent distortions (elongation) due to repeated heating and cooling through the transformation point. The reported electrical resistivity results are corrected for the permanent geometrical changes. The magnitude of this correction was about 1%. At 293 K, the average electrical resistivity ($42.8 \times 10^{-8} \Omega\cdot m$) of the three specimens used in this work is within 3.5% of the values reported in the literature by Adenstedt [10] ($44.1 \times 10^{-8} \Omega\cdot m$) and by Powell and Tye [11] ($42.2 \times 10^{-8} \Omega\cdot m$ and $44.3 \times 10^{-8} \Omega\cdot m$). Some of the differences in the electrical resistivity values may be due to differences in the chemical composition of the specimens.

The hemispherical total emittance values reported in this work are higher (10-25%) than those reported by Timrot and Peletskii [12], Peletskii et al. [9] and Zhorov [8]. Considerable differences in hemispherical total emittance results of various investigators may be due to differences in specimen surface conditions. Changes in the specimen's surface conditions were noticed during this work, with the initial smooth polished surface changing to an uneven rough surface as the result of repeated heating and cooling through the transformation point. This may partially account for the high emittance values.

Acknowledgement

The authors express their gratitude to C. W. Beckett for his encouragement of research in high-speed thermophysical measurements and to M. S. Morse for his help with the electronic instrumentation.

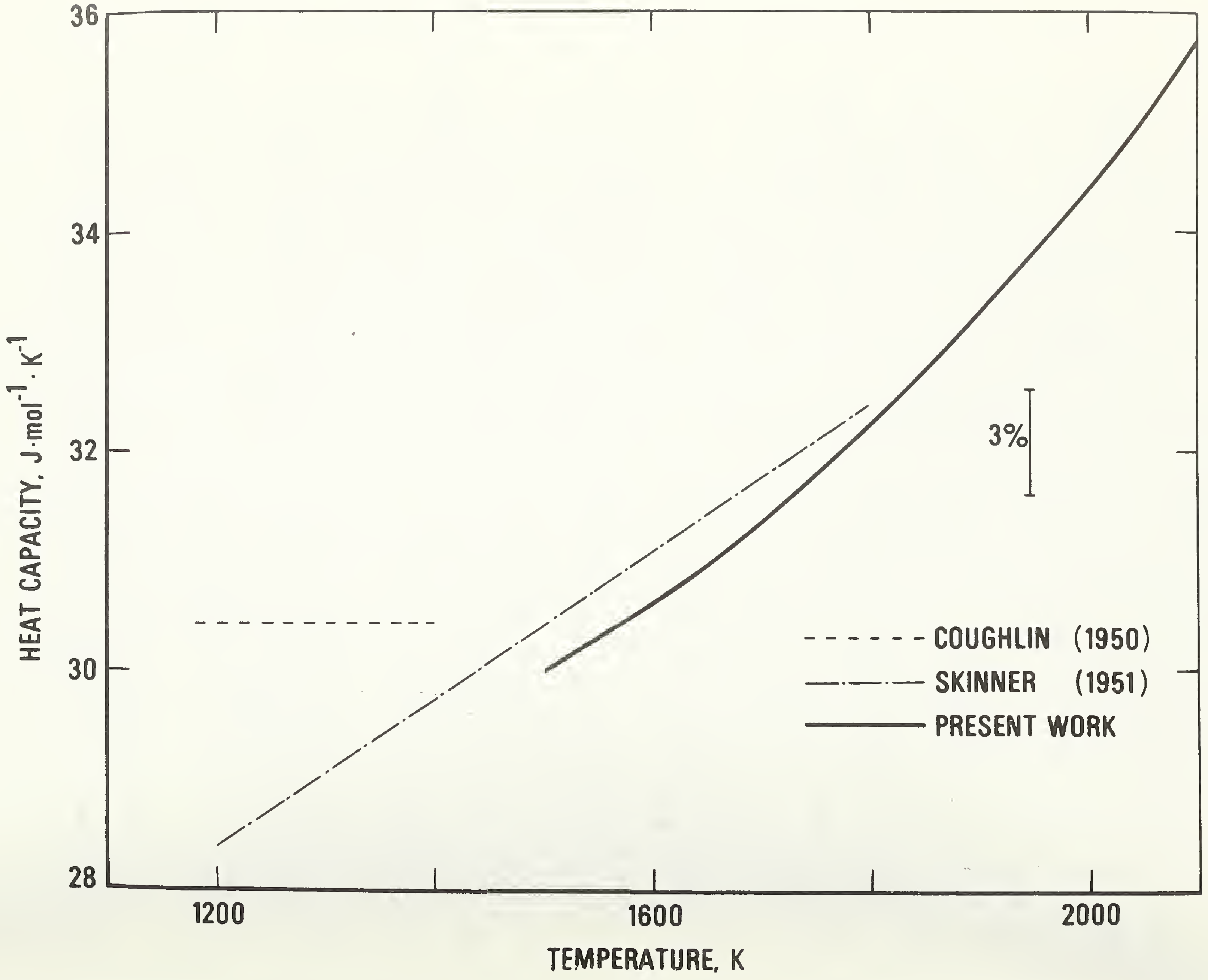

FIGURE 1. Heat capacity of zirconium reported in the literature.

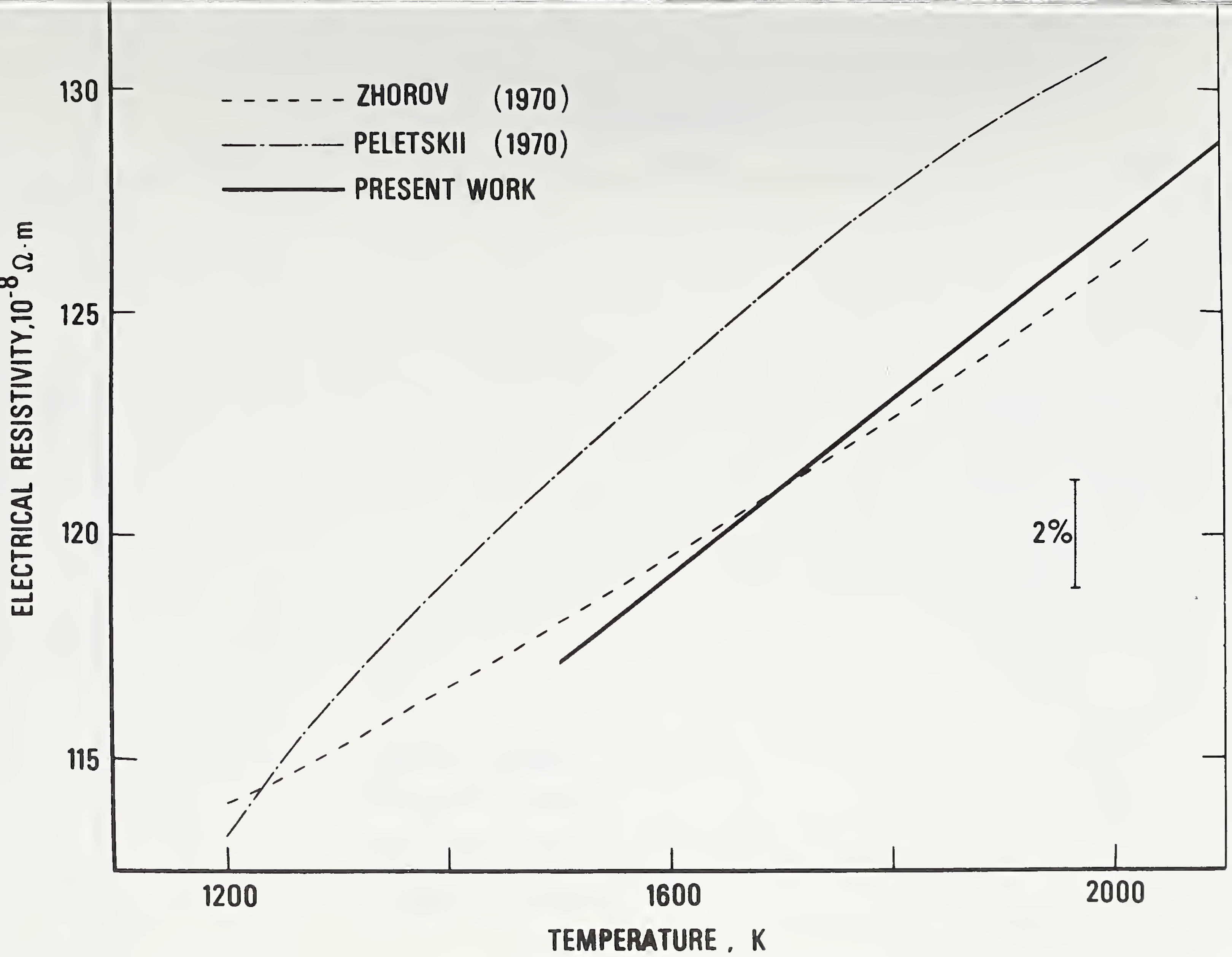

FIGURE 2. Electrical resistivity of zirconium reported in the literature.

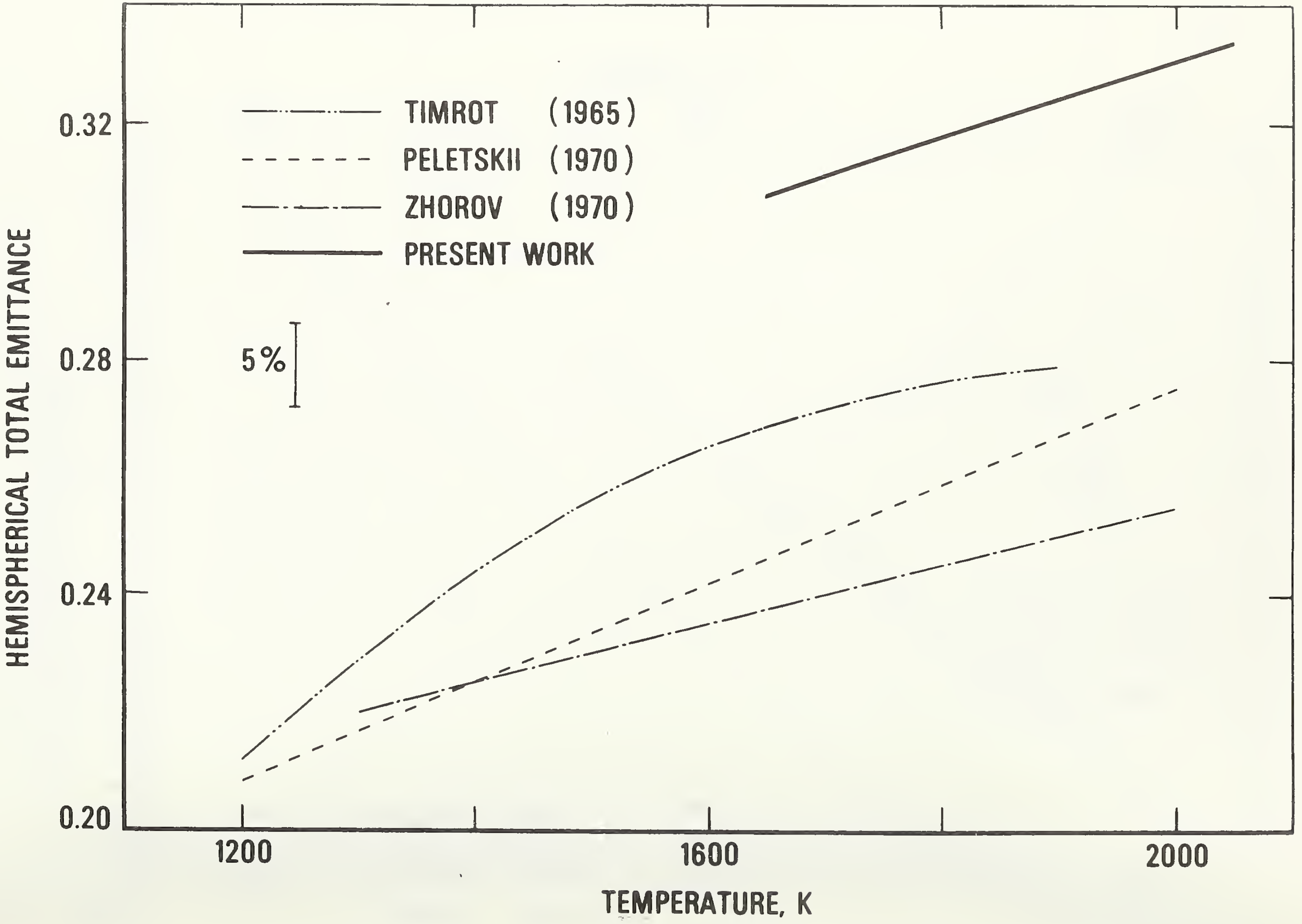

FIGURE 3. Hemispherical total emittance of zirconium reported in the literature.

4. Appendix

TABLE A-1

Experimental results on heat capacity of zirconium

Range	Temperature (K)	specimen-1		specimen-2		specimen-3			
		C_p ($J \cdot mol^{-1} \cdot K^{-1}$)	ΔC_p^* (%)	C_p ($J \cdot mol^{-1} \cdot K^{-1}$)	ΔC_p^* (%)	C_p ($J \cdot mol^{-1} \cdot K^{-1}$)	ΔC_p^* (%)	C_p ($J \cdot mol^{-1} \cdot K^{-1}$)	ΔC_p^* (%)
I	1500	29.87	- 0.52	29.72	- 1.03	29.73	- 1.00	30.02	- 0.02
	1550	30.38	+ 0.20	30.16	- 0.53	30.22	- 0.33	30.38	+ 0.20
	1600	30.91	+ 0.86	30.61	- 0.11	30.72	+ 0.25	30.72	+ 0.25
	1650	31.45	+ 1.42	31.05	+ 0.15	31.22	+ 0.69	31.65	+ 2.04
II	1700	31.54	+ 0.46	31.10	- 0.95	31.32	- 0.24	31.32	- 0.24
	1750	32.05	+ 0.72	31.79	- 0.10	31.79	- 0.10	31.83	+ 0.03
	1800	32.57	+ 0.90	32.22	- 0.18	32.25	- 0.09	32.36	+ 0.25
	1850					32.71	- 0.18	32.89	+ 0.37
	1900					33.17	- 0.37	33.42	+ 0.38
III	1850	32.66	- 0.34	32.42	- 1.08				
	1900	33.31	+ 0.05	33.05	- 0.74				
	1950	33.99	+ 0.41	33.72	- 0.39				
	2000	34.70	+ 0.74	34.40	- 0.12				
	2050	35.44	+ 1.05						
IV	1850	32.96	+ 0.58	32.77	0.00				
	1900	33.21	- 0.25	33.02	- 0.83				
	1950	33.63	- 0.66	33.43	- 1.26				
	2000	34.25	- 0.56	34.01	- 1.27				
	2050	35.12	+ 0.15	34.79	- 0.79				
	2100	36.31	+ 1.62	35.82	+ 0.27				

---

[*] The quantity ΔC_p is percentage deviation of the individual results from the smooth function represented by the pertinent equation in table 3.

TABLE A-2

Experimental results on resistivity of zirconium

Range	Temperature	specimen-1		specimen-2		specimen-3			
		ρ	$\Delta\rho$*	ρ	$\Delta\rho$	ρ	$\Delta\rho$*	ρ	$\Delta\rho$*
	(K)	($10^{-8}\Omega\cdot m$)	(%)	($10^{-8}\Omega\cdot m$)	(%)	($10^{-8}\Omega\cdot m$)	(%)	($10^{-8}\Omega\cdot m$)	(%)
I	1500	115.97	- 1.02	116.07	- 0.93	117.55	+ 0.34	117.67	+ 0.44
	1550	117.06	- 0.91	117.16	- 0.82	118.62	+ 0.42	118.85	+ 0.61
	1600	118.14	- 0.81	118.30	- 0.67	119.75	+ 0.54	119.98	+ 0.74
	1650	119.25	- 0.69	119.39	- 0.57	120.87	+ 0.66	121.10	+ 0.85
II	1700	120.36	- 0.57	120.50	- 0.45	122.00	+ 0.78	122.00	+ 0.78
	1750	121.41	- 0.50	121.56	- 0.38	123.06	+ 0.85	123.07	+ 0.86
	1800	122.50	- 0.40	122.57	- 0.34	124.10	+ 0.89	124.10	+ 0.89
	1850					125.13	+ 0.93	125.13	+ 0.93
	1900					126.14	+ 0.95	126.23	+ 1.02
III	1850	123.60	- 0.29	123.61	- 0.29				
	1900	124.62	- 0.25	124.60	- 0.27				
	1950	125.65	- 0.21	125.59	- 0.26				
	2000	126.68	- 0.16	126.58	- 0.24				
	2050	127.71	- 0.12						
IV	1850	123.60	- 0.29	123.61	- 0.29				
	1900	124.64	- 0.24	124.67	- 0.21				
	1950	125.65	- 0.21	125.68	- 0.18				
	2000	126.63	- 0.20	126.66	- 0.18				
	2050	127.61	- 0.19	127.62	- 0.19				
	2100	128.61	- 0.17	128.59	- 0.19				

The quantity $\Delta\rho$ is percentage deviation of the individual results from the smooth function represented by the pertinent equation in table 3.

TABLE A-3

Experimental results on hemispherical total emittance of zirconium

specimen-1			specimen-2		
Temperature (K)	ε	Δε* (%)	Temperature (K)	ε	Δε* (%)
1674.7	0.307	- 0.87	1650.5	0.301	- 2.37
1680.1	0.309	- 0.33	1655.5	0.304	- 1.47
1685.7	0.310	- 0.12	1660.7	0.307	- 0.58
1691.4	0.312	+ 0.40	1666.0	0.310	+ 0.28
1697.1	0.313	+ 0.61	1671.4	0.312	+ 0.81
1703.0	0.314	+ 0.80	1676.9	0.315	+ 1.65
1848.8	0.320	- 0.24	1980.7	0.326	- 0.96
1856.9	0.322	+ 0.23	1991.0	0.327	- 0.86
1865.3	0.324	+ 0.68	2001.6	0.328	- 0.75
1873.7	0.325	+ 0.82	2012.3	0.329	- 0.65
1882.4	0.327	+ 1.26	2023.3	0.329	- 0.87
1891.3	0.328	+ 1.39	2034.5	0.330	- 0.78
2003.3	0.330	- 0.18			
2014.3	0.332	+ 0.22			
2025.6	0.333	+ 0.30			
2037.1	0.334	+ 0.38			
2048.9	0.335	+ 0.45			
2061.0	0.336	+ 0.52			

*The quantity Δε is percentage deviation of the individual results from the smooth function represented by the pertinent equation in table 3.

5. References

[1] Cezairliyan, A., Design and operational characteristics of a high-speed (millisecond) system for the measurement of thermophysical properties at high temperatures. J. Res. Nat. Bur. Stand. (U. S.) 75C (Eng. and Instr.), 7 (1971).

[2] Cezairliyan, A., Morse, M. S., Berman, H. A., and Beckett, C. W., High-speed (subsecond) measurement of heat capacity, electrical resistivity, and thermal radiation properties of molybdenum in the range 1900 to 2800 K. J. Res. Nat. Bur. Stand. (U.S.) 74A (Phys. and Chem.), 65 (1970).

[3] International Practical Temperature Scale of 1968. Metrologia 5, 35 (1969).

[4] IUPAC Commission on Atomic Weights, Atomic Weights of the elements 1969. Pure Appl. Chem. 21, 91 (1970).

[5] Foley, G. M., High-speed optical pyrometer, Rev. Sci. Instr. 41, 827 (1970).

[6] Skinner, G. B., Thermodynamic and structural properties of zirconium. Ph.D. Thesis, Ohio State University, 1951.

[7] Coughlin, J. P., and King, E. G., High-temperature heat contents of some zirconium-containing substances. J. Am. Chem. Soc. 72, 2262 (1950).

[8] Zhorov, G. A., Emissivity of metals of the IVb subgroup at high temperatures. High Temp. 8, 501 (1970).

[9] Peletskii, V. É., Druzhinin, V. P., and Sobol', Ya. G., Emissivity, thermal conductivity, and electrical conductivity of remelted zirconium at high temperatures. High Temp. 8, 732 (1970).

[10] Adenstedt, H. K., Physical, thermal and electrical properties of hafnium and high purity zirconium. Trans. A.S.M. 44, 949 (1952).

[11] Powell, R. W., and Tye, R. P., The thermal and electrical conductivities of zirconium and of some zirconium alloys. J. Less-Common Metals 3, 202 (1961).

[12] Timrot, D. L., and Peletskii, V. É., The thermal conductivity and integral blackness of zirconium. High Temp. 3, 199 (1965).

Chapter 4

MEASUREMENT OF MELTING POINT, RADIANCE TEMPERATURE (AT MELTING POINT), AND ELECTRICAL RESISTIVITY (ABOVE 2100 K) OF ZIRCONIUM BY A PULSE HEATING METHOD[*]

A. Cezairliyan and F. Righini[**]
Institute for Materials Research
National Bureau of Standards
Washington, D. C. 20234

Abstract

A subsecond duration pulse heating method is used to measure the melting point, radiance temperature (at 650 nm) at the melting point, and electrical resistivity (above 2100 K) of zirconium. The results yield a value of 2128 K for the melting point on the International Practical Temperature Scale of 1968. The radiance temperature (at 650 nm) of zirconium at its melting point is 1940 K, and the corresponding normal spectral emittance is 0.367. At 2100 K electrical resistivity is 128.7×10^{-8} Ω·m. Estimated inaccuracy is: 8 K in the melting point and in the radiance temperature, and 3% in the normal spectral emittance and in the electrical resistivity.

---

[*] This work was supported in part by the U. S. Air Force Office of Scientific Research.

[**] Guest scientist from the Istituto di Metrologia "G. Colonnetti" in Torino, under a fellowship from the Consiglio Nazionale delle Ricerche of Italy.

1. Introduction

A millisecond resolution pulse heating technique was developed earlier in connection with the measurement of selected thermophysical properties of electrical conductors at high temperatures [1]. This technique was also applied to the measurement of the melting point of molybdenum [2], tungsten [3] and niobium [4], and the radiance temperature (at 650 nm) of niobium at its melting point [5].

In the present study, the same technique is used for the measurement of the melting point, radiance temperature at the melting point, and electrical resistivity (above 2100 K) of zirconium.

The method is based on rapid resistive self-heating of the specimen from room temperature to high temperatures (above 1500 K) in less than one second by the passage of an electrical current pulse through it; and on measuring, with millisecond resolution, such experimental quantities as current through the specimen, potential drop across the specimen, and specimen temperature. Temperature is measured with a high-speed photoelectric pyrometer [6], which permits 1200 evaluations of specimen temperature per second. Details regarding the construction and operation of the measurement system, the methods of measuring experimental quantities, and other pertinent information, such as the formulation of relations for properties, error analysis, etc. are given in earlier publications[1, 7].

2. Measurements

Measurements were performed on zirconium specimens in the form of tubes and strips, all of the same grade and obtained from the same manufacturer. The specimens were 99.98% pure and manufacturer's typical analysis indicated the presence of the following impurities in ppm by weight: O, 125; Hf, 40; Fe, 30; C, 6; H, 3.3; Al, 3; N, 2.1; Ni, Si, 1.5 each; and Ti, 1. The total amount of all other detected elements was less than 6 ppm, each element being below 1 ppm limit.

Melting point and electrical resistivity measurements were performed on three zirconium specimens in the form of tubes, designated as specimen-I, II and III. The nominal dimensions of the tubes were: length, 76.2 mm; outside diameter, 6.3 mm and thickness, 0.25 mm. A small rectangular hole (0.5 x 1 mm) fabricated in the wall at the middle of the specimen approximated blackbody conditions for temperature measurements.

The radiance temperature measurements at the melting point were performed on thirteen zirconium specimens in the form of strips. The nominal dimensions of the strips were: length, 50.8 mm; width, 4.7 mm and thickness, 0.24 mm. The thin oxide coating present on the specimens (strip) in the "as received" condition was removed using abrasive. Four different grades of abrasive were used yielding four different surface roughnesses (ranging from 0.23 μm to 0.95 μm) for different specimens.

All the experiments, with one exception, were performed with the specimen in a vacuum environment of approximately 1.3 x 10^{-3} $N \cdot m^{-2}$ (~ 10^{-5} torr), and in one case the specimen was in an argon environment at atmospheric pressure. The heating rate for the tubular specimens was approximately 3000 $K \cdot s^{-1}$ which corresponds to a specimen heating period (from room temperature to melting point) of approximately 600 ms. The heating rate for the strips varied from 400 $K \cdot s^{-1}$ to 3200 $K \cdot s^{-1}$, and the corresponding heating periods changed from 1200 ms to 280 ms. The magnitude of the current pulses near the melting point was about 750 A in the case of tubular specimens and ranged from 40A to 300A for the strips.

The high-speed pyrometer and the neutral density filters used for its operation at different ranges were calibrated before and after the entire set of experiments, using a tungsten filament standard lamp, which in turn was calibrated against the NBS "Temperature Standard."

All temperatures reported in this paper, except where explicitly noted, are based on the International Practical Temperature Scale of 1968 [8].

3. Experimental results

3.1. Melting point

Temperature of the tubular specimens was measured near and during the initial melting period, until the specimen collapsed. Typical results for the variation of the specimen temperature as a function of time (for specimen I) are shown in figure 1. The plateau in temperature indicates the region of solid and liquid equilibrium. The complete results

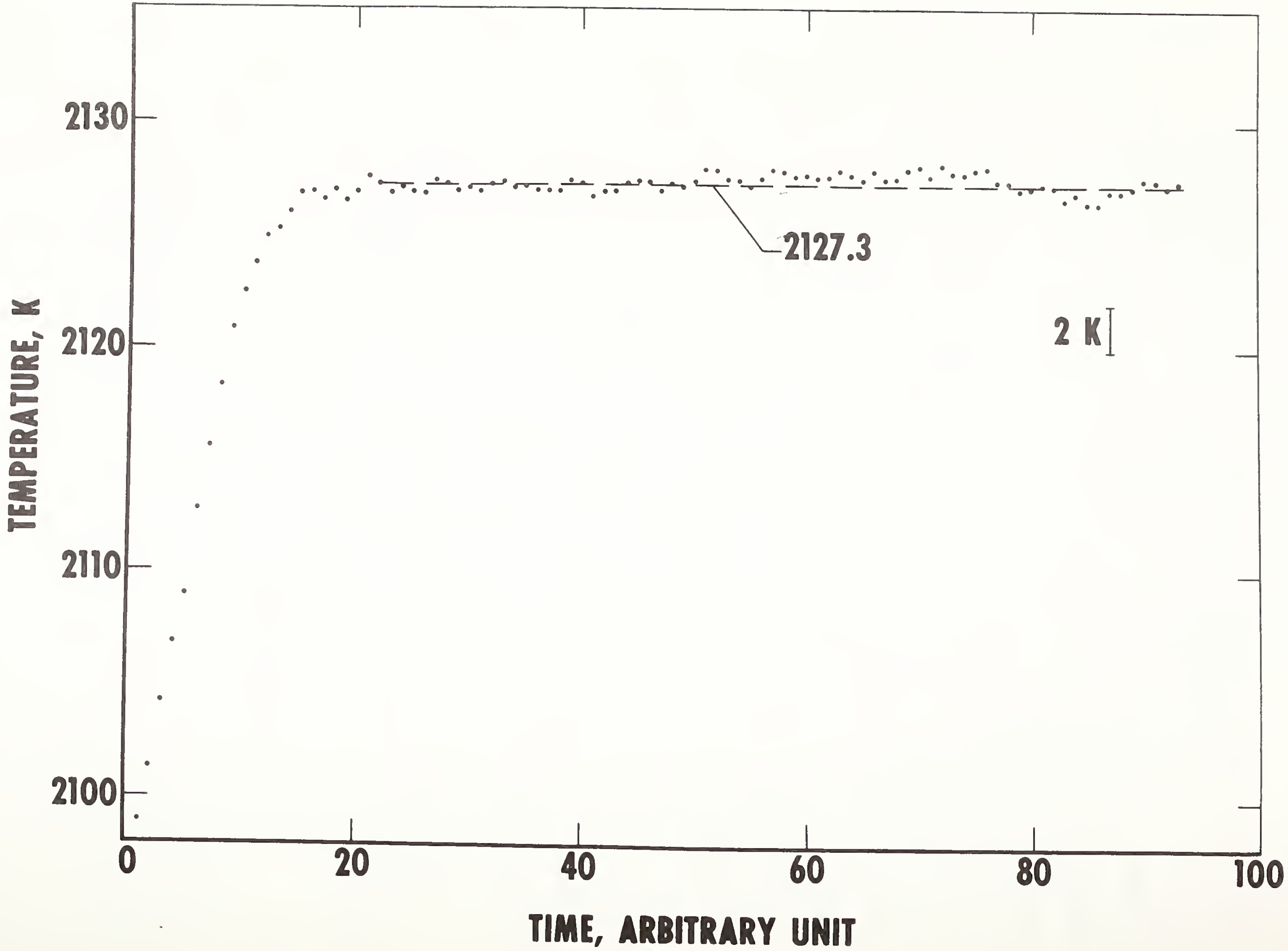

Figure 1. Variation of temperature of zirconium (specimen I) as a function of time near and at the melting point (1 time unit = 0.833 ms).

Table 1

Experimental results of the melting point of tubular zirconium specimens

Specimen number	Number of temperatures at plateau	Melting point (K)	Standard deviation (K)
I	73	2127.3	0.4
II	20	2127.5	0.4
III	28	2127.8	0.6

for the three tubular zirconium specimens are presented in table 1. The value of the melting point was obtained by averaging temperature points on the plateau of a given specimen. The duration of the plateau for specimens II and III was shorter than that of specimen I. This may be attributed to an early collapse of these specimens. To determine the trend of measured temperatures at the plateau, temperatures for specimen I were fitted to a linear function in time using the least squares method. The slope of the linear function was 4.7 $K \cdot s^{-1}$, which corresponds to a maximum temperature difference of less than 0.3 K between the begining and the end of the plateau. This procedure gave a standard deviation of 0.4 K, the same as that obtained by averaging the temperatures. Values of the same order of magnitude were found for specimens II and III. The average melting point of the three specimens is 2127.5 K with an average absolute deviation from the mean of 0.3 K. It may be concluded that the melting point of zirconium measured in this work is 2128 K.

3.2. Radiance temperature at the melting point

Radiance temperature measurements were performed on strips at 650 nm which corresponds to the effective wavelength of the pyrometer's interference filter. The bandwidth of the filter was 10 nm. The circular area viewed by the pyrometer was 0.2 mm in diameter.

Radiance temperature of zirconium at its melting point for the thirteen experiments (corresponding to thirteen specimens) and other pertinent results are reported in table 2. The variation of radiance temperature as a function of time near and at the melting point is shown in figure 2 for three typical experiments representing three

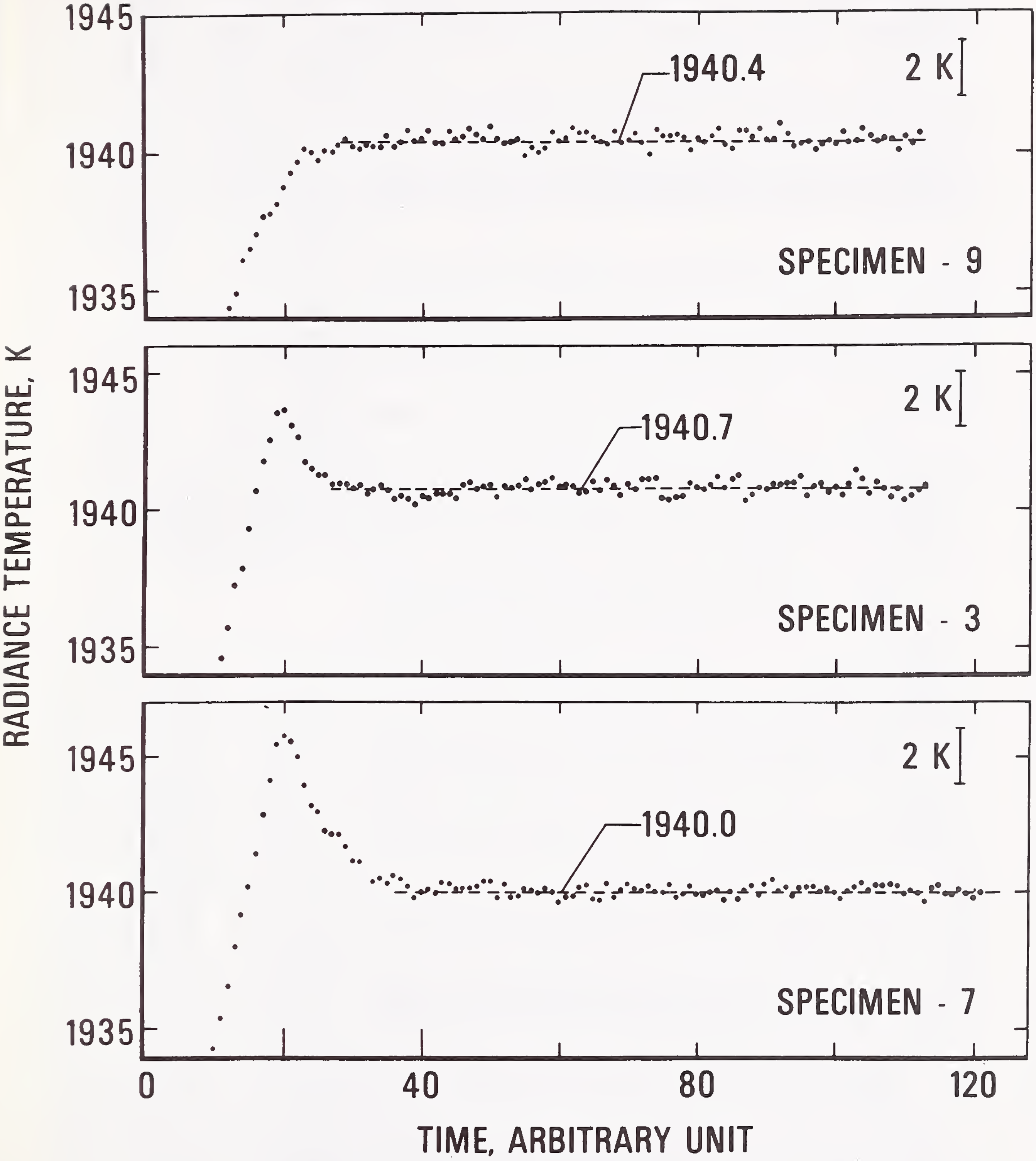

Figure 2. Variation of radiance temperature (at 650 nm) of zirconium as a function of time near and at its melting point for three typical experiments (1 time unit = 0.833 ms).

Table 2

Summary of experiments for the measurement of radiance temperature of zirconium during melting

Specimen number[a]	Surface roughness[b]	Premelting period		Melting period				
		Heating rate[c] $(K \cdot s^{-1})$	Standard deviation[d] (K)	Number of temperatures[e]	Slope at plateau[f] $(K.s^{-1})$	Plateau temp. difference[g] (K)	Radiance temperature[h] (K)	Standard deviation[i] (K)
1	B	1400	0.2	90	4.5	0.3	1940.1	0.2
2	C	1400	0.3	60	11.4	0.5	1940.7	0.3
3	B	1500	0.3	84	2.1	0.1	1940.7	0.3
4	C	1400	0.3	90	1.6	0.1	1940.6	0.2
5	C	1500	0.4	54	6.1	0.3	1940.7	0.2
6	D	1500	0.3	60	3.8	0.2	1940.3	0.2
7	D	1600	0.3	84	0.3	0.1	1940.0	0.2
8	A	1600	0.3	102	2.9	0.2	1939.8	0.3
9	A	1600	0.3	84	-0.2	-0.1	1940.4	0.2
10	B	1300	0.4	60	7.3	0.4	1940.7	0.3
11	B	1300	0.3	36	-2.5	-0.1	1940.6	0.2
12	B	400	0.3	72	9.2	0.5	1940.7	0.2
13	B	3200	0.5	12	23.3	0.2	1940.7	0.2

[a] Also represents the experiments in chronological order.

[b] The notations used for surface conditions correspond to the following typical roughnesses in µm: A, 0.23; B, 0.38; C, 0.53; and D, 0.95.

[c] Heating rate evaluated at a temperature approximately 10 K below the melting point.

[d] Represents standard deviation of an individual temperature as computed from the difference between the measured value and that from the smooth temperature versus time function (quadratic) obtained by the least squares method. Data extend approximately 100 K below the melting point.

[e] Number of temperatures used in averaging the results at the plateau to obtain an average value for the radiance temperature at the melting point of the specimen.

[f] Derivative of the temperature versus time function obtained by fitting the temperature data at the plateau to a linear function in time using the least squares method.

[g] Maximum radiance temperature difference between the beginning and the end of the plateau based on the linear temperature versus time function.

[h] The average (for a specimen) of measured radiance temperatures at the plateau.

[i] Standard deviation of an individual temperature as computed from the difference between the measured value and that from the average plateau radiance temperature.

specimens with different initial surface conditions. The magnitude of the spike before the melting plateau for two of the specimens is related to the degree of initial surface roughness of the specimens. However, regardless of the initial surface and operational conditions, radiance temperature at the melting plateau is approximately the same for all the specimens.

A single value for the radiance temperature at the plateau for each specimen was obtained by averaging the temperatures at the plateau. The number of temperatures used for averaging ranged from 12 to 102, depending both on the heating rate and on the behavior of the specimen during melting. The standard deviation of an individual temperature from the average was in the range 0.2 to 0.3 K for all the experiments. Similar values (for standard deviation) were obtained when fitting the temperature data corresponding to the premelting period to a quadratic function in time. This indicates that during melting no undesirable effects took place, such as vibration of the specimen, development of hot spots in the specimen and random changes in the specimen surface conditions.

To determine the trend of measured temperatures at the plateau, temperatures for each experiment were fitted to a linear function in time using the least squares method. The detailed results are reported in table 2. The temperature difference between the beginning and the end of the plateau (corresponding to the slope in the plateau) is in the range 0.1-0.5 K. The standard deviation of an individual temperature from the linear function was approximately the same as the standard deviation obtained by direct averaging of the temperatures.

The average radiance temperature at the melting point for the thirteen zirconium specimens was 1940.5 K with an average absolute difference of 0.3 K and a maximum difference of 0.7 K. The results are presented in figure 3. It may be concluded that the radiance temperature (at 650 nm) of zirconium at its melting point is 1940 K.

The normal spectral emittance at the melting point was determined using the results of the radiance temperature (obtained from the measurements on strip-shape specimens) and the melting point (obtained from the measurements on tube-shape specimens). The results yield a value of 0.367 for the normal spectral emittance (at 650 nm) at the melting point of zirconium.

Several additional experiments were conducted on zirconium strips in the "as received" condition. The results of a typical experiment are shown in figure 4. The temperature plateau during melting has a considerable slope and the temperature values are 2 to 5 K higher than the values obtained on specimens with clean surfaces. This may be attributed to the presence of a thin oxide coating on the specimens; the high temperature values are consistent with the general behavior of the zirconium-oxygen system [9].

3.3 Electrical resistivity

Electrical resistivity of the tubular zirconium specimens was computed using the relation $\rho = RA/L$ where R is the resistance, A the cross-section area and L the length of the specimen between the potential probes. The dimensions were based on their room temperature values; the cross-section area was determined from the measurement of weight and

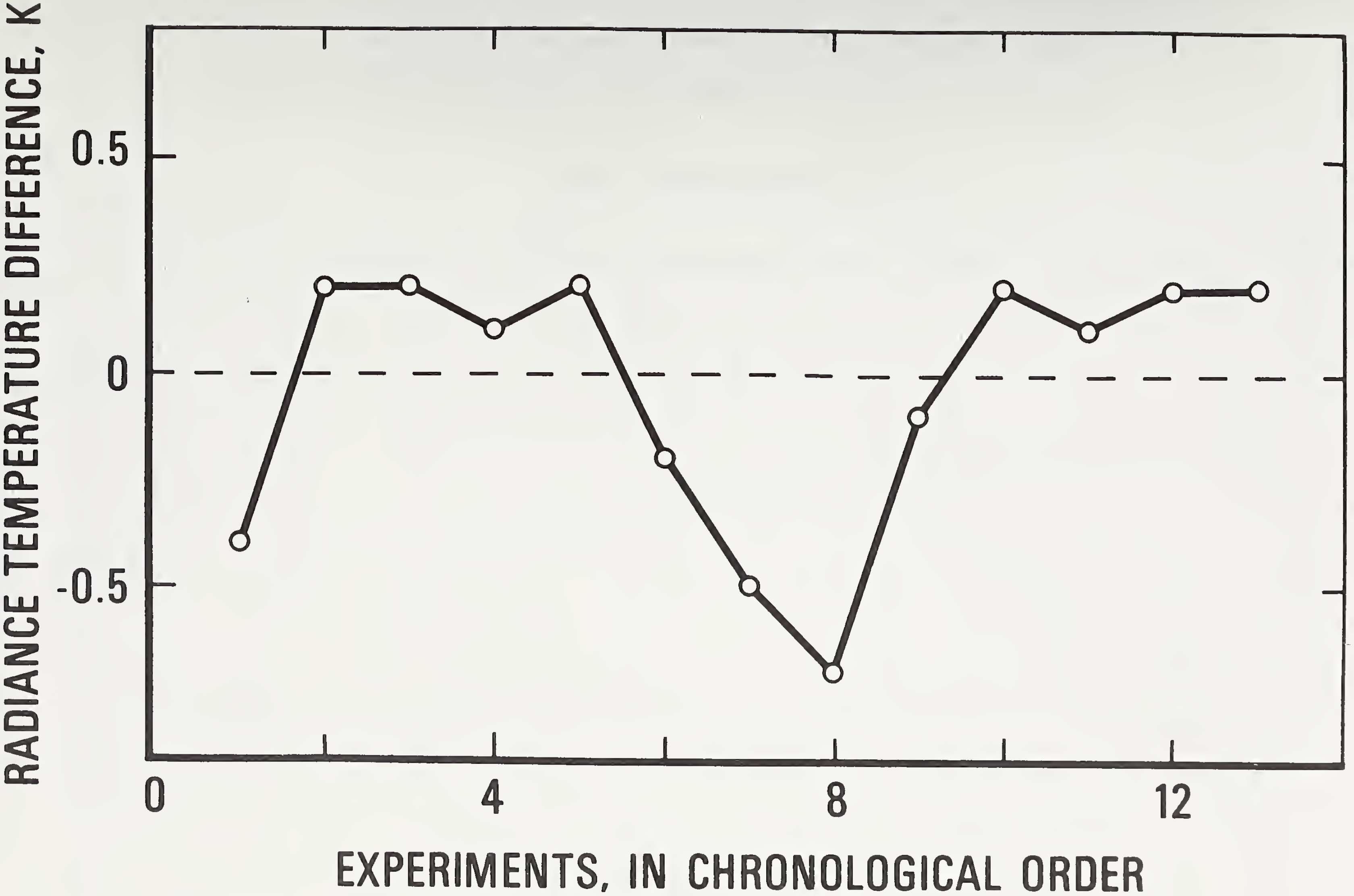

Figure 3. Difference of radiance temperature (at the melting point of zirconium, at 650 nm) for individual experiments from their average value of 1940.5 K (represented by the "zero" line).

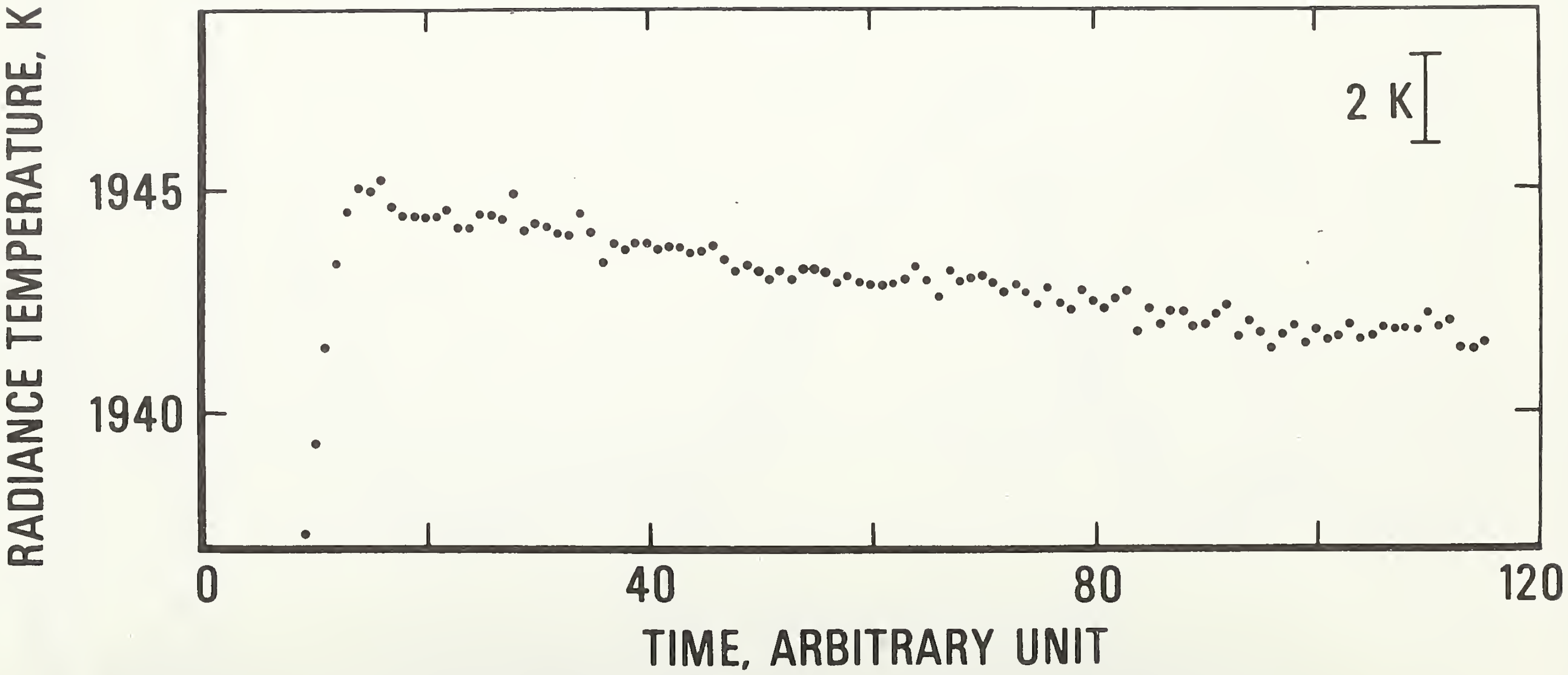

Figure 4. Typical variation of radiance temperature (at 650 nm) of zirconium (with oxide coating) as a function of time near and at its melting point (1 time unit = 0.833 ms).

density. Resistivity values above 2100 K are available only for specimens II and III, since the melting point determination of specimen I was made without the voltage probes.

Zirconium undergoes a solid-solid phase transformation around 1150 K [10]. As mentioned in an earlier publication [11], the measurements of the geometrical quantities of a zirconium specimen after a number of experiments indicated permanent distortions (elongation) due to repeated heating and cooling through the transformation point. The reported electrical resistivity results were corrected for the permanent geometrical changes. The results for the electrical resistivity of specimen II above 2100 K are shown in figure 5. The average absolute difference in the measured electrical resistivity of the two zirconium specimens in the range 2100-2125 K was approximately 0.2%. The final results for the electrical resistivity of zirconium were obtained by averaging the results for the two specimens. This yielded the values 128.7×10^{-8} $\Omega \cdot m$ at 2100 K and 128.9×10^{-8} $\Omega \cdot m$ at 2120 K. As shown in figure 5, the electrical resistivity continued to increase during melting of the specimen.

4. Estimate of errors

Sources and estimates of errors in experiments similar to the ones conducted in this study are given in detail in earlier publications [1, 2]. Specific items in the error analysis were recomputed whenever the present conditions differed from those in the earlier publications.

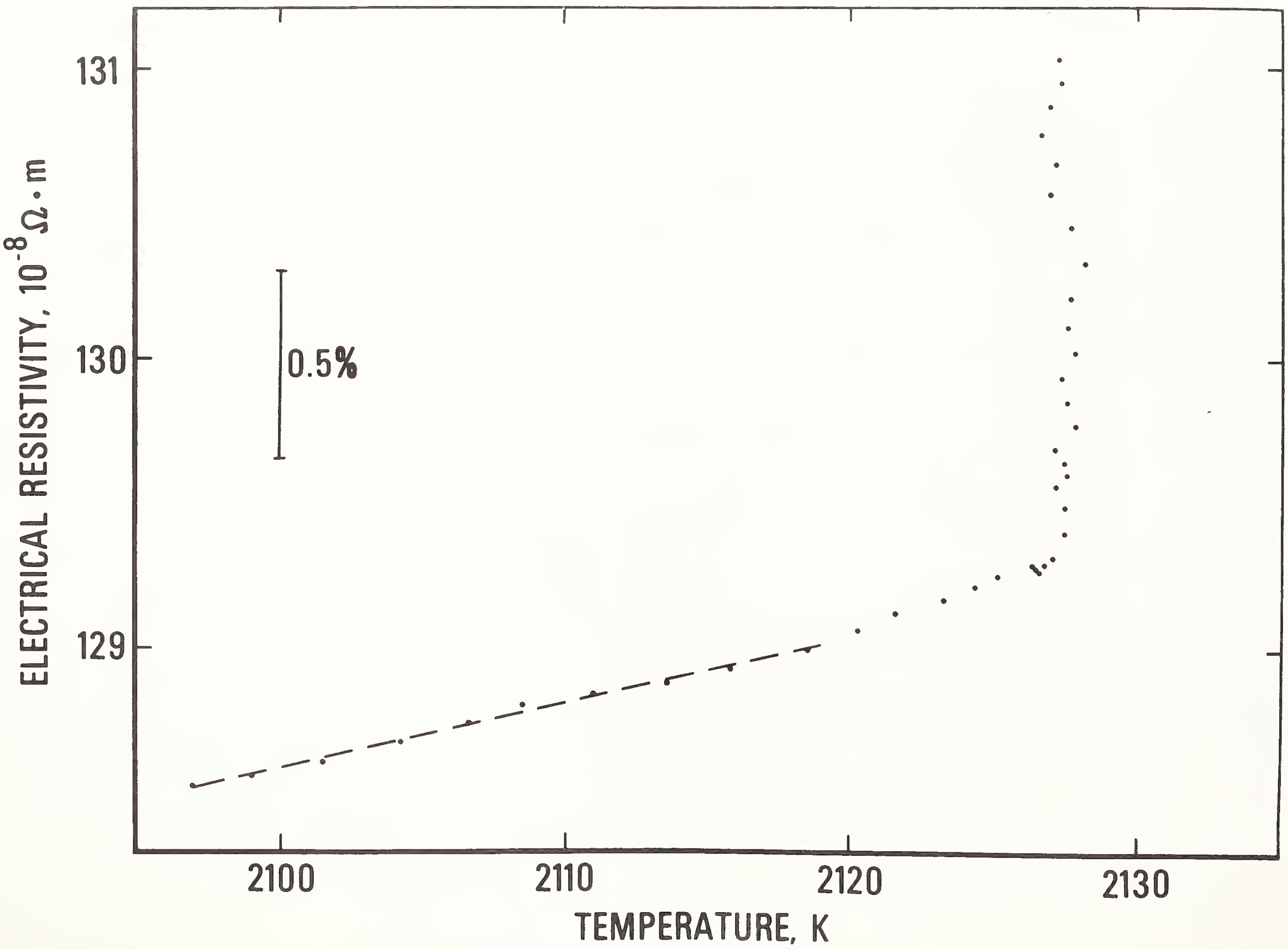

Figure 5. Variation of electrical resistivity of zirconium (specimen II) as a function of temperature near and at the melting point.

A summary of the results on imprecision[1] and inaccuracy[2] of some of the measured and computed quantities is given in table 3.

It may be seen from table 3 that the imprecision of blackbody temperature measurements during heating of the specimen (before reaching the melting point) was approximately the same as that during the melting period. This indicates that in the experiment the initial melting phase progressed normally and that there were no undesirable effects during melting of the specimen, such as vibration of the specimen, movement of the blackbody sighting hole in the specimen, and the instantaneous development of hot spots or zones in the specimen. Also the imprecision of the radiance temperature measurements was the same as that of blackbody temperature measurements, which indicates that the surface conditions of the specimen did not change in a random fashion during the melting period.

5. Discussion

The values of the melting point of zirconium reported in the literature are given in table 4. No large discrepancies are found: all values are within the combined inaccuracies of the measurements. There

---

[1] Imprecision refers to the standard deviation of an individual point as computed from the difference between measured value and that from the smooth function obtained by the least squares method.

[2] Inaccuracy refers to the estimated total error (random and systematic).

Table 3

Imprecision and inaccuracy of measured and computed quantities

Quantity	Imprecision	Inaccuracy
Temperature: blackbody (during heating)	0.5 K	5 K
Temperature: blackbody (during melting)	0.5 K	5 K
Temperature: radiance (during melting)	0.3 K	5 K
Voltage	0.03%	0.1%
Current	0.03%	0.1%
Melting point of zirconium	0.5 K	8 K
Radiance temperature of zirconium at its melting point	0.3 K	8 K
Normal spectral emittance	0.3%	3%
Electrical resistivity	0.05%	3%

Table 4

Values of the melting point of zirconium reported in the literature

Investigator	Reference	Year	Temperature[a] (K)	Imprecision[b] (K)	Inaccuracy[b] (K)
deBoer and Fast	12	1930	2128		
Adenstedt	13	1952	2116		25
Oriani and Jones	14	1954	2128	2	
Williams	15	1955	2136	10	
Deardorff and Hayes	16	1956	2131	3	15
Sara	17	1965	2136		18
Ackermann and Rauh	18	1972	2134	4	
Present work			2128	0.5	8

[a] All temperatures reported in the original references are converted to IPTS-68.

[b] As reported by the authors of the original papers.

are indications that the specimens used in some of the earlier measurements were less pure than those used in the present study. Some of the high values may be attributed to relatively large hafnium (melting point about 2500 K) content of the specimens.

Normal spectral emittance (at 0.645 nm) of zirconium at its melting point is reported to be 0.318 [19]; this is approximately 13% lower than the value obtained in this work. Since in both cases, the same value for the melting point was considered, the difference in emittance may be attributed to the difference in radiance temperature at the melting point, which is 22 K. No satisfactory explanation for this large discrepancy has been found.

In an earlier publication [11], measurements of the electrical resistivity of zirconium were reported for temperatures up to 2100 K. At 2100 K the difference between the present value and that reported earlier is approximately 0.1%. Electrical resistivity of zirconium up to 2000 K were reported by Peletskii et al. [20] and by Zhorov [21]. Extrapolation of those results to 2100 K give the values 127.9×10^{-8} $\Omega\cdot$m and 132.0×10^{-8} $\Omega\cdot$m, respectively. The results of this work differ from the extrapolated values by 0.7% in the case of Peletskii et al. [20] and by 2.6% in the case of Zhorov [21]. Electrical resistivity behaved normally until approximately 5-10 K below the melting point (figure 5). Above this, a departure from normalcy was observed which may be due to: (a) premelting effects of impurities present in the specimen, and (b) increase in vacancy concentration. Small temperature gradients in the specimen also may partially account for this.

As it may be noted from table 2, the linear fitting of radiance temperatures at the plateau shows a bias toward positive slopes. Two possible explanations may be given for this gradual increase: (a) a small change in the normal spectral emittance of zirconium during melting, and (b) partial formation of zirconium oxide on the specimen surface, due to the high chemical reactivity of zirconium. It may be noted that, with the present system, it was not possible to follow the entire melting process because the specimen collapsed and opened the main electrical circuit prior to the completion of melting. Approximate calculations in the case of zirconium strips indicate that approximately one third of the specimen was melted during the experiment.

In conclusion, the results of this study have yielded new values for the melting point and the electrical resistivity of zirconium above 2100 K, and have shown the constancy and reproducibility of the radiance temperature of zirconium at its melting point. The scheme of measuring radiance temperature at the melting point, so far demonstrated for niobium [5] and zirconium, may be an easy, accurate and practical way for performing secondary calibrations and for conducting overall on-the-spot checks on complicated measurements systems at high temperatures.

Acknowledgement

The authors express their gratitude to C. W. Beckett for his encouragement of research in high-speed thermophysical measurements and to M. S. Morse for his help with the electronic instrumentation.

6. References

1. A. Cezairliyan, M. S. Morse, H. A. Berman and C. W. Beckett. - High-speed (subsecond) measurement of heat capacity, electrical resistivity, and thermal radiation properties of molybdenum in the range 1900-2800 K. J. Res. Nat. Bur. Stand. (U.S.), 1970, 74A (Phys. and Chem.), 65-92.

2. A. Cezairliyan, M. S. Morse and C. W. Beckett. - Measurement of melting point and electrical resistivity (above 2840 K) of molybdenum by a pulse heating method. Rev. Int. Hautes Tempér. et Réfract., 1970, 7, 382-388.

3. A. Cezairliyan. - Measurement of melting point and electrical resistivity (above 3600 K) of tungsten by a pulse heating method. High Temp. Science, 1972, 4, 248-252.

4. A. Cezairliyan. - Measurement of melting point, normal spectral emittance (at melting point), and electrical resistivity (above 2650 K) of niobium by a pulse heating method. High Temp.-High Press., 1972, 4, 453-458.

5. A. Cezairliyan. - Radiance temperature of niobium at its melting point. J. Res. Nat. Bur. Stand. (U.S.), 1973, 77A (Phys. and Chem.), 333-339.

6. G. M. Foley. - High-speed optical pyrometer. Rev. Sci. Instr., 1970, 41, 827-834.

7. A. Cezairliyan. - Design and operational characteristics of a high-speed (millisecond) system for the measurement of thermophysical properties at high temperatures. J. Res. Nat. Bur. Stand. (U.S.), 1971, 75C (Eng. and Instrum.), 7-18.

8. International Committee for Weights and Measures. - The International Practical Temperature Scale of 1968. Metrologia, 1969, 5, 35-44.

9. R. F. Domagala and D. J. McPherson. - System zirconium-oxygen. Trans. AIME, 1954, 200, 238-246.

10. A. Cezairliyan and F. Righini. - Thermodynamic studies of the $\alpha \rightarrow \beta$ phase transformation in zirconium using a subsecond pulse heating technique. J. Res. Nat. Bur. Stand. (U.S.), in press.

11. A. Cezairliyan and F. Righini. - Simultaneous measurements of heat capacity, electrical resistivity and hemispherical total emittance by a pulse heating technique: zirconium, 1500 to 2100 K. J. Res. Nat. Bur. Stand. (U.S.), 1974, 78A (Phys. and Chem.), in press.

12. J. H. deBoer and J. D. Fast. - Über die darstellung der reinen metalle der titangruppe durch thermische zersetzung ihrer jodide. III. Hafnium. Z. anorg. u. allg. Chem., 1930, 187, 193-208.

13. H. K. Adenstedt. - Physical, thermal and electrical properties of hafnium and high purity zirconium. Trans. A.S.M., 1952, 44, 949-973.

14. R. A. Oriani and T. S. Jones. - An apparatus for the determination of the solidus temperatures of high-melting alloys. Rev. Sci. Instr., 1954, 25, 248-250.

15. J. T. Williams. - Vanadium-zirconium alloy system. Trans. AIME, 1955, 203, 345-350.

16. D. K. Deardorff and E. T. Hayes. - Melting point determination of hafnium, zirconium, and titanium. Trans. AIME, 1956, 206, 509-511.

17. R. V. Sara. - The system zirconium-carbon. J. Am. Cer. Soc., 1965, 48, 243-247.

18. R. J. Ackermann and E. G. Rauh. - Determination of liquidus curves for the Th-W, Th-Ta, Zr-W, and Hf-W systems: the anomalous behavior of metallic thorium. High Temp. Science, 1972, 4, 272-282.

19. D. W. Bonnell, J. A. Treverton, A. J. Valerga, and J. L. Margrave. -"The emissivities of liquid metals at their fusion temperatures". in Temperature - its measurement and control in science and industry. H. H. Plumb ed. Vol. 4, part 1 (ISA, Pittsburgh,1972), pp. 483-487.

20. V. É. Peletskii, V. P. Druzhinin and Ya. G. Sobol'. - Emissivity, thermal conductivity, and electrical conductivity of remelted zirconium at high temperatures. High Temp., 1970, 8, 732-736.

21. G. A. Zhorov. - Emissivity of metals of the IVb subgroup at high temperatures. High Temp., 1970, 8, 501-504.

Thermodynamic Studies of the $\alpha \rightarrow \beta$ Phase Transformation in Zirconium Using a Subsecond Pulse Heating Technique [*]

A. Cezairliyan and F. Righini[**]
Institute for Materials Research
National Bureau of Standards
Washington, D. C. 20234

Abstract

Measurements of the temperature and energy of the $\alpha \rightarrow \beta$ phase transformation, and the electrical resistivity near and at the transformation point of zirconium using a subsecond duration pulse heating technique are described. The results yield 1147 K for the transformation temperature and 3980 $J \cdot mol^{-1}$ for the transformation energy. Electrical resistivity is found to decrease by 17% during the transformation. Estimated inaccuracies of the measured properties are: 10 K for the transformation temperature, 5% for the transformation energy, and 2% for the electrical resistivity.

---

[*] This work was supported in part by the U. S. Air Force Office of Scientific Research.

[**] Guest scientist from the Istituto di Metrologia "G. Colonnetti" in Torino, under a fellowship from the Consiglio Nazionale delle Ricerche of Italy.

1. Introduction

In another publication [1][1], the applicability of a rapid pulse heating technique to studies of solid-solid phase transformations at high temperatures was demonstrated by measurements on iron at the $\gamma \rightarrow \delta$ transformation point.

The objective of this paper is to apply the same technique to studies of the $\alpha \rightarrow \beta$ phase transformation in zirconium. Measurements of the temperature and energy of the phase transformation, and electrical resistivity near and at the transformation point are reported.

The method is based on rapid resistive self-heating of the specimen from room temperature to high temperatures in less than one second by the passage of an electrical current pulse through it; and on measuring, such experimental quantities as current through the specimen, potential drop across the specimen, and specimen temperature. Recordings of the experimental quantities are made digitally every 0.4 ms with a full-scale signal resolution of approximately one part in 8000. Specimen temperature is measured with a high-speed photoelectric pyrometer [2]. The details regarding the construction and operation of the measurement system are given in earlier publications [3, 4].

---

[1] Figures in brackets indicate the literature references at the end of this paper.

2. Measurements

The measurements were made on three zirconium specimens of 99.98% purity. The specimens were tubes fabricated from rods by removing the center portion using an electro-erosion technique. The nominal dimensions of the specimens were: length, 76.2 mm; outside diameter, 6.3 mm; and wall thickness, 0.5 mm. The outer surfaces of the specimens were polished to reduce heat loss due to thermal radiation. According to the manufacturer's analysis, the specimens contained the following impurities, in ppm by weight: O, 125; Hf, 40; Fe, 30; C, 6; H, 3.3; Al, 3; N, 2.1; Ni and Si, 1.5 each; and Ti, 1. The total amount of all other detected elements was less than 6 ppm, each element being below 1 ppm limit.

Duration of the current pulses ranged from 220 to 620 ms. Specimen heating rates varied from 1800 $K \cdot s^{-1}$ to 4000 $K \cdot s^{-1}$. All the experiments were conducted with the specimens in a vacuum environment of approximately 1.3×10^{-3} $N \cdot m^{-2}$ ($\sim 10^{-5}$ torr).

The $\alpha \rightarrow \beta$ transformation (from hexagonal close-packed form to body-centered cubic) was manifested by a plateau in the temperature versus time relation for the specimen during heating. The transformation temperature for each specimen was obtained by averaging the temperatures at the plateau.

The transformation energy was obtained from the time integral of the power absorbed by the specimen during the transformation as defined by the plateau. The instantaneous value of the absorbed power was obtained by subtracting the power loss due to thermal radiation from the imparted power (current through the specimen times the potential drop across the specimen). The hemispherical total emittance needed at 1147 K was obtained from the extrapolation of the measurements above 1500 K reported in an earlier publication [5]. Since at the transformation temperature power loss from the specimen due to thermal radiation was approximately 0.7% of the imparted power, even considerable uncertainties (10%) in the emittance do not contribute any significant errors to the absorbed power.

3. Experimental results

Except where explicitly noted, all temperatures reported in this paper are based on the International Practical Temperature Scale of 1968 [6]. In all computations, the geometrical quantities are based on their dimensions at room temperature (298 K). The experimental results for the temperature and energy of the α → β phase transformation are presented in table 1.

The average value for the transformation temperature is 1146.6 K with a maximum and average absolute difference from this value of 1.8 K and 1.2 K, respectively. The average value for the transformation energy is 3977 $J \cdot mol^{-1}$ with a maximum and average absolute difference from this value of 0.4% and 0.3%, respectively. It may be concluded that for α → β transformation in zirconium, the transformation temperature

Table 1

Results for the $\alpha \rightarrow \beta$ transformation temperature and transformation energy of zirconium

Specimen Number	Heating rate[a] ($K \cdot s^{-1}$)	Number of Temperatures[b]	Transformation Temperature (K)	Standard Deviation[c] (K)	Transformation Energy ($J \cdot mol^{-1}$)
1	4000	27	1144.9	3.4	3993
2	1600	61	1148.4	3.2	3970
3	3100	47	1146.6	3.4	3968

[a] Evaluated approximately 50 K below the transformation point.

[b] Number of temperatures at the plateau used to obtain the average transformation temperature for a specimen.

[c] Standard deviation of an individual temperature at the plateau from the average transformation temperature for a specimen.

is 1147 K and the transformation energy is 3980 $J \cdot mol^{-1}$.

As discussed in an earlier publication [5], the measurements of the geometrical quantities of a zirconium specimen after a number of experiments indicated permanent distortions (elongation) due to repeated heating and cooling through the transformation point. The values reported in this paper correspond to the first experiment for a specimen for which no correction was needed.

Typical experimental results are presented in figures 1, 2, and 3, all referring to specimen 3. Specimen temperature near and at the transformation point is shown in figure 1. Figure 2 shows the variation of electrical resistivity as a function of time, while the variation of resistivity with temperature is shown in figure 3. The dashed lines in figure 3 are the best least squares fittings of the resistivity versus temperature data in the respective regions. It may be seen that the change in the electrical resistivity ($100(\rho_{before} - \rho_{after})$ during the transformation was about 17%. Extrapolation of the resistivity values about the transformation to 1500 K is in agreement, within 0.3%, with those reported in an earlier publication [5].

The details for estimating errors in measured and computed quantities using the present measurement system are given in an earlier publication [4]. In this paper the specific items were recomputed whenever the present conditions differed from those in the earlier publication.

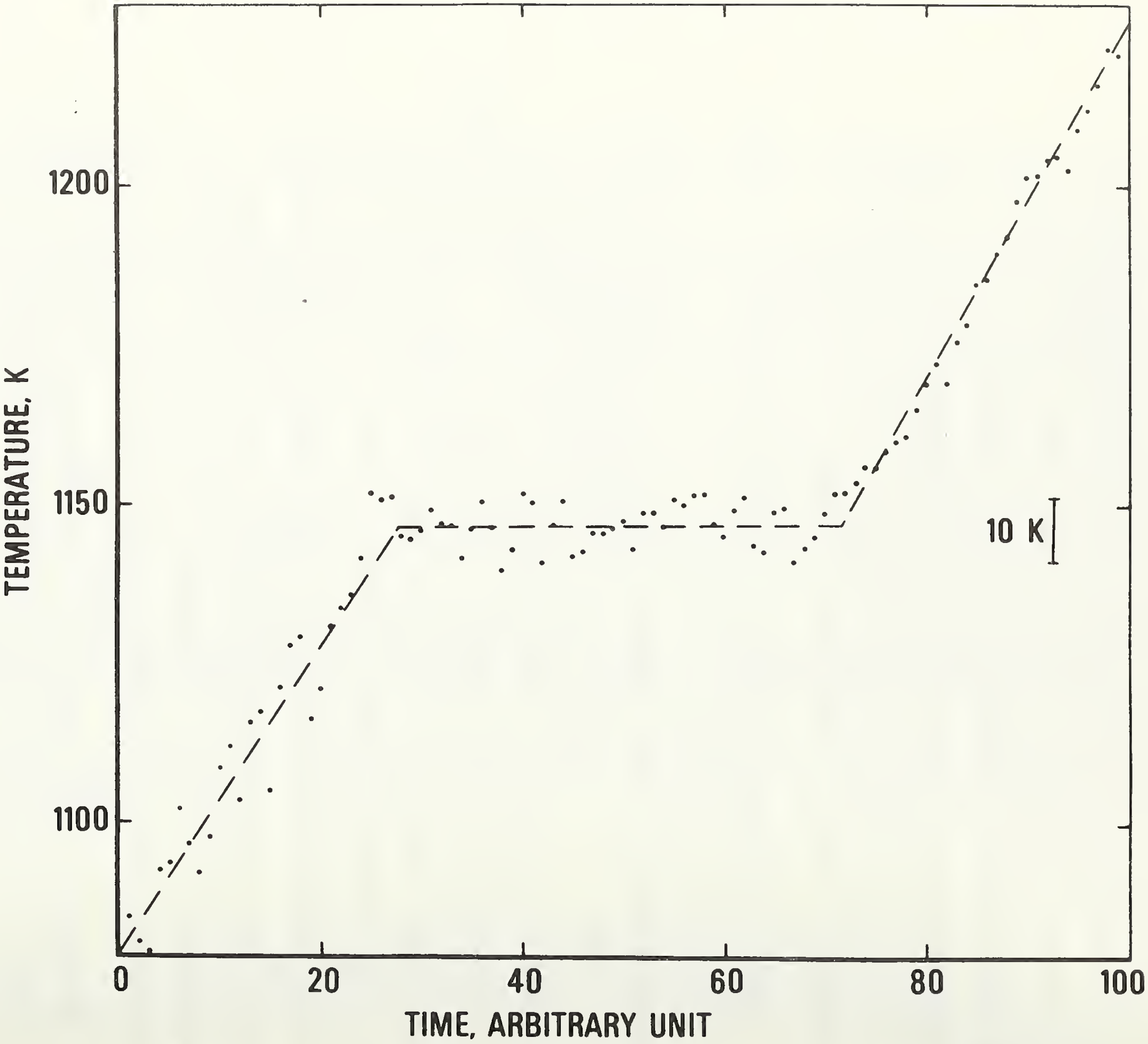

Figure 1. Variation of temperature as a function of time, near and at the transformation point of zirconium.

(The curve refers to specimen 3; 1 time unit = 0.833 ms).

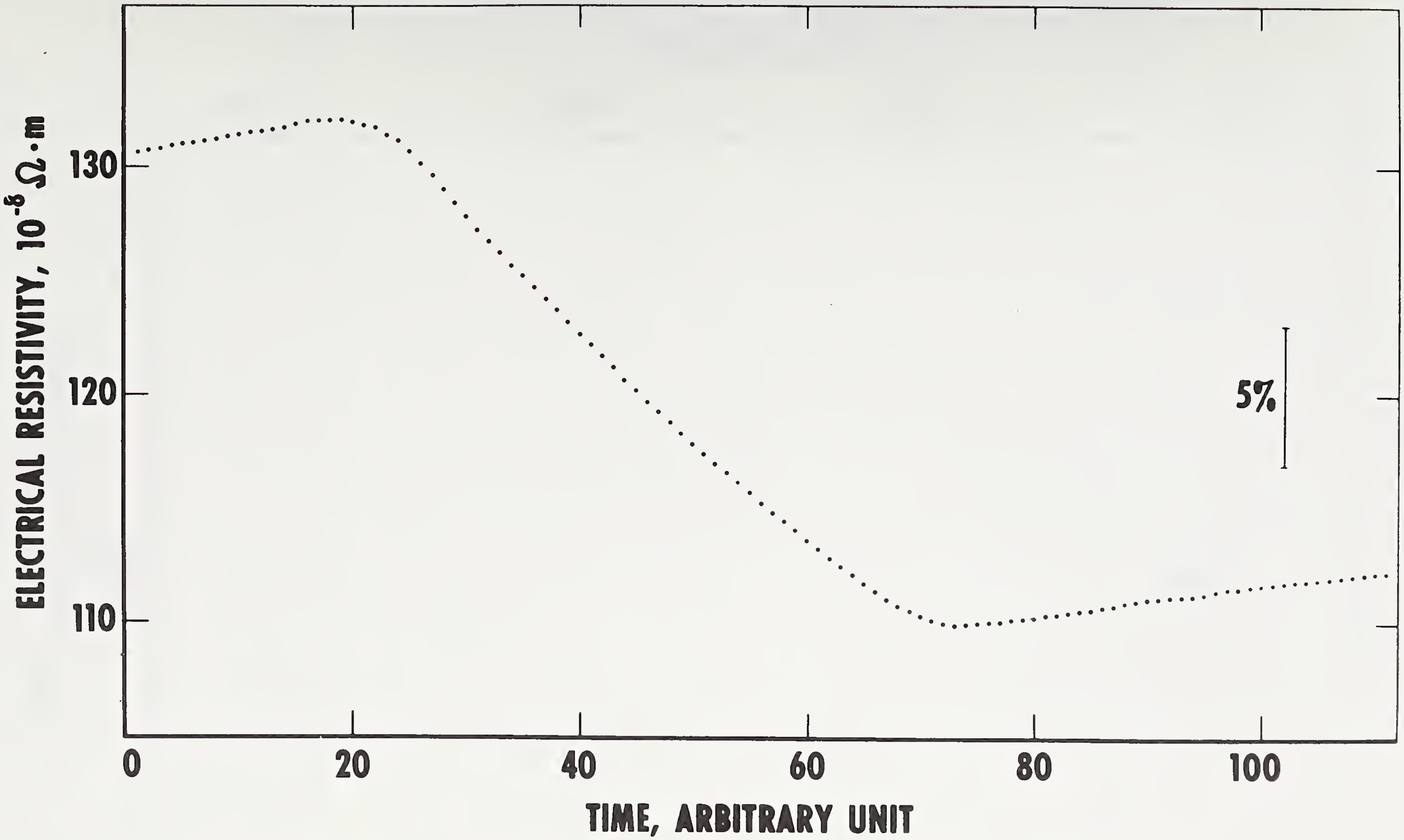

Figure 2. Variation of resistivity as a function of time near and at the transformation point of zirconium.

(The curve refers to specimen 3; 1 time unit = 0.833 ms).

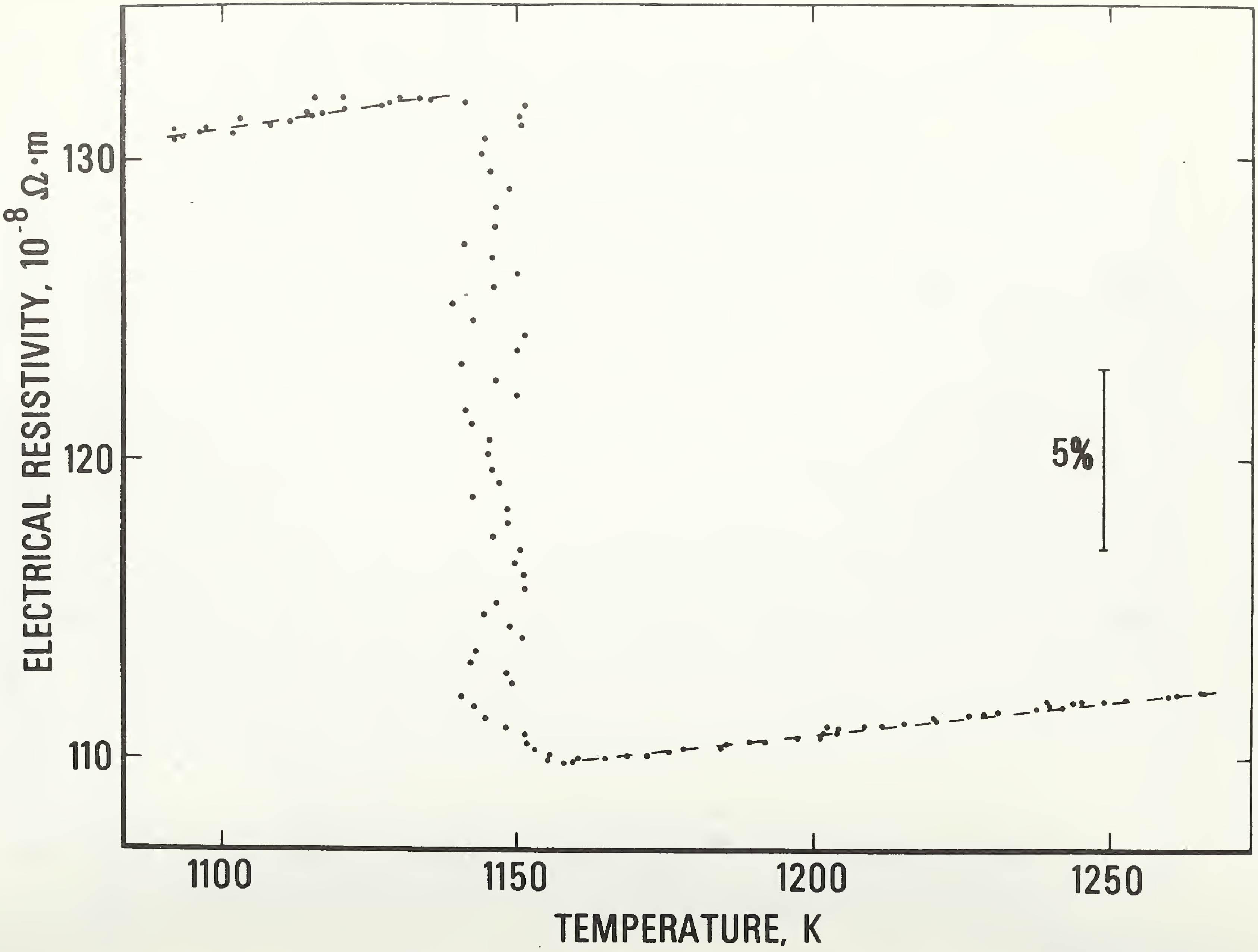

Figure 3. Variation of resistivity as a function of temperature near and at the transformation point of zirconium..

The results for imprecision[2] and inaccuracy[3] are: 3 K and 10 K for the transformation temperature, 1% and 5% for the transformation energy, and 0.5% and 2% for the electrical resistivity.

In the case of temperature, the standard deviation of an individual point from the average transformation temperature in a given experiment is approximately 3 K. For the three experiments, the average absolute difference of transformation temperatures from their mean is 1.2 K. In the case of energy, the imprecision includes the uncertainty in the computation of the time duration of the transformation plateau. Different ways in selecting temperature points belonging to heating or plateau regions lead to average energy differences of 0.6%.

4. Discussion

The first evidence of a possible solid-solid phase transformation in zirconium was presented by Zwikker in 1926 [7]. Since his experiments were performed on zirconium heated in air, the transformation occurred over an extended temperature range. A sharp transformation was reported by Vogel and Tonn [8] from dilatometric and metallographic measurements and was confirmed by de Boer et al. [9], who noted that the temperature

---

[2] Imprecision refers to the standard deviation of an individual point as computed from the difference between measured value and either the average or the smooth function obtained by the least squares method.

[3] Inaccuracy refers to the estimated total error (random and systematic).

range was extended by small amounts of oxygen and nitrogen in zirconium. The values for the $\alpha \rightarrow \beta$ transformation temperature for zirconium reported in the literature are given in table 2. Some of the old results could not be corrected to IPTS-68, due to insufficient information in the original papers. However, the contribution of the possible differences in the temperature scales may not exceed a few degrees at the transformation temperature.

The present value for the transformation temperature is higher than most of the values given in the literature. This may partly be due to the high heating rates used in this work. A similar effect, though in the opposite direction, was observed by Duwez [10] in experiments on rapid quenching of zirconium specimens (cooling rates from 4 to 10,000 $K \cdot s^{-1}$). The transformation temperature was found to decrease with increasing cooling rate by as much as 15 K. This behavior was confirmed by Hayes and Kaufman [15]. The result of the energy of transformation of zirconium obtained in this work (3980 $J \cdot mol^{-1}$) is 6% higher than the value (3740 $J \cdot mol^{-1}$) of Douglas and Victor [14], 3% higher than the value (3850 $J \cdot mol^{-1}$) of Coughlin and King [16], and 0.1% higher than the most recent value (3975 $J \cdot mol^{-1}$) of Vollmer et al. [13].

The general trend of the behavior of electrical resistivity near and at the transformation point of zirconium is as follows (figures 2 and 3). Resistivity reaches a maximum about 10 K below the transformation point, then it decreases slightly and undergoes a large change (decrease) at the transformation point, after which it decreases some more and

Table 2

Values of the α-β transformation temperature of zirconium reported in the literature

Investigator	Reference	Year	Temperature[a] (K)
Vogel and Tonn	8	1931	1135 ± 5
de Boer et al.	9	1936	1138 ± 10
Duwez	10	1951	1123 to 1138
Domagala and McPherson	11	1954	1135
Kneip and Betterton	12	1956	1138 to 1146
Vollmer et al.	13	1967	1155
Present work			1147 ± 10

[a] All temperatures in this table are those reported by the authors of the original papers. No correction to IPTS-68 was possible, due to insufficient information in the original papers.

reaches a minimum at about 5-10 K above the transformation point. Above this minimum, resistivity increases with temperature almost linearly.

Because of the strong dependence of the electrical resistivity on composition for zirconium at the transformation point, it is difficult to compare resistivity values reported in the literature on an absolute basis. However, a meaningful comparison may be made based on the ratio of the maximum to the minimum resistivities for a given specimen. The results of such a comparison are given in table 3. High values for the ratio and small temperature range during which transformation is completed are indications of the high purity of the specimens.

Acknowledgement

The authors express their gratitude to C. W. Beckett for his encouragement of research in high-speed thermophysical measurements and to M. S. Morse for his help with the electronic instrumentation.

Table 3

Change of the electrical resistivity of zirconium during the $\alpha \rightarrow \beta$ transformation reported in the literature

Investigator	Reference	Year	Temperature[a] of maximum resistivity (K)	Temperature[a] of minimum resistivity (K)	Ratio, $\frac{\rho_{max}}{\rho_{min}}$
Zwikker	7	1926	1150	1430	1.14
de Boer et al.	9	1936	1130	1145	1.19
Squire and Kaufman	17	1941	1067	1142	1.12
Adenstedt	18	1952	1118	1143	1.20
Rogers and Atkins	19	1955	1127	1173	1.19
Powell and Tye	20	1961	1129	1177	1.18
Present work			1134	1158	1.20

[a] All values in this table are based on the results reported by the authors of the original papers. No correction of values to IPTS-68 was possible, due to insufficient information in the original papers.

5. References

[1] Cezairliyan, A. and McClure, J. L., A subsecond pulse heating technique for the study of solid-solid phase transformations at high temperatures: application to iron. in preparation.

[2] Foley, G. M., High-speed optical pyrometer. Rev. Sci. Instr., 41, 827 (1970).

[3] Cezairliyan, A., Design and operational characteristics of a high-speed (millisecond) system for the measurement of thermophysical properties at high temperatures. J. Res. Nat. Bur. Stand. (U.S.), 75C (Eng. and Instr.), 7 (1971).

[4] Cezairliyan, A., Morse, M. S., Berman, H. A., and Beckett, C. W., High-speed (subsecond) measurement of heat capacity, electrical resistivity, and thermal radiation properties of molybdenum in the range 1900 to 2800 K. J. Res. Nat. Bur. Stand. (U.S.), 74A (Phys. and Chem.), 65 (1970).

[5] Cezairliyan, A. and Righini, F., Simultaneous measurements of heat capacity, electrical resistivity and hemispherical total emittance by a pulse heating technique: zirconium, 1500 to 2100 K. J. Res. Nat. Bur. Stand. (U.S.), 78A (Phys. and Chem.), in press.

[6] International Practical Temperature Scale of 1968. Metrologia, 5, 35 (1969).

[7] Zwikker, C., Modificatieveranderingen bij zirkoon en hafnium. Physica, 6,361 (1926).

[8] Vogel, R. and Tonn, W., Über einen umwandlungspunkt des zirkons. Z. anorg. allgem. Chem., 202, 292 (1931).

[9] de Boer, J. H., Clausing, P. and Fast, J. D., The α-β transition with mechanically treated and with untreated zirconium. Rec. Trav. Chim., 55, 450 (1936).

[10] Duwez, P., Effect of rate of cooling on the alpha-beta transformation in titanium and titanium-molybdenum alloys. Trans. AIME, 191, 765 (1951).

[11] Domagala, R. F. and McPherson, D. J., System zirconium-oxygen. Trans. AIME, 200, 238 (1954).

[12] Kneip, G. D. and Betterton, Jr., J. O., Floating zone purification of zirconium. J. Electrochem. Soc., 103, 684 (1956).

[13] Vollmer, O., Braun, M. and Kohlhaas, R., Die Atomwärme des Zirkons zwischen 300 und 1700 K. Z. Naturforsch., 22, 833 (1967).

[14] Douglas, T. B. and Victor A. C., Heat content of zirconium and of five compositions of zirconium hydride from 0 to 900°C. J. Res. Nat. Bur. Stand., 61, 13 (1958).

[15] Hayes, E. E. and Kaufmann, A. R., "Observations on the alpha-beta transformation in zirconium" in Zirconium and Zirconium Alloys, p. 241 (American Society for Metals, Cleveland, Ohio 1953).

[16] Coughlin, J. P., and King, E. G., High-temperature heat contents of some zirconium - containing substances. J. Am. Chem. Soc., 72, 2262 (1950).

[17] Squire, C. F. and Kaufmann, A. R., The magnetic susceptibility of Ti and Zr. J. Chem. Phys., 9, 673 (1941).

[18] Adenstedt, H. K., Physical, thermal and electrical properties of hafnium and high purity zirconium. Trans. A.S.M., 44, 949 (1952).

[19] Rogers, B. A. and Atkins, D. F., Zirconium-columbium diagram. Trans. AIME, 203, 1034 (1955).

[20] Powell, R. W. and Tye, R. P., The thermal and electrical conductivities of zirconium and of some zirconium alloys. J. Less-Common Metals, 3, 202 (1961).

Chapter 6

RADIANCE TEMPERATURE (at 650 nm) OF MOLYBDENUM AT ITS MELTING POINT

Ared Cezairliyan
National Bureau of Standards
Washington, D. C. 20234

Measurements of the radiance temperature (at 650 nm) of molybdenum (99.95 percent pure) at its melting point were performed on 14 specimens in the form of strips. The nominal dimensions of the strips were: length, 50.8 mm; width, 4.7 mm and thickness, 0.24 mm. Before the experiments, specimen surface was treated using abrasive ; three different grades of abrasive were used yielding three different surface roughnesses (ranging from approximately 0.2 to 0.5 μm) for different specimens.

All the experiments were performed with the specimen in an argon environment at atmospheric pressure. The heating rates for different specimens were in the range 1200 $K \cdot s^{-1}$ to 3500 $K \cdot s^{-1}$, corresponding to specimen heating periods (from room temperature to the melting point) in the range 0.4 - 1 s.

Radiance temperature of molybdenum at its melting point for the 14 specimens and other pertinent results are reported in Table 1. The variation of radiance temperature as a function of time near and at the melting point is shown in Figure 1 for three typical experiments representing three specimens with different initial surface conditions. The magnitude of the spike before the melting plateau for the specimens is related to the degree of initial surface roughness of the specimens. However, regardless of the initial surface and operational conditions, radiance temperature at the melting plateau is approximately the same for all the specimens. Temperature of the spike in all the experiments ranged from 4 to 16 K above the plateau temperature.

A single value for the radiance temperature at the plateau for each specimen was obtained by averaging the measured values of the temperatures at the plateau. The number of measurements used for averaging ranged from 25 to 99, depending both on the heating rate and on the behavior of the specimen during melting. The standard deviation of an individual measurement from the average was in the range 0.3 to 0.4 K for all the experiments. Similar values (for standard deviation) were obtained when fitting the temperature data corresponding to the premelting period to a quadratic function in time. This indicates that during melting no undesirable effects took place, such as vibration of the specimen, development of hot spots in the specimen and random changes in the specimen surface conditions.

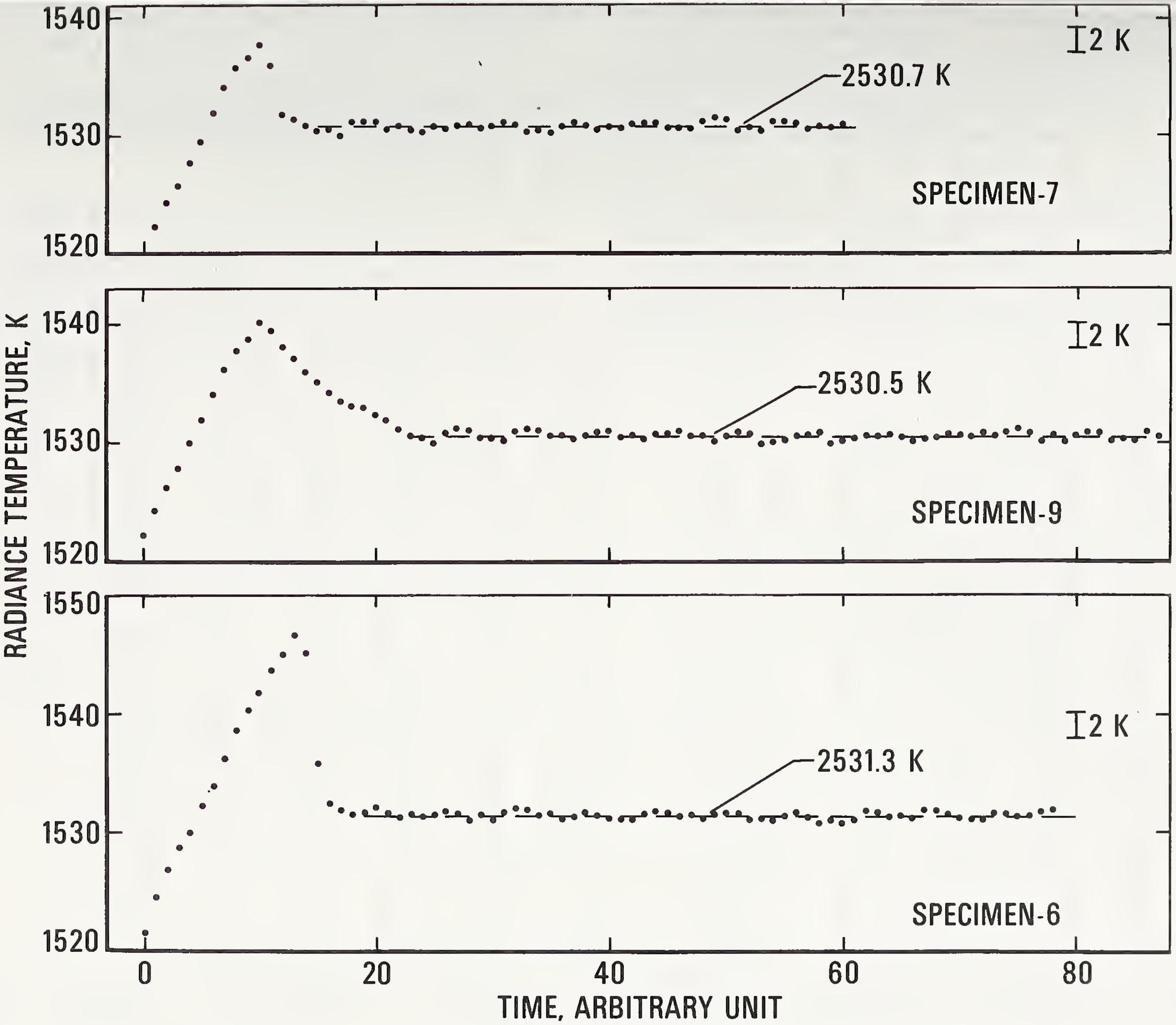

Figure 1. Variation of radiance temperature (at 650 nm) of molybdenum as a function of time near and at its melting point for three typical experiments (1 time unit = 0.833 ms).

Table 1

Summary of experiments for the measurement of radiance temperature (at 650 nm) of molybdenum during melting

		Premelting period		Melting period				
Specimen number[a]	Surface roughness[b]	Heating rate[c] K · s-1	Standard deviation[d] K	Number of temperatures[e]	Slope at plateau[f] K · s-1	Plateau temp. difference[g] K	Radiance temperature[h] K	Standard deviation[i] K
1	B	3500	0.3	39	8.9	0.3	2530.6	0.3
2	B	3400	0.2	32	-8.2	-0.2	2529.3	0.3
3	C	3300	0.3	49	-3.7	-0.2	2530.5	0.3
4	A	3300	0.3	25	0	0	2530.2	0.2
5	B	2500	0.3	67	6.6	0.4	2530.7	0.3
6	C	2500	0.4	58	0	0	2531.3	0.3
7	A	2400	0.4	47	5.6	0.2	2530.7	0.3
8	A	2400	0.3	75	0	0	2530.4	0.3
9	B	2500	0.3	78	0	0	2530.5	0.3
10	C	2500	0.3	48	9.3	0.4	2529.2	0.4
11	A	2400	0.4	45	7.7	0.3	2530.7	0.3
12	B	1200	0.4	99	0	0	2530.4	0.4
13	A	2600	0.4	28	0	0	2530.7	0.4
14	A	2500	0.4	51	11	0.5	2530.9	0.4

[a] Also represents the experiments in chronological order.

[b] The notations used for surface conditions correspond to the following typical roughnesses in μm: A, 0.23; B, 0.38; C, 0.53.

[c] Heating rate evaluated at a temperature approximately 10 K below the melting point.

[d] Represents standard deviation of an individual temperature as computed from the difference between the measured value and that from the smooth temperature versus time function (quadratic) obtained by the least squares method. Data extend approximately 100 K below the melting point.

[e] Number of temperatures used in averaging the results at the plateau to obtain an average value for the radiance temperature at the melting point of the specimen.

[f] Derivative of the temperature versus time function obtained by fitting the temperature data at the plateau to a linear function in time using the least squares method.

[g] Maximum radiance temperature difference between the beginning and the end of the plateau based on the linear temperature versus time function.

[h] The average (for a specimen) of measured radiance temperatures at the plateau.

[i] Standard deviation of an individual temperature as computed from the difference between the measured value and that from the average plateau radiance temperature.

To determine the trend of measured temperatures at the plateau, temperatures for each experiment were fitted to a linear function in time using the least squares method. The detailed results are reported in Table 1. The temperature difference between the beginning and the end of the plateau (corresponding to the slope in the plateau) is in the range 0 – 0.5 K. The standard deviation of an individual temperature from the linear function was approximately the same as the standard deviation obtained by direct averaging of the temperatures.

The average radiance temperature at the melting point for the 14 molybdenum specimens was 2530.4 K with a standard deviation of 0.6 K and a maximum absolute difference of 1.2 K. The results are presented in Figure 2. It may be noted that the maximum absolute difference of the results for the specimens with condition A surfaces (least rough) is only 0.7 K. The two experiments (corresponding to specimen-2 and specimen-10) with relatively large negative deviations (about -1.1 K and -1.2 K) have caused a downward shift of the average by about 0.2 K. In order to reduce the contribution of these two experiments, the average temperature is rounded-off to the higher value. This is also compatible with the average (2530.6 K) of the results for the specimens with condition A surfaces. It may be concluded that the radiance temperature of molybdenum at its melting point is 2531 K, with an estimated inaccuracy of 10 K.

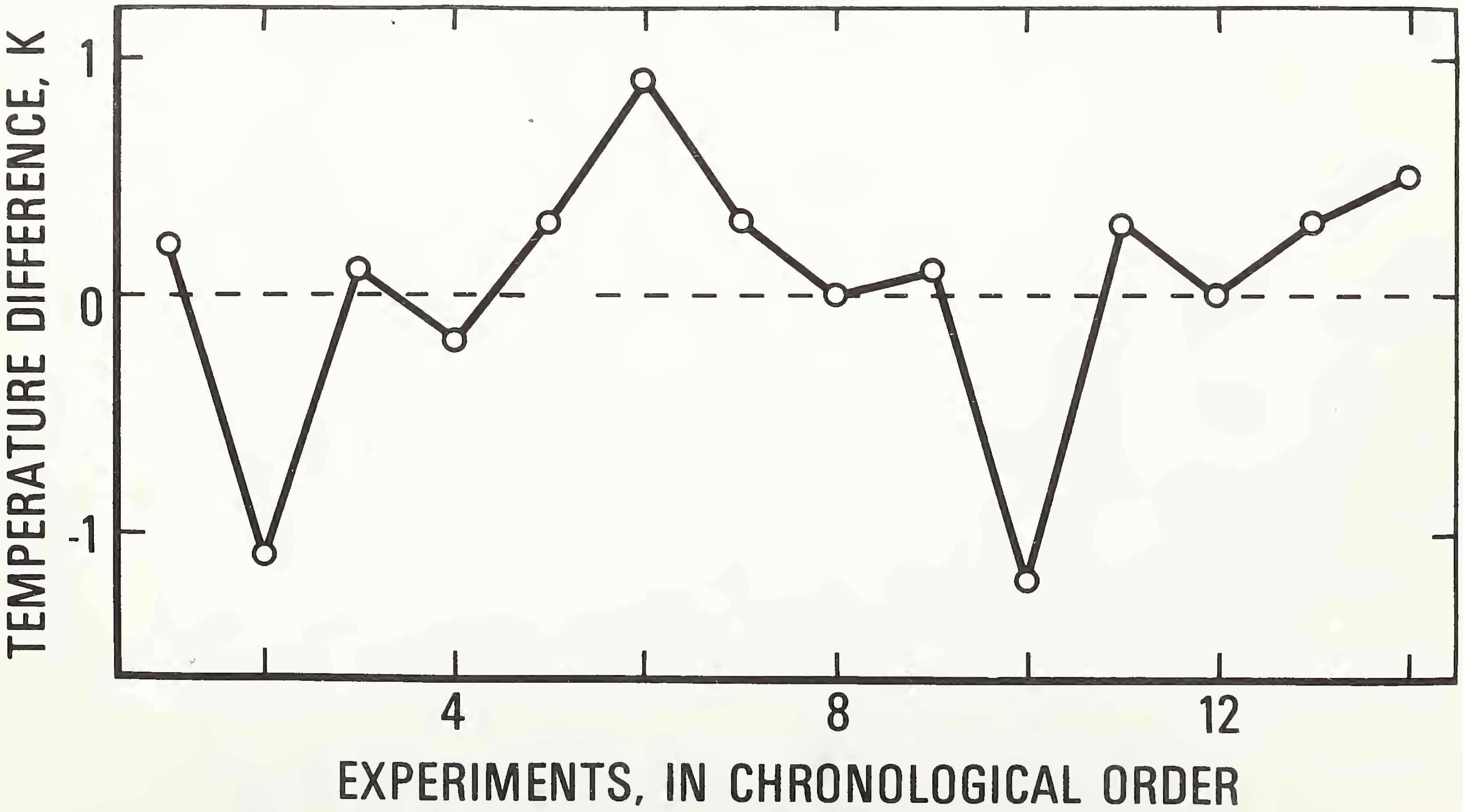

Figure 2. Difference of radiance temperature (at the melting point of molybdenum, at 650 nm) for individual experiments from their average value of 2530.4 K (represented by the "zero" line).

The radiance temperature (2531 K) and the melting point (2894 K) measured with the present system [1] yield a value of 0.334 for the normal spectral emittance (at 650 nm) of molybdenum at its melting point.

Several additional experiments were conducted on molybdenum in "as received" condition. The results of these experiments were generally 3-5 K higher than the value 2531 K. The higher values might be attributed to contamination on the specimen surface. Because of the high vapor pressure of molybdenum at its melting point, it was not possible to conduct meaningful experiments with the specimen in a vacuum environment.

Bonnell et al. [2] have reported a value of 2510 K for the radiance temperature (at 645 nm) of molybdenum (99.9 percent pure) at its melting point. No satisfactory explanation for the large discrepancy (21 K) between the result of Bonnell et al. and that of the present work has been found. In the past [3, 4], differences of the same magnitude and direction were also noted in the results obtained by the two laboratories for other refractory metals. The differences were 20 K for niobium (at 2425 K) and 22 K for zirconium (at 1940 K).

References

1. Cezairliyan, A., Morse, M. S., and Beckett C.W. Measurement of melting point and electrical resistivity (above 2840 K) of molybdenum by a pulse heating method. Rev. Int. Hautes Tempér. et Réfract., 7, 382, (1970).

2. Bonnell, D. W., Treverton, J. A., Valerga, A. J. and Margrave J. L., "The emissivities of liquid metals at their fusion temperatures". in Temperature - its measurement and control in science and industry, H. H. Plumb. ed., Vol. 4, part 1 (ISA, Pittsburgh, 1972), p. 483.

3. Cezairliyan, A., Radiance temperature of niobium at its melting point. J. Res. Nat. Bur. Stand. (U.S.), 77A (Phys. and Chem.), 333 (1973).

4. Cezairliyan, A., and Righini, F., Measurement of melting point, radiance temperature (at melting point), and electrical resistivity (above 2100 K) of zirconium by a pulse heating method. In preparation.

Matrix Isolation Studies on the Reaction of Iron Vapor with Oxygen

S. Abramowitz and N. Acquista
National Bureau of Standards
Institute for Materials Research
Washington, D. C. 20234

Introduction

The reactions of metallic vapor beams with oxygen species such as N_2O, O, O_2, and O_3, are often exothermic enough to populate electronically excited levels of the diatomic oxides formed. Recently several groups (1,2) have shown that reactions of Ba(g) with N_2O and O_3 give high yields of electronically excited BaO (on the order of 10% of the barium vapor consumed results in photons emitted in the A-X system of BaO). In order to fully understand such processes and to evaluate them for possible use as chemical laser systems a knowledge of the rates of all the reactions involved and the nature of any chemical intermediates is necessary.

The methods of matrix isolation spectroscopy are particularly useful for identifying possible intermediates in oxidation processes. The infrared spectra of matrix isolated BaO_2 formed by the reaction of Ba(g) with O_2 has been observed (3). Simple oxides of metals such as Pb(4), Sn(5), Ge(6), Ni(7), Pt(8), Pd(8), Cu(9), Cr(9), Li(10,11), Na(12),K(13) and Rb(13) have been identified using this method. In addition to these species reaction of alkali metals (14,15,16) and some alkaline-earth metals with O_3/Ar (17) have given infrared spectra of matrix isolated MO_3 species. In some cases where the ΔH of reaction is sufficient to yield the monoxide (when the metal vapor is reacted with O_2) the monoxide, dioxide and higher oxides are observed. Mole ratios of the observed oxides can often be controlled by the O_2/Ar (or other matrix gas) used. Such was the case for the reaction of $U_{(g)}$ (18) and $Th_{(g)}$ (19) with O_2 or N_2O where varying ratios of UO, UO_2 and UO_3 (and ThO, ThO_2) are observed as a function of the O_2 or N_2O concentration. The UO_2, UO_3 and ThO_2 formed in these reactions have the same structures as those obtained by generating the metallic oxides using standard Knudsen effusion techniques. The reaction of Fe(g) with O_2 and N_2O is reported in this study. The reaction of Fe(g) with O_2 to produce FeO is endothermic by about 20 kcal/mole and is not expected to proceed. Rather a FeO_2 species is expected. The reaction of Fe + N_2O to give FeO + N_2 is exothermic by 60 kcal/mole and is expected to proceed.

Experimental

The experimental apparatus used in these studies has been described (18). An Air Products closed cycle helium refrigerator was used to obtain liquid hydrogen temperatures. Temperatures of the deposition holder were measured using a hydrogen bulb thermometer and a gold-iron vs. chromel thermocouple.

A heater at the deposition plate allowed temperatures to be varied to obtain good matrices and to carry out controlled diffusion studies. The iron was vaporized from tungsten and molybdenum Knudsen cells. In some of the experiments boron or carbon liners were used to minimize reactions of the iron with the tungsten and molybdenum. Temperatures of the Knudsen cell were measured using W 25% Re vs W3% Re or Pt vs. Pt/Rh thermocouples, or in some cases an optical pyrometer. An electron beam furnace is used to generate the iron vapor in the one to ten micron pressure range. Argon and nitrogen were used as the matrix gases. Isotopically enriched oxygen samples obtained from the Miles-Yeda company were used in some of the studies.

Infrared spectra were observed with a Perkin-Elmer model 99G monochromator equipped with either a 40 or 150ℓ/mm diffraction grating for the 500 and 1000 cm^{-1} region. Interference filters were used to block out higher order radiation. A Perkin-Elmer model 301 was used to obtain infrared spectra in those parts of the 500 cm^{-1} region where water vapor lines are strong. Calibration of both infrared instruments is accomplished with water and ammonia lines. It is estimated that the frequencies are good to ±0.5 cm^{-1} in both regions studied with the 99G. The PE 301 spectra observed in the 500 cm^{-1} are probably accurate to ±0.8 cm^{-1}.

Results

The infrared spectrum of the product of the reaction of Fe(g) with O_2/Ar (1/100) is shown in Figure 1. The extent of reaction and/or the absorptivity coefficient of the species formed is small since many hours of reaction are required in order to obtain the spectrum shown. Spectrum a is that of Fe(g) + $^{16}O_2$/Ar (1/100). The main peak in the spectrum is at 945.9 cm^{-1}. Other peaks at 954.7, 969.5, 918.8 and 915.3 cm^{-1} are due to polymeric features (or those possibly involving one iron atom and more than one O_2 unit). These features are increased in intensity relative to the 945.9 cm^{-1} which diminishes in intensity when controlled diffusion of the matrix at temperatures of about 30K is allowed to proceed. These features are also more prominent when lower dilutions of O_2/Ar are used. The 945.9 cm^{-1} is extremely narrow with a $\Delta\nu_{1/2}$ (on an absorbance scale) of about 1 cm^{-1}. In addition to this feature at 945.9 cm^{-1} another band attributable to a low molecular weight species appears at 517.1 cm^{-1}. This feature also loses intensity at about the same rate as the 945.9 cm^{-1} upon controlled diffusion. Other weak features in the 300 cm^{-1} region are not reproducibly present and do not behave in a similar manner upon controlled diffusion. The 517.1 cm^{-1} feature is much weaker than its 945.9 cm^{-1} counterpart. A rough measurement of peak intensities indicate about a seven to one ratio. The 517.1 cm^{-1} feature appears to be also narrow, however due to its weakness it is difficult to measure its half width.

An isotopically enriched sample of O_2 was used in the spectrum b. The oxygen contained 30.5% $^{18}O_2$, 19.5% $^{16}O_2$, 48.7% $^{16}O^{18}O$ and insignificant amounts of $^{17}O_2$, $^{17}O^{18}O$, and $^{16}O^{17}O$. The single peak at 945.9 cm^{-1} is replaced with three peaks in the peak intensity ratio of about 2:5:3 at

945.9, 930.8, and 911.4 cm^{-1}. (These spectra are direct reproductions of those obtained on the PE 99G, which is a single beam instrument. Therefore, the Io is not flat, but rather tends to increase in going to higher frequency due to the blackbody characteristics of the Globar source, transmission of the interference filter, and the diffraction grating efficiency.) This ratio is in good agreement with that of the isotopically enriched oxygen sample used. In the 500 cm^{-1} region a feature is found at 508.1 cm^{-1}. The weakness of this feature precludes the observation of the 517.1 cm^{-1} feature in the same spectrum. Similarly it wasn't possible to observe the feature which will be seen to be assignable to $Fe^{18}O_2$ in this spectrum.

In order to observe the features due to $Fe^{18}O_2$ it was necessary to use an isotopically enriched $^{18}O_2$ sample containing 86.0% $^{18}O_2$, 12.2% $^{16}O^{18}O$, 0.4% $^{16}O_2$, and similarly insignificant amounts of $^{17}O^{18}O$, $^{17}O^{16}O$ and an $^{17}O^{16}O$ and an $^{17}O_2$ concentration about two orders of magnitude smaller. The spectrum in Figure 1c is that of the product of the reaction of Fe(g) with this oxygen sample diluted in 50 parts argon. The 911.4 cm^{-1} feature assigned to $Fe^{18}O_2$ is prominent in this spectrum. The 930.8 cm^{-1} feature, assignable to $Fe^{16}O^{18}O$ is also clearly seen. The intensity of this feature relative to that of $Fe^{18}O_2$ is approximately 7:1 in agreement with the isotopic abundances of $^{18}O_2$ and $^{16}O^{18}O$ in the isotopically enriched oxygen sample used. A peak at 494.0 cm^{-1} was also found. As was the case in the experiments with the sample containing 48.7% $^{16}O^{18}O$ and lesser amounts of the other isotopic varieties it was not possible to see any features due to $^{16}O^{18}O$ in this region. The low intensity of all the features in the 500 cm^{-1} is responsible for this. It might be added for completeness that these low intensities only allowed controlled diffusion experiments to be performed with the $^{16}O_2$ sample. (This is the only sample containing essentially 100% of one isotopic variety of oxygen.)

In a separate set of experiments the reaction of Fe(g) with N_2O/Ar has been studied. FeO is the principal product of this reaction and was found in the argon matrix at about 880 cm^{-1} in good agreement with the gas phase value derived from its electronic spectrum. Another peak located at somewhat higher frequency is also observed. It is believed this peak is assignable to a Fe-nitrogen complex, possibly FeN_2. However a proof of this and elucidation of the bonding obviously requires isotopic studies; utilizing N_2 and $^{14}N^{15}N$.

Discussion

A MO_2 species can either have a side-on or end-on structure.

M-O=O

end-on

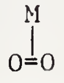

$$\begin{array}{c} M \\ | \\ O{=}O \end{array}$$

side-on

The side-on structure shown is a monodentate model while an isosceles triangle structure is

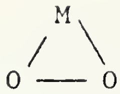

also possible. Both limiting models of the side-on structure have C_{2v} structure. The end-on structure will either have $C_{\infty v}$ or C_s symmetry depending upon whether the molecule is linear or bent. End-on structures have been found for several metal nitrogen complexes. The spectrum expected for the end-on and both limiting cases of the side-on models in the O-O stretching region are shown below for a 1:2:1 mixture of $M^{16}O_2$, $M^{16}O^{18}O$ and $M^{18}O_2$.

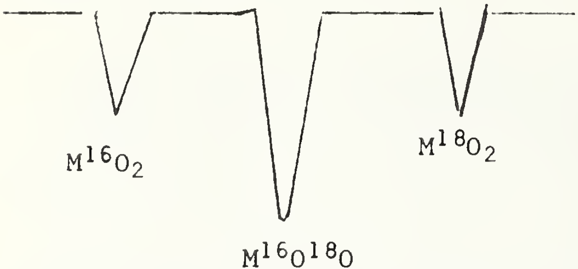

side-on

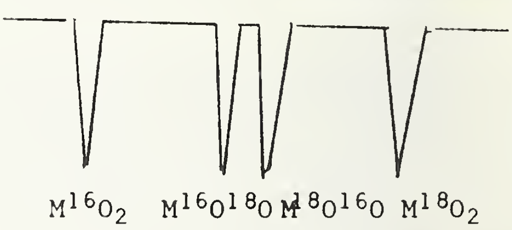

end-on

A three line spectrum with an intensity ratio of 1:2:1 is expected for a side-on model. The central component shows the spectral equivalence of the mixed isotopic species for this model. The end-on model gives a four line spectrum with a closely spaced doublet with absorption intensities in the ratio of 1:1:1:1. The inequivalence but equal probability of $M^{16}O^{18}O$ and $M^{18}O^{16}O$ results in a small separation and equal intensities of the central doublet.

The MO stretching region would show either a triplet or quartet for side-on and end-on models of MO_2 respectively. These modes are expected to be as shown below for an isotopic abundance of $1^{16}O_2$: $2^{16}O^{18}O$: $1^{18}O_2$.

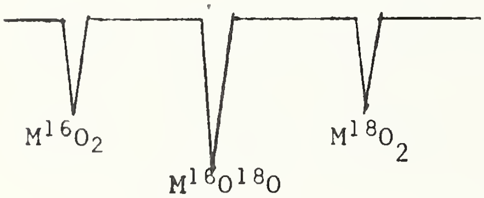

side-on

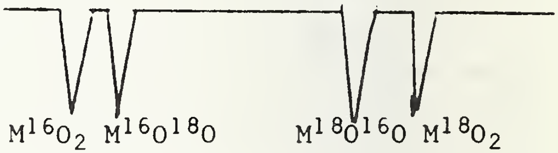

end-on

The side-on model would exhibit the same type pattern as shown for oxygen stretching region. The end-on model (be it $C_{\infty v}$ or C_s symmetry) is expected to have two closely spaced doublets with no absorption in between. The spacing of the doublets is expected to be small since only a small frequency difference is to be expected in the MO stretching between the pairs of molecules $M^{16}O^{16}O$ and $M^{16}O^{18}O$, and $M^{18}O^{18}O$ and $M^{18}O^{16}O$.

The observed spectrum in the oxygen stretching region has been shown in Figure 1. The three lines observed are in the proper intensity ratios for a side-on MO_2 molecule. The reduction in the observed frequency from the 1060-1120 cm^{-1} region expected for O_2^- seems to indicate some charge transfer from O=O to the MO bond. The narrowness of the $Fe^{16}O^{18}O$ feature which appears to have a $\Delta\nu_{1/2}$ of about 1 cm^{-1} would make the presence of another unresolved component to the doublet (as would be required for end-on bonding) improbable.

The M-O stretching modes in the 500 cm^{-1} region have already been discussed. The weakness of these modes made diffusion experiments difficult for all but the $^{16}O_2$ case. It was also not possible to observe all the modes of the three isotopic species $Fe^{16}O_2$, $Fe^{16}O^{18}O$, and $Fe^{18}O_2$ in one experiment. Three separate experiments were necessary to obtain the modes of the three isotopic species. Despite these difficulties, however it should be noted that a synthesis of the three observed spectra gives a three line spectrum with features at 517.1, 508.1 and 494.0 cm^{-1}. This pattern is expected for a side-on model of FeO_2. It should also be noted that the relative intensities of the 517.1, 508.1 and 494.0 cm^{-1} to their counterparts at 945.9, 930.8 and 911.4 cm^{-1} are approximately the same for each pair. This coupled with the controlled diffusion experiment, possible with only the $Fe^{16}O_2$ sample, showing similar ratios of disappearance of the 945.9 and 517.1 cm^{-1} features lends some confidence to the assignment of the O-O stretching mode and an Fe-O stretching mode of a side-on FeO_2 molecule.

A detailed assignment of the observed vibrations of FeO_2 to normal modes is not possible since only two of the three vibrations have been observed. Prolonged periods of deposition of Fe(g) + O_2/Ar have not yielded any other features assignable to FeO_2. It is expected that the missing fundamental which is a Fe-O stretching mode is at a lower frequency than the observed 517.1 cm^{-1} for $Fe^{16}O_2$. The observation of only two vibrational modes is not unexpected. Of the previous molecular complexes of this type observed, three modes have been observed for only alkali dioxides such as LiO_2. Indeed for most of the molecules studied such as PdO_2, NiO_2 etc., only two modes have been observed for the $M^{16}O_2$ species. Two modes have also been observed for $Ba^{16}O_2$ and $Ba^{18}O_2$ and only a BaO stretching mode for $Ba^{18}O^{16}O$. The ratio of the observed frequencies for the O-O stretching mode of $Fe^{18}O_2$ and $Fe^{16}O_2$ 911.4/945.9 = 0.9635 is considerably greater than 0.9428 expected for a pure O-O stretching mode. This indicates that this vibration is mixing with an FeO stretching mode. The product rule for ν_1 ν_2 of a C_{2v} XY_2 end-on model is

$$\frac{\nu_1^i\nu_2^i}{\nu_1\nu_2} = \left(\frac{2m_{y_i} + m_x}{2m_y + m_x}\right)\left(\frac{m_y^2 m_x}{m_{y_i}^2 m_x}\right) = 0.9089$$

The observed ratio for $(\nu_1\ \nu_2)\ Fe^{18}O_2/(\nu_1\ \nu_2)\ Fe^{16}O_2$ is

$$\frac{\nu_1\ \nu_2}{\nu_1^i\ \nu_2^i} = \left(\frac{(911.4)\ \ (494.0)}{(945.9)\ \ (517.1)}\right) = 0.9205$$

This is larger by about 1.3% than the ratio expected for harmonic vibrations. An alternative assignment of the 494.0 and 517.1 cm^{-1} features as due to ν_3 the asymetric stretching mode of a C_{2v} model is not very satisfying. Using these two frequencies an O-Fe-O angle of 87.3° is computed. This angle is larger than one would expect for such a molecule. A summary of the results obtained is given in Table 1.

There have been several solid and liquid phase studies of the molecular complexes of oxygen and hemoglobin type molecules. These studies were designed to elucidate the bonding between oxygen and iron in hemoglobin. A preliminary report on an X-ray diffraction study of a model porphryn molecule seems to indicate end-on bonding with a bent Fe-O-O bond (21). Some infrared (22) and resonance Raman spectroscopic studies (23) would seem to support this view. Both the infrared and Raman studies only investigated $^{16}O_2$ and $^{18}O_2$ samples. As was seen in the O-O stretching region previously, both end-on and side-on bonding would give similar spectra. The spectra of the mixed isotope, $^{16}O^{18}O$ bonded to Fe would clearly distinguish between the two proposed models in these condensed phases.

Conclusion

Spectra of the molecular complex formed by the reaction Fe(g) with oxygen have been studied by the methods of infrared matrix isolation spectroscopy. Spectra were observed using both normal and isotopically enriched oxygen samples. While a complete spectrum was not obtainable due to the weakness of the observed bands the weight of evidence is indicative of a side-on isoceles triangle (C_{2v}) model for FeO_2.

Table 1

Observed Fundamental Modes for FeO_2(cm^{-1})

Assignment	$Fe^{16}O_2$	$Fe^{18}O_2$	$Fe^{16}O^{18}O$
O-O Stretch	945.9	911.4	930.8
Fe-O Stretch	517.1	494.0	508.1

Fig. 1. The Infrared Spectrum of Matrix Isolated FeO_2

a) Fe(g) vs. $^{16}O_2$/Ar (1/100).

b) Fe(g) vs. ($2\,^{16}O_2$:$5\,^{16}O^{18}O$:$3\,^{18}O_2$)/Ar (1/50)

c) Fe(g) vs. $^{18}O_2$/Ar (1/50)

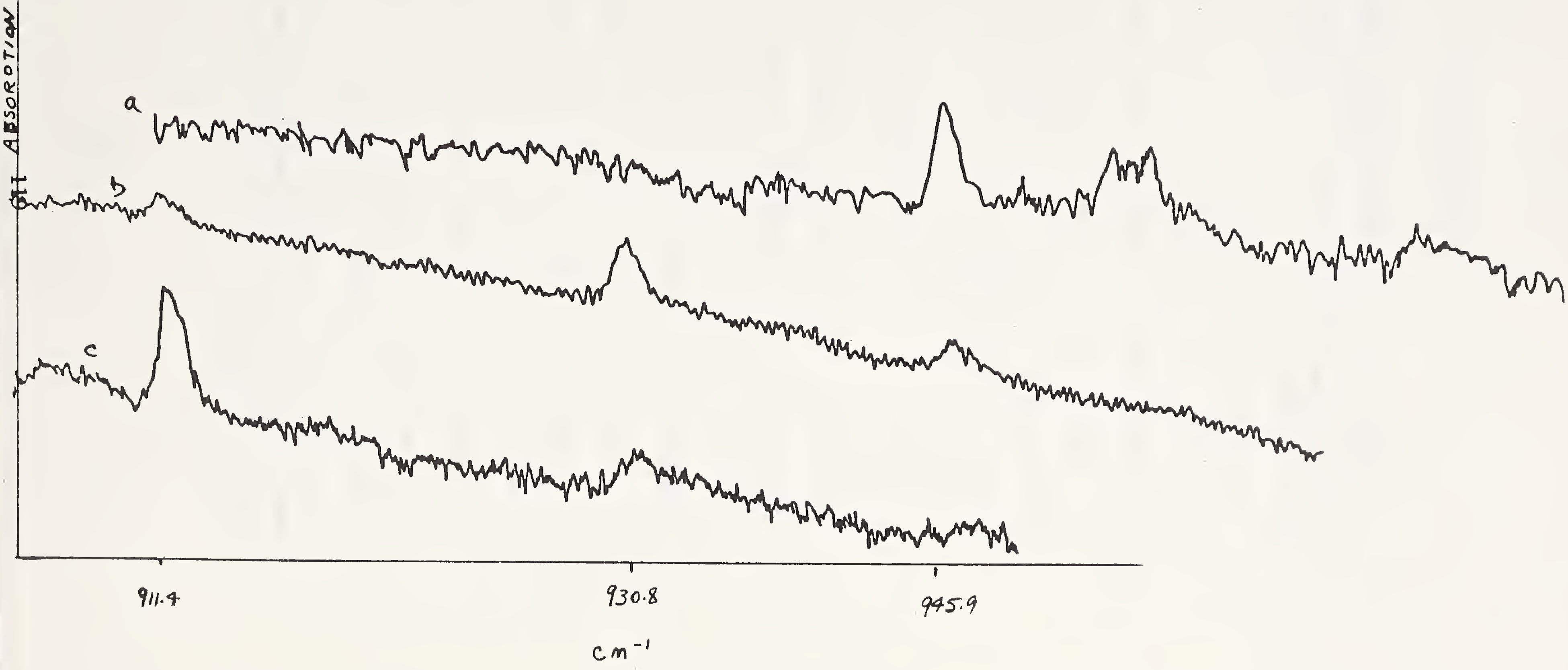

References

1. C. R. Jones and H. P. Broida, J. Chem. Phys. 59, 6677 (1973).
2. D. J. Eckstrom, S. A. Edelstein, S. W. Benson, J. Chem. Phys. 60, 2930 (1974).
3. S. Abramowitz and N. Acquista, J. Res. NBS 75A, 23 (1971).
4. J. S. Ogden and M. J. Ricks, J. Chem. Phys. 56, 1658 (1972).
5. J. S. Ogden and M. J. Ricks, J. Chem. Phys. 52, 352 (1970).
6. J. S. Ogden and M. J. Ricks, J. Chem. Phys. 53, 896 (1970).
7. H. Huber and G. A. Ozin, Can. J. Chem. 50, 3746 (1972).
8. H. Huber, W. Klotzenbucher, G. A. Ozin, A. Vander Voet, Can. J. Chem. 51, 2722 (1973).
9. J. H. Darling, M. B. Garton-Sprenger, J. S. Ogden, Faraday Symposium, In proof.
10. L. Andrews, J. Chem. Phys. 50, 4288 (1969).
11. L. Andrews and R. R. Smardewski, J. Chem. Phys. 58, 2258 (1973).
12. L. Andrews, J. Phys. Chem. 73, 3922 (1969).
13. L. Andrews, J. Chem. Phys. 54, 4935 (1971).
14. M. E. Jacox and D. E. Milligan, J. Mol. Spectroscopy 43, 148 (1972).
15. R. C. Spiker and L. Andrews, J. Chem. Phys. 59, 1851 (1973).
16. L. Andrews and R. C. Spiker, J. Chem. Phys. 59, 1863 (1973).
17. D. M. Thomas and L. Andrews, J. Mol. Spectroscopy 50, 220 (1974).
18. S. Abramowitz and N. Acquista, J. Res. NBS 78A, 421 (1974).
19. N. Acquista, S. Abramowitz, M. Linevsky, to be published.
20. Certain commercial instruments are identified in this paper to specify completely the experimental procedure. In no case does such identification imply a recommendation or endorsement by the National Bureau of Standards.

21. J. P. Collman, R. P. Gagne, C. A. Reed, W. T. Robinson, G. A. Rodley, Proc. Nat. Acad. Sci. 71, 1326 (1974).

22. C. H. Barlow, J. C. Maxwell, W. J. Wallace, W. S. Caughey, Biochem. and Biophys. Res. Comm. 55, 91 (1973).

23. J. S. Loehr, T. B. Freedman, T. W. Loehr, Biochem. and Biophys. Res. Comm. 56, 510 (1974).

Studies of the Reactions of Ba(g) with $O_3^{\neq}$

W. Braun, M. Kurylo, S. Abramowitz

The kinetics of the reaction of Ba(g) with ozone is being studied using modulation techniques. By exciting ozone vibrationally with a mechanically chopped monochromatic carbon dioxide laser, one can measure several parameters. In addition to being able to measure the ratio of the rates, k_1 and k_2

$$Ba(g) + O_3 \xrightarrow{k_1} BaO + O_2 + h\nu$$

$$Ba(g) + O_3^{\neq} \xrightarrow{k_2} BaO + O_2 + h\nu$$

one can measure (by using a suitable multichannel analyzer) the rates of growth and decay of luminescence (produced by the reaction) in the millisecond time regime. In this way, one can in principle measure the rates of production and loss of the various excited species that may be present in the flame.

The projected experiments will measure these variables as a function of argon pressure, in order to try to elucidate the proposed mechanisms. The luminescence will also be passed through a fast monochromator in order to investigate its wavelength dependence as a function of argon pressure and time.

Very preliminary data using the total luminescence obtainable from the reaction indicate a rate enhancement when vibrationally excited ozone is used. In these experiments pressures of barium in the ten micron range are used. The barium is driven by Ar through a resistively heated 1/4" O.D. stainless steel tube into a small reaction chamber. The ozone which is generated, using a commercial ozonator, is vibrationally pumped with the P_{30} line of a CO_2 laser. Chopping speeds are used such that a full on-off wave of 10 milliseconds is investigated. Argon pressures of about 5 torr were utilized in the initial experiments.

Chapter 9

DISSOCIATION ENERGIES OF THE SCANDIUM GROUP AND RARE-EARTH GASEOUS MONOXIDES

Ralph F. Krause, Jr.

Abstract

The dissociation energies of the scandium group and rare-earth gaseous monoxides are evaluated by reviewing the literature available on Knudsen effusion rates and mass-spectrometric data. The rate of effusion data for vaporizing the solid sesquioxides to form gaseous monoxides and monatomic oxygen are corrected for the presence of other vapor species. These include metal atoms, dioxides, diatomic oxygen, and oxides of the container and except for the metal atoms were not considered in the original sources. The results from various sources are compared by using the same auxiliary data which are needed to derive the dissociation energy of each monoxide. Selected values of thermodynamic properties are provided for all of the vapor species and solid sesquioxides under consideration. Corrections of the rate of effusion data for the presence of neodymium dioxide are found ambiguous. Using the dioxide data from one source leads to a molar ratio of dioxide to monoxide near unity. From another source the dioxide data, though inconsistent with the rate of effusion data, indicates this molar ratio to be negligible. This ambiguity suggests that the extent of forming this dioxide and perhaps others should be examined further. When a tantalum container is used, corrections of the rate of effusion data for the presence of tantalum oxides are found substantial in all the cases of the sesquioxides effused. When a tungsten container is used, corresponding corrections appear appreciable only in the case of europium sesquioxide whose effusion also appears to require an appreciable correction for diatomic oxygen. Corrections for the presence of metal atoms seem negligible in most cases, but they are appreciable in the effusion of the sesquioxides of europium, thulium, and ytterbium. Finally, differences between dissociation energies of several pairs of monoxides are compiled from published mass-spectrometric studies of isomolecular oxygen exchange reactions.

I. Introduction

The scandium group and rare-earth metals L appear as possible candidates for chemical lasers in the visible spectrum. Consider the bimolecular gaseous reaction,

$$L + XO \rightarrow LO^{*} + X \tag{1}$$

in which XO may be N_2O or O_3. A test for a metal atom to be a candidate is that the monoxide is formed in an excited state which has an excess energy equivalent to an electronic transition in the visible spectrum, namely more than 40 kcal mol^{-1}. These metal monoxides meet this criterion because their dissociation energies are greater than the sum of the above minimum transition energy and the dissociation energy of either XO.

Values of the dissociation energies $\underline{D}^{\circ}$, corresponding to the all gaseous reaction,

$$LO \rightarrow L + O \tag{2}$$

are provided in table 1. The last column gives values obtained from the present work; details are given in subsequent sections. Other columns give values reported earlier in other compilations. Those of Suchard (1974) and Rosen (1970), are both primarily collections of spectroscopic data. Although Schumm *et al.* (1973) made selections from among published values which they adjusted to be consistent with their values of the heats of formation of related compounds, the documentation of their efforts has yet to be published. Brewer and Rosenblatt (1969) estimated Gibbs free energy functions for the gaseous monoxides and recalculated dissociation energies from the published values of selected equilibria measurements. Ames *et al.* (1967) performed an extensive series of measurements. They used the Knudsen method to study the vaporization of sesquioxides and mass-spectrometry to study several isomolecular exchange reactions.

Determining accurate dissociation energies from weight-loss and mass-spectrometric data is fraught by several difficulties. An erroneous assessment of the vapor composition could made an otherwise accurate set of weight-loss data become misleading. It appears that earlier investigators failed to consider adequately the possible effects that the presence of gaseous dioxides might extend. Other errors in weight-loss data will result from vapor unsaturation and also from reactions between the sample and its container. Reliable results from ion intensity data depend upon identifying the ion which was produced by electron impact and properly selecting its molecular progenitor. While temperature dependent errors limit the accuracy of results obtained by the 2nd Law method, errors in the Gibbs free energy functions will cause a systematic dispersion of results obtained by

Table 1. Compilations of Dissociation Energies for the Gaseous Monoxides.

$D_0^\circ(\mathrm{LO})/(\mathrm{kcal\ mol^{-1}})^{a}$

Oxide LO	Gaydon (1968)	Ames et. et. (1967)[b]	Brewer et. al. (1969)	Rosen (1970)	Schumm et. al. (1973)[c]	Suchard (1974)	Present Work
ScO	160.9 ± 3.5	165.1 ± 5	154 ± 5	160.4 ± 2	162.4^{d}	160.4	161
YO	168.5 ± 2	171.8 ± 5	161 ± 5	170.4 ± 2.5	$168._{5}^{d}$	170.4 ± 2.5	170
LaO	189 ± 2	193.2 ± 5	187 ± 5	190.3 ± 2.5	190.6^{d}	190.3 ± 3	191
CeO	185 ± 5	193.2 ± 5	-	193.0 ± 3	$190._{2}$	193.0 ± 3	190
PrO	171 ± 7	181.7 ± 5	179 ± 8	181.7 ± 3	$182._{2}$	178.2 ± 3	178
NdO	164 ± 5	172.5 ± 5	167 ± 8	172.5 ± 3	167.7	172.5 ± 3	166
PmO	-	(160)[e]	-	-	-	-	-
SmO	-	142.0 ± 5	133 ± 8	142.1 ± 3	$139._{2}$	142 ± 3	141
EuO	-	133.7 ± 5	129 ± 10	133.8 ± 3	$132._{4}^{f}$	133.8 ± 3	130
GdO	161 ± 12	173.0 ± 5	161 ± 6	173.0 ± 3	$171._{3}$	-	169
TbO	-	173.4 ± 5	164 ± 8	173.4 ± 3	$171._{3}$	-	170
DyO	-	150.4 ± 5	145 ± 10	150.4 ± 3	$148._{0}$	-	150
HoO	175 ± 35	152.7 ± 5	148 ± 10	152.7 ± 3	$153._{3}$	152.7 ± 3	154
ErO	-	151.7 ± 5	146 ± 10	151.7 ± 3	$148._{1}$	-	154
TmO	-	139.3 ± 5	121 ± 15	139.3 ± 3	$133._{8}$	-	135
YbO	122 ± 35	<88.3 ± 5	97 ± 15	88.3	-	-	100
LuO	-	166.7 ± 5	158 ± 8	166.7 ± 3	$164._{2}$	166.7 ± 3	162

[a] 1 cal = 4.184 joules

[b] The values of the source were converted, using 23.06 kcal mol^{-1}/ev.

[c] The values given in this column were calculated from values of the heats of formation of the gaseous monoxide, gaseous metal, and atomic oxygen which were selected by the source.

[d] Wagman et. al. (1971)

[e] This is a predicted value which was interpolated from a graph of the source.

[f] This value is at 298.15 K.

the 3rd Law method. Although it is beyond the scope of this paper to examine the extent of all these errors, an attempt has been made to become critical of some.

II. Weight-Loss Vaporization of Sesquioxides

Several investigators have studied the vaporization of the sesquioxides by weight-loss methods, including Knudsen-effusion in tungsten, tantalum, or rhenium cells, Langmuir-torsion in molybdenum cages, and entrainment in a container of the sample itself. In many cases investigators had assumed that the vaporization process occurred practically as

$$L_2O_3(s) \rightarrow 2\ LO(g) + O(g). \qquad (3)$$

Even though reaction 3 may not be a practical process for evaluating the weight-loss data of all the sesquioxides, it will be taken in this paper as a convenient reaction whose equilibrium will be evaluated.

Vapor pressure measurements as a function of temperature are meaningful if the chemical system is univariant. When the sample container is excluded, one may realize from the Gibbs Phase Rule that a two component system will be univariant if three phases, for example two solids and the gas phase, are present. Although White et al. (1962) perceived by x-ray powder analysis only a single solid phase during the complete process of vaporizing each of several sesquioxides, the composition of this phase remained constant for a particular sesquioxide and varied among them from 2.96 to 2.99 atomic oxygen per 2 L. White et al. also observed constant effusion rates between the limits of 20 and 80% of sample vaporized. Consequently, it appears that these sesquioxides vaporize as azeotropes, making a two component system univariant. If the solid phase were a mixture of L_2O_3 and LO, the mol fraction of the latter would appear as high as 0.077; and if the solid phase were an ideal solution, this mol fraction would be the error in the pressure of LO(g). It can be shown that for measurements at 2500 K a correction for this error would lower the calculated dissociation energy by 0.6 kcal mol^{-1}.

In accord with reaction 3, weight-loss data alone would uniquely define the vapor composition if the vapor contained only two gas species. In general, the vapor may be considered to contain many species for which an investigator should account. When a sesquioxide is, for example, in a tungsten container, vaporization may be expressed as

$$L_2O_3(s) + n\ W(s) \rightarrow a\ O(g) + b\ O_2(g) + c\ L(g) + d\ LO(g) +$$
$$e\ LO_2(g) + \Sigma\ k_i\ W_xO_y(g) + \ldots \qquad (4)$$

If reaction 4 is assumed to vaporize congruently, a mass balance provides

$$c + d + e + \ldots = 2 \qquad (5)$$

$$a + 2b + d + 2e + \Sigma\, y_i k_i + \ldots = 3 \qquad (6)$$

and

$$\Sigma\, x_i k_i = n \qquad (7)$$

The vapor composition of more than two gas species is not defined by weight-loss data unless other data are available to relate all the variables. Table 2 gives thermodynamic values for several equilibria which involve gas species implicated by reaction 4.

One of the gas species which remains undefined is the metal atom. Table 3 shows that the mass-spectrometric ion-intensities from sesquioxide vaporization indicate that the L^+/LO^+ ratio has two cycles of increasing values for the series of rare earths including lanthanum. These values might be on the high side because the high ionization potentials which were used might have fragmented the LO^+. Ackermann et al. (1964) point out that some caution must be exercised in evaluating a meaningful L^+/LO^+ ratio, which they believe cannot be obtained at a single arbitrarily selected electron energy. Using ionization efficiency curves, they observed a saturation plateau for Y^+ at approximately 10-12 eV and for YO^+ at approximately 20 eV; from these they evaluated the Y^+/YO^+ saturation ratio to be 0.015, which is about 1/4 that observed by Ames et al. Extrapolating these curves to zero intensity they found appearance potentials of 5.5 and 6.0 eV for YO^+ and Y^+, respectively. If they had observed an appearance potential for Y^+ near 13 eV, one would have suspected its presence due solely to fragmentation of YO^+, which their ionization efficiency curve showed to be appreciable above 20 eV. Conversion of a ratio of ion-intensities to a ratio of pressures in the last column of table 3 depends on the proportionality of the following relation

$$P_i \propto I_i^+ T/\sigma_i \qquad (8)$$

in which σ_i is a cross-section for detection of the species i in a particular instrument. Using rate of effusion data, Ames et al. (1967) deduced σ_i for Y^+, YO^+, La^+, and LaO^+ with respect to that of Ag^+. The results for the L^+/LO^+ ratio of cross-sections averaged 1.6 with a difference of 0.2. Although the values in the last column of table 3 may be useful for comparison, a preferrable method, which is similar to one used by White et al. (1962), provides a relationship between the pressure of a metal atom and the published data for the atomization of its sesquioxide.

$$L_2O_3(s) \rightarrow 2\,L(g) + 3\,O(g) \qquad (9)$$

and this method will be described below.

The weight-loss method which was predominantly used for the sesquioxide vaporization measurements in the literature was the Knudsen effusion method. At temperature T the vapor pressure P_i for a vapor species of molecular weight M_i is obtained from

Table 2. Some Equilibria Involved with the Vaporization of Sesquioxides.

Reaction[e]	ΔH_0° kcal mol^{-1}	$\Delta[-(G^\circ-H_0^\circ)/T]$/cal $mol^{-1}K^{-1}$ 2000 K	2200 K	2400 K	2600 K	Ref.
$2\ O \rightarrow O_2$	-117.98	-29.91	-30.10	-30.26	-30.41	a
$Nd + NdO_2 \rightarrow 2\ NdO$	- 10.5	4.01	3.96	3.65	3.07	b
$NdO_2 \rightarrow NdO + O$	101[c]	26.93	27.01	27.06	27.11	
$Ta(s) + O \rightarrow TaO$	- 6.88	7.24	6.95	6.69	6.44	d
$Ta(s) + 2\ O \rightarrow TaO_2$	-163.93	-27.10	-27.41	-27.67	-27.90	d
$W(s) + O \rightarrow WO$	42.74	9.41	9.11	8.84	8.57	a
$W(s) + 2\ O \rightarrow WO_2$	-99.10	-20.02	-20.41	-20.76	-21.08	a
$W(s) + 3\ O \rightarrow WO_3$	-245.92	-57.65	-58.04	-58.38	-58.69	a
$2\ W(s) + 6\ O \rightarrow (WO_3)_2$	-630.70	-146.71	-147.03	-147.31	-147.56	a
$3\ W(s) + 8\ O \rightarrow W_3O_8$	-878.30	-212.72	-213.15	-213.51	-213.84	a
$3\ W(s) + 9\ O \rightarrow (WO_3)_3$	-1011.56	-247.87	-248.30	-248.65	-248.97	a
$4\ W(s) + 12\ O \rightarrow (WO_3)_4$	-1374.59	-344.85	-345.27	-345.61	-345.92	a

[a] Stull and Prophet (1971).

[b] Pupp and Gingerich (1971).

[c] Calculated by the 3rd Law from the K_p data of Staley and Norman (1969).

[d] Schick (1966).

[e] Gaseous species except where noted.

Table 3. Ratio of Mass-Spectrometric Ion Intensities from Vaporization of the Sesquioxides.

Solid	I_L^+/I_{LO}^+ Panish (1961), 20 eV	Shchukarev & Semenov (1961) 10 eV	45 eV	Ames et. al. (1967) 25 eV	Average	P_L/P_{LO}[a]
Sc_2O_3	-	1/8[b]	-	0.2	0.16	0.1
Y_2O_3	-	-	-	1/16	0.06	0.04
La_2O_3	-	-	0.16	<0.01	0.08	0.05
Ce_2O_3	-	-	0.20	-	0.2	0.12
Pr_2O_3	<0.1	-	0.36	-	0.2	0.1
Nd_2O_3	<0.1	-	0.25	<0.01	0.1	0.06
Sm_2O_3	0.5 to 1.0	1.3	1.0	0.5	0.9	0.6
Eu_2O_3	8±2, 9±1	7	5	10	9	6
Gd_2O_3	<0.1	1.2	0.3	-	0.5	0.3
Tb_2O_3	<0.1	0.9	0.2	-	0.4	0.3
Dy_2O_3	0.4	1.7	0.5	0.5	0.8	0.5
Ho_2O_3	1.0	2.2	1.3	0.5	1.2	0.8
Er_2O_3	1.5 ± 0.5	1.4	1.0	0.5	1.1	0.7
Tm_2O_3	15 ± 5	-	10	10	12	8
Yb_2O_3	(>30)	-	-	>50	50	30
Lu_2O_3	<0.1	1.7	1.1	0.5	0.8	0.5

[a] The ratio of cross-sections (L^+/LO^+) was assumed as 1.6; see text.

[b] Semenov (1965).

$$P_i = w_i \sqrt{2\ RT/M_i} \Big/ (tBW_b f) \tag{10}$$

in which w_i is the mass of species i that effuses in time t through an orifice with a Clausing factor W_b and an area B. The value of the constant R is $(8.31434)10^7$ erg $K^{-1}mol^{-1}$, and 1 atm is $(1.01325)10^6$ dyn cm^{-2}. Paule and Margrave (1967) show that the fraction of saturation f of the vapor in a Knudsen cell with a Clausing factor W_a and an area A may be estimated by

$$f = [1 + (BW_b/A)(\alpha^{-1} + W_a^{-1} - 2)]^{-1} \tag{11}$$

in which α is the vaporization coefficient of the condensed sample. Values of Clausing factors are tabulated in an appendix of reference 35 as functions of the length and radius of a cylinder. The mass w_i of species i is related to the total mass w of sesquioxide of molecular weight M by

$$w_i = w\ k_i M_i / M \tag{12}$$

in which k_i is the coefficient of a vapor species in reaction 4. When eq. 10 is used to calculate a hypothetical Knudsen P_k corresponding to the w and M of a sesquioxide,

$$P_i = k_i\ P_k \sqrt{M_i/M} \tag{13}$$

Using eq. 13, the k_i of species i may be expressed as a function of a known K_p for a reaction in which the species i is also involved; for example in the case of a metal atom L in reaction 9

$$c^2 = K_p\ M^{5/2} \Big/ (a^3 P_k^5\ M_L M_O{}^{3/2}) \tag{14}$$

The K_p of a reaction at a given temperature is calculated from the corresponding ΔH_0° and $\Delta[-(G^\circ - H_0^\circ)/T]$ as

$$K_p = \exp\{\Delta[-(G^\circ - H_0^\circ)/T]/R - \Delta H_0^\circ/(RT)\} \tag{15}$$

In like manner the procedure of the preceding example may be applied to other equilibria, such as those in table 2, which contribute to the definition of vapor species in reaction 4. After values of a and d are evaluated by simultaneous solution of eqs. 5 and 6, the K_p of reaction 3 may be calculated simply as

$$K_p(3) = P_{LO}{}^2\ P_O \tag{16}$$

in which the P_i are determined by eq. 13. When the Langmuir method is employed, eq. 13 could also be used since it involves using the $\sqrt{M_i}$ term of eq. 10 similar to the Knudsen method. If reliable P_k data as a function of temperature are available, the $d(\ell n\ P_k)/d(1/T)$ could be applied to define an unknown variable in eqs. 5 and 6.

In principle the entrainment method offers yet another means to evaluate an unknown variable in eqs. 5 and 6 when it is combined with the Knudsen method. In practice, however, experimental imprecision of the two methods often outweighs any meaningful contribution. The entrainment method, which is truly a vapor density measurement, would result in defining the pressure of vapor species i as

$$P_i = (w_i/V)RT/M_i \qquad (17)$$

When eq. 17 is used to calculate a hypothetical entrainment P_e corresponding to the w and M of a sesquioxide,

$$P_i = k_i\ P_e \qquad (18)$$

which is analogous to eq. 13.

III. Auxiliary Data

The published data necessary to evaluate the K_p of reaction 9 are assembled in tables 4 and 5. Holley et al. (1968) had reviewed extensively the published thermodynamic data for the sesquioxides. Table 4 includes some revised values which have been measured recently. The values of $(H°-H°_0)$ and $-(G°-H°_0)/T$ in table 4 are extrapolations which were calculated using expressions of the form

$$(H°-H°_{298}) = A + BT + CT^2 + D/T \qquad (19)$$

which Holley et al. had determined from relative enthalpy data. Holley et al. had selected the coefficients D so that the high temperature data joined smoothly with the low temperature heat capacity data. Since the sources in table 5 gave values of the Gibbs free energy functions with respect to 298.15 K, they were appropriately adjusted to zero Kelvin.

Since reaction 9 is the sum of reaction 3 and twice reaction 2, the dissociation energy of a monoxide is related as

$$D°(LO) = [\Delta H°(9) - \Delta H°(3)]/2 \qquad (20)$$

Table 4. Selected Values[a] of Chemical Thermodynamic Properties for the Solid Sesquioxides

Oxide (structure)[b]	$-\Delta H^\circ_{298}$ f kcal mol^{-1}	$(H^\circ_{298}-H^\circ_0)$ kcal mol^{-1}	S°_{298} cal mol^{-1}K^{-1}	$(H^\circ-H^\circ_0)$/kcal mol^{-1}				$-(G^\circ-H^\circ_0)/T$/cal mol^{-1}K^{-1}			
				2000 K	2200 K	2400 K	2600 K	2000 K	2200 K	2400 K	2600 K
Sc_2O_3 (C)	456.2 ± 0.5	3.335	18.43 ±.06	54.42	61.06	67.80	74.65	45.84	48.46	50.90	53.18
Y_2O_3 (C)	455.4 ± 0.5	3.989	23.69 ± .07	55.72	62.02	68.31	74.61	51.87	54.54	57.01	59.29
La_2O_3 (H)	428.7 ± 0.2	4.731	30.5 ± 0.2	59.16	66.28	73.54	80.92	59.39	62.24	64.88	67.36
Ce_2O_3 (H)	429.3 ± 0.7[c]	5.152	36.2 ± 0.5	-	-	-	-	-	-	-	-
Pr_2O_3 (H)	432.5 ± 0.7[d]	(5.0)	(37.9)[k]	65.72	74.07	82.66	91.49	69.44	72.61	75.58	78.36
Nd_2O_3 (H)	432.4 ± 0.2	5.00	37.4 ± 0.3	63.86	71.30	78.74	86.18	67.93	71.00	73.83	76.47
Sm_2O_3 (M)	435.9 ± 0.5[e]	5.036	36.1 ± 0.3	64.58	71.96	79.34	86.72	67.59	70.69	73.55	76.21
Eu_2O_3 (M)	394.7 ± 0.8[f]	(5.0)	(35)[k]	65.53	73.43	81.48	89.68	67.24	70.40	73.33	76.07
Gd_2O_3 (M)	434.9 ± 0.9[g]	4.45[i]	36.0 ± 0.8[i]	57.03	63.95	71.00	78.19	64.02	66.76	69.32	71.71
Tb_2O_3 (C)	445.6 ± 1.8	(5.0)	(37.5)[k]	63.86	71.92	80.21	88.74	68.27	71.35	74.23	76.93
Dy_2O_3 (C)	445.3 ± 0.8[h]	5.04	35.8 ± 0.3	60.60	67.48	74.36	81.24	65.66	68.57	71.26	73.74
Ho_2O_3 (C)	449.5 ± 1.2	5.017	37.8 ± 0.5	58.79	65.77	72.89	80.13	66.70	69.52	72.15	74.60
Er_2O_3 (C)	453.6 ± 0.5	4.79	36.6 ± 0.3	58.01	64.86	71.81	78.86	65.08	67.87	70.45	72.87
Tm_2O_3 (C)	451.4 ± 1.4	4.99[j]	(36.5)[k]	58.49	64.88	71.26	77.65	65.80	68.59	71.17	73.55
Yb_2O_3 (C)	433.7 ± 0.5	4.69	31.8 ± 0.3	58.25	64.67	71.09	77.52	61.48	64.27	66.85	69.22
Lu_2O_3 (C)	448.9 ± 1.8	4.192[j]	26.3[j]	55.88	62.40	68.97	75.60	53.96	56.65	59.13	61.44

[a] Values in parentheses are estimates. Non-superscripted values were taken from the review by Holley et. al. (1968).

[b] The structure is indicated by (C) cubic, (H) hexagonal, and (M) monoclinic.

[c] Baker and Holley (1968).

[d] Fitzgibbon et. al. (1973).

[e] Baker et.al. (1972).

[f] Fitzgibbon et. al. (1972).

[g] The value reported by Huber and Holley (1955), who used an atomic weight of 156.9 g mol^{-1} for Gd, was corrected by the new atomic weight listed in Table 5.

[h] Huber et. al. (1971).

[i] This value applies to the cubic form, but it is used here since no low-temperature measurements have been made on the monoclinic form.

[j] Justice et. al. (1969).

[k] Westrum and Grønvold (1962).

Table 5. Selected Values of Chemical Thermodynamic Properties of the Atomic Metals and Atomic Oxygen

Element	M	ΔH°_{298} f[a]	$(H^\circ_{298}-H^\circ_0)$/kcal mol^{-1} [a]		$-(G^\circ-H^\circ_0)/T$/ cal mol^{-1}K^{-1}				Ref.
	g mol^{-1}	kcal mol^{-1}	gas	solid	2000 K	2200 K	2400 K	2600 K	
Sc	44.956	90.32 ± 1	1.674	1.247	46.257	46.745	47.192	47.604	a
Y	88.905	101.5 ± 0.5	1.639	1.426	48.012	48.525	48.992	49.424	a
La	138.91	103.0 ± 1	1.509	1.593	49.638	50.292	50.895	51.456	a
Ce	140.12	101.0 ± 3	1.594	1.740	52.527	53.289	53.994	54.649	a
Pr	140.907	85.0 ± 0.5	1.487	1.773	50.868	51.458	52.007	52.510	c
Nd	144.24	78.3 ± 0.5	1.498	1.705	51.061	51.690	52.272	52.813	c
Sm	150.35	49.4 ± 0.5	1.953	1.810	50.400	51.060	51.658	52.203	c
Eu	151.96	41.9 ± 0.2	1.481	1.914[b]	49.586	50.061	50.497	50.900	c
Gd	157.25	95.0 ± 0.5	1.825	2.172	52.094	52.674	53.208	53.704	c
Tb	158.924	92.9 ± 0.5	1.779	2.253	53.938	54.543	55.102	55.622	d
Dy	162.50	69.4 ± 1	1.481	2.119	51.378	51.885	52.353	52.788	c
Ho	164.930	71.9 ± 0.3	1.481	1.911	51.244	51.735	52.187	52.607	c
Er	167.26	75.8 ± 1	1.481	1.767	50.918	51.437	51.928	52.397	d
Tm	168.934	55.5 ± 1	1.481	1.768	49.902	50.379	50.815	51.218	d
Yb	173.04	36.35 ± 0.2	1.481	1.604	45.840	46.313	46.745	47.143	c
Lu	174.97	102.2 ± 0.4	1.482	1.527	49.278	49.836	50.348	50.820	c
O	15.999	59.559	1.608	2.075[f]	43.002	43.485	43.926	44.330	e

[a] Hultgren *et*. *al*. (1973).

[b] Gerstein *et*. *al*. (1967).

[c] Feber and Herrick (1965).

[d] Feber and Herrick (1967).

[e] Stull and Prophet (1971).

[f] Value for $O_2(g)$.

The 2nd or 3rd Law Method may be used to obtain the ΔH_0° of reaction 3 from measured values of the corresponding $\underline{K}_p$. If $\underline{K}_p$ data are available as a function of temperature, the 2nd Law would give

$$\Delta H_0^\circ = -R[d(\ell n\ K_p)/d(1/T)] - \Delta(H_T^\circ - H_0^\circ) \qquad (21)$$

in which values of $(H_T^\circ - H_0^\circ)$ for atomic oxygen were obtained from Stull and Prophet (1970) and values of $(H_T^\circ - H_0^\circ)$ for all these monoxides were obtained from Ames et. al. as 16.82, 18.59, 20.37, and 22.15 cal $mol^{-1}K^{-1}$ at 2000, 2200, 2400, and 2600 K, respectively. At a given temperature the 3rd Law gives

$$\Delta H_0^\circ = T\left\{\Delta[-(G^\circ - H_0^\circ)/T] - R\ \ell n\ K_p\right\} \qquad (22)$$

in which values of $-(G^\circ - H_0^\circ)/T$ for all these monoxides were also obtained from Ames et. al. and are given in table 6. Differences in the results of the two methods indicate either errors in $\underline{K}_p$, in its derivative with temperature, or in the auxiliary thermodynamic functions.

The $-(G^\circ - H_0^\circ)/T$ values in table 6 are those used in the present work, but they appear somewhat uncertain. Table 7 shows $-(G^\circ - H_0^\circ)/T$ values which were estimated either by Ames et. al. (1967) or by Brewer and Rosenblatt (1969). Using the values of the latter would lead to values of dissociation energies which are approximately 6 kcal mol^{-1} smaller than those derived from table 6. Both sources appear to have selected, respectively, similar ground state vibrational frequencies for all the rare-earth monoxides, and these estimates are approximately the same as those which DeKock and Weltner (1971) observed recently in the infrared between 808 and 832 cm^{-1} by matrix isolation.

The major cause of the discrepancy is that the above two sources chose different electronic multiplicities for the ground and low-lying states. These multiplicities affect mainly the entropy of a monoxide. While both sources reported using a divalent-ion model for the electronic partition functions, Brewer and Rosenblatt used higher multiplicity values; for example, with ScO Ames et.al. considered only the ground state and assumed it to have a multiplicity of 2, whereas Brewer et. al. used 4 along with that of 6 for an assumed low-lying energy level which they took as 197 cm^{-1}, the value for the divalent ion. The values of Ames et. al. are nevertheless preferred. Approximate wavefunctions for ScO were calculated by Carlson et. al. (1965) who concluded that $^2\Sigma^+$ is the ground state of the molecule. Kasai and Weltner (1965) presented experimental evidence which they believed was conclusive that ScO, YO, and LaO all have $^2\Sigma$ ground states. Finally Green (1971) presented evidence that the unobserved low-lying electronic states of ScO, YO, and LaO can be interpreted using a model, but he concluded that these states make no appreciable contribution to the electronic partition functions.

Table 6. Values of the Gibbs Free Energy Functions for the Gaseous Monoxides.

Oxide	Electronic Multiplicity	$-(G^\circ-H^\circ_o)/T$ / cal $mol^{-1}K^{-1}$ 2000 K	2200 K	2400 K	2600 K
ScO	2	61.19	61.99	62.72	63.39
YO	2	63.55	64.35	65.09	65.77
LaO	2	64.97	65.78	66.51	67.20
CeO	3	65.71	66.52	67.25	67.93
PrO	4	66.37	67.18	67.92	68.60
NdO	5	66.86	67.67	68.41	69.09
SmO	7	67.66	68.46	69.20	69.88
EuO	8	67.96	68.76	69.50	70.18
GdO	9	68.29	69.09	69.83	70.51
TbO	8	68.09	68.90	69.63	70.31
DyO	7	67.89	68.70	69.43	70.11
HoO	6	67.63	68.43	69.17	69.85
ErO	5	67.31	68.11	68.85	69.53
TmO	4	66.90	67.70	68.44	69.12
YbO	3	66.40	67.20	67.94	68.62
LuO	2	65.61	66.42	67.15	67.83

Reference: Ames *et. al.* (1967).

Table 7. Differences in Dissociation Energies from Different Values of the Gibbs Free Energy Functions for the Gaseous Monoxides.

Oxide	T/K	$-(G^\circ-H^\circ_o)/T$ / cal $mol^{-1}K^{-1}$ Ames et. al. (1967)	Brewer et. al. (1969)	$\Delta D^\circ_o(LO)^a$ kcal mol^{-1}
ScO	2600	63.39	66.46	8.0
YO	2600	65.77	68.53	7.2
LaO	2400	66.51	68.79	5.5
CeO	2000	65.71	68.90	6.4
PrO	2000	66.37	53.0[b]	-
NdO	2400	68.41	54.4[b]	-
SmO	2400	69.20	71.5	5.5
EuO	2200	68.76	70.7	4.3
GdO	2600	70.51	72.55	5.3
TbO	2000	68.09	69.2	2.2
DyO	2600	70.11	72.4	6.0
HoO	2600	69.85	72.2	6.1
ErO	2600	69.53	72.0	6.4
TmO	2400	68.44	71.0	6.1
YbO	2400	67.94	70.6	6.4
LuO	2600	67.83	53.6[b]	-

[a] Calculated as Ames' value of $[-(G^\circ-H^\circ_o)/T]$ less Brewer's value.

[b] Apparently an error in the source's text.

IV. Errors in Vapor Composition

A possibly serious systematic error in the calculations using weight-loss data might exist if the formation of metal dioxides and more complex oxides are neglected. As shown above in table 2, Staley and Norman (1969) and Pupp and Gingerich (1971) have studied equilibria involving NdO_2. Since their data will be shown to be disparate, the extent of NdO_2 formation is difficult to evaluate. The last column of table 8 shows values of $\underline{D}_0^\circ$ for NdO which were calculated by varying the ΔH_0° as shown in column 1. Corrections were applied for the formation of diatomic oxygen, tungsten oxides, and the Nd atom, using the sesquioxide atomization data. A value of ΔH_0° for reaction *c* that is as low as that shown in the last line of column 2 is inconsistent with the rate of effusion data because there is produced $P_{Nd}/P_{NdO} < 0$. In the next to the last line the mol fraction of NdO_2 is assumed zero. If the data of Pupp and Gingerich were believed, one would judge from the results in line 1 that Nd_2O_3 vaporizes practically as

$$Nd_2O_3(s) \rightarrow NdO(g) + NdO_2(g) \qquad (23)$$

Also, the negligible amount of atomic oxygen shown in line 1 would correspond to the fact that no tungsten oxides were detected mass-spectrometrically by Goldstein *et al*. (1961). The presence of other metal dioxides are apparent. De Kock and Weltner have observed infrared spectra which they have assigned to CeO_2, PrO_2, and TbO_2. The extent of formation of these and other dioxides would help define the vapor composition of weight-loss studies and provide more accurately calculated dissociation energies.

The use of mass-spectrometry to study equilibria involving LO_2 might entail some difficulties especially when too high an ionization potential is used. Using ionization efficiency curves for CeO^+ and CeO_2^+, Ackermann and Rauh (1971), ref. 3, found appearance potentials of 5.2 and 10.3 eV, respectively, based on the known 5.5 eV ionization potential for Ce^+. They found the onset of fragmentation of CeO_2 to CeO^+ at about 11 eV and of CeO to Ce^+ at about 13.5 eV. After an interval of time they observed the amount of CeO^+ had increased by a factor of 7 and the amount of CeO_2^+ had decreased by a factor of 2. A decrease in the pressure of atomic oxygen would account for the shift of CeO_2 to CeO. It seems entirely possible that the use of mass-spectrometry could miss LO_2 entirely unless a sufficient pressure of oxygen were present.

Errors which result from sample reaction with its container appear most pronounced when sesquioxides are vaporized in tantalum Knudsen cells. Using the rate of effusion data of Kulvarskaia and Maslovskaia (1960), eqs. 5 and 6 were solved simultaneously with and without corrections for the tantalum oxides. The results are shown in table 9. Corrections for diatomic oxygen and the sample-metal atoms, using the atomization data for the sesquioxides, were applied; but the sample-

Table 8. Effect of the Uncertainty of Forming Neodymium Dioxide Gas on Calculations Using Sesquioxide Rate of Effusion Data[a]

Assumed	Calculated	Averaged Results (30 runs, 2255-2434 K)					
ΔH°_0 (b)	ΔH°_0(c)	P_{Nd}/P_{NdO}	Mole Ratio per Nd_2O_3 (vaporized)				$D^\circ_0(NdO)$[f]
kcal mol^{-1}	kcal mol^{-1}		W (vaporized)	O(g)	NdO(g)	NdO_2(g)	kcal mol^{-1}
-10[d]	148.3	0.016	$(2)10^{-5}$	0.007	0.97	1.01	158.2
-20	141.7	0.002	$(9)10^{-5}$	0.026	1.02	0.98	161.7
-30	135.0	$(3)10^{-4}$	$(5)10^{-4}$	0.094	1.09	0.91	165.0
-40	128.2	$(5)10^{-5}$	0.003	0.27	1.28	0.72	168.2
-50	120.9	$(1.4)10^{-5}$	0.012	0.56	1.60	0.40	170.9
-	-	$(6)10^{-5}$	0.03	0.87	2.00	0	173.0
-	101[e]	<0	-	-	-	-	-

[a] Goldstein *et al.* (1961).

[b] $Nd(g) + NdO_2(g) \rightarrow 2\ NdO(g)$

[c] $NdO_2(g) \rightarrow NdO(g) + O(g)$

[d] Pupp and Gingerich (1971)

[e] Staley and Norman (1969)

[f] Third Law values

Table 9. Effects of Correcting for Gaseous Tantalum Oxides on Calculations Using Sesquioxide Rate of Effusion Data[a]

L_2O_3(s)	Without Correction			With Correction			
	P_L/P_{LO}	Mole Ratio $O(g)/L_2O_3$(vaporized)	$D^\circ_0(LO)$[b]	P_L/P_{LO}	Mole Ratio per L_2O_3(vaporized)		$D^\circ_0(LO)$[b]
			kcal mol^{-1}		Ta(vaporized)	O(g)	kcal mol^{-1}
La_2O_3	10^{-9}	0.61	208	10^{-6}	0.58	0.0033	197
Pr_2O_3	10^{-6}	0.85	190	10^{-4}	0.68	0.009	180
Nd_2O_3	10^{-5}	0.87	179	10^{-2}	0.72	0.014	169
Sm_2O_3	10^{-4}	0.80	154	0.28	0.90	0.009	143
Eu_2O_3	10^{-4}	0.41	140	2.0	1.23	0.0032	125
Gd_2O_3	10^{-6}	0.91	187	10^{-3}	0.72	0.011	177
Dy_2O_3	10^{-4}	0.94	164	0.11	0.94	0.021	155
Ho_2O_3	10^{-4}	0.97	166	0.13	1.03	0.023	156
Er_2O_3	10^{-3}	0.99	166	0.16	1.12	0.027	157
Yb_2O_3	10^{-3}	0.76	138	3.1	1.44	0.010	123
Lu_2O_3	10^{-6}	0.90	193	10^{-4}	0.76	0.012	183

[a] Kulvarskaia and Maslovskaia (1960).

[b] Third Law values.

metal dioxides were assumed absent. The general effect of correcting for the tantalum oxides is to reduce the value of the calculated dissociation energy by approximately 10 kcal mol^{-1}. The correction of course depends upon the pressure of atomic oxygen; so if the formation of a sample-metal dioxide were appreciable, alternative results would be obtained. Goldstein et al. (1960) detected no tantalum oxides mass-spectrometrically when they studied sesquioxide effusion in a tantalum cell, but they observed that the total weight-loss of the cell and sample exceeded the sample mass.

The effects that other assumptions have upon the calculations of dissociation energies are shown in table 10. Here are analysed the sesquioxide rate of the effusion data of Goldstein et al. (1961) and of Ames et al. (1967), both of whom had used a tungsten cell. The variation in the calculated dissociation energy for LaO is representative of those for the monoxides of Sc, Y, Nd, Sm, Gd, Dy, Ho, Er, and Lu. Calculations using the effusion data for Yb_2O_3 yielded negative P(L)/P(LO). In assumptions 1 through 4, the sample-metal atoms were corrected by the atomization data for the sesquioxides. The first assumption, which is the one employed by Ames et al., considers that only the a, c, and d of reaction 4 are important. The second assumption includes b, and the third assumption includes the k_i for the various tungsten oxides. Assumptions 3 and 5 differ in that the latter uses values in the last column of table 3 instead of the atomization data. The P(L)/P(LO) calculated by assumption 3 for all the sesquioxides follows the same two cyclic pattern as table 3 except that assumption 3 gives them one or more orders of magnitude smaller. Even though Ames et al. detected no tungsten oxides mass-spectrometrically, they did observe nearby 0.1 mole of tungsten-loss per mole of L_2O_3. The results in table 10 indicate that the corrections for the tungsten oxides have appreciable effects mainly for the case of Eu_2O_3. This correction is confirmed to some extent by the results of Petzel and Greis (1971) who used iriduim-lined Knudsen cells to study the vaporixation of Eu_2O_3 in the presence of W.

An approximation of the effect of vapor unsaturation in the Knudsen cell is shown by assumption 4 in table 10. Although vapor unsaturation produces a shift in the vapor equilibria of complex vaporization, the approximation is based upon an estimate of f by eq. 11. The cell dimensions reported by Goldstein et al. (1961) and used by Ames et al. were such that A/B, W_a, and W_b were evaluated as 16, 0.3, and 0.5, respectively. Goldstein et al. (1961) believed that $\alpha > 0.5$; so it appears that they and Ames et al. reported mass-effusion rates which included a value of f as 0.91. More recently Messier (1967) observed Knudsen effusion rates for Gd_2O_3 through each of two orifices of different size. As will be described later in Section VI under Messier, the vaporization coefficient α for Gd_2O_3 was deduced to be 0.074. When this value of α is used to revise the work of Goldstein et al., f becomes 0.68 instead of 0.91 to produce the results of assumption 4.

Table 10. Effects of Other Assumptions on Calculations Using Sesquioxide Rate of Effusion Data

Assumptions (see text for full explanation.)	P_L/P_{LO}	Averaged Results		
		Mole Ratio per L_2O_3 (vaporized)		$D^{\circ}_0(LO)^c$
		W (vaporized)	O(g)	kcal mol^{-1}
La_2O_3, (22 runs, 2234-2441 K)[a]				
1. Formation of Metal Atom	$(6)10^{-7}$	-	1.00	193.2
2. Including Diatomic Oxygen	$(6)10^{-7}$	-	0.91	193.0
3. Including Tungsten Oxides	$(8)10^{-7}$	0.059	0.79	192.7
4. Using Revised Vap. Coeff.	$(4)10^{-7}$	0.082	0.72	194.5
5. Using Mass-Spect. P(L)/P(LO)	0.05	0.073	0.84	192.6
Eu_2O_3, (9 runs, 1984-2188 K)[b]				
1. Formation of Metal Atom	0.001	-	1.00	135.7
2. Including Diatomic Oxygen	0.003	-	0.56	134.5
3. Including Tungsten Oxides	0.02	0.29	0.14	131.6
4. Using Revised Vap. Coeff.	0.01	0.30	0.11	132.9
5. Using Mass-Spect. P(L)/P(LO)	6	0.84	0.17	123.8
Tm_2O_3, (11 runs, 2450-2641 K)[b]				
1. Formation of Metal Atom	0.73	-	1.85	134.9
2. Including Diatomic Oxygen	0.74	-	1.84	134.9
3. Including Tungsten Oxides	0.76	0.018	1.82	134.8
4. Using Revised Vap. Coeff.	0.39	0.016	1.52	137.8
5. Using Mass-Spect. P(L)/P(LO)	8	0.033	2.69	127.4

[a] Goldstein et. al. (1961).

[b] Ames et. al. (1967).

V. Equilibria Data by Mass Spectrometry

Differences between the dissociation energies of several pairs of monoxides, LO and MO, have been determined from equilibria studies of isomolecular oxygen exchange reactions in the gas phase

$$L + MO \rightarrow LO + M \qquad (24)$$

Several investigators have used mass-spectrometry to measure ion-intensities as a function of temperature for different condensed mixtures of two or more metals and oxides, or of oxides only. They calculated the $\underline{K_p}$ of reaction 24 by assuming that the corresponding ratio of cross-sections were unity, which seems satisfactory according to the measurements of the cross-sections for Y^+, YO^+, La^+, and LaO^+ discussed in Section II above. Results by the 2nd and 3rd Law methods are assembled in table 11. The extent of fragmentation of LO to L^+ was neglected; however, Smoes et al. (1965) and Ackermann and Rauh (ref. 2) were so concerned about the ill-effects of fragmentation that they used lower ionization potentials. Values of the dissociation energies in the last column of table 11 were calculated from the selected values in the next to the last column. The results for LaO has particular significance because it depends upon that for SiO which was derived from an independent review by Stull and Prophet (1971).

Another method which has been used to evaluate dissociaiton energies by mass-spectrometry involves measuring the LO^+/L^+ ratio of ion-intensities for the vapor species which are in thermodynamic equilibrium with both $L(\ell)$ and $L_2O_3(s)$. A difficulty with this method is the uncertain activities of the condensed phases, i.e. their mutual solubilities. Using eq. 8 and independent data for the pressure of L(g), the $\underline{K_p}$ of reaction 25

$$1/3\ L(g) + 1/3\ L_2O_3(s) \rightarrow LO(g) \qquad (25)$$

may be calculated from

$$K_p = P_L^{2/3}\,(I_{LO}^+/I_L^+)(\sigma_L^+/\sigma_{LO}^+) \qquad (26)$$

in which the L^+/LO^+ ratio of cross-sections was shown in Section II above to be approximately 1.6.

A third application of mass-spectrometry involves measuring as a function of temperature the LO^+ ion-intensity which is proportional to the pressure of LO vapor in equilibrium with $L_2O_3(s)$. When the pressure of atomic oxygen is assumed proportional to the pressure of the monoxide over the temperature interval of measurement, the enthalpy change of reaction 3 may be approximated from

$$\Delta H^\circ_T = -3R[d(\ln P_{LO})/d(1/T)] \qquad (27)$$

Table 11. Mass-Spectrometrically Determined Enthalpy Changes of Isomolecular Exchange Reactions

$L + MO \rightarrow LO + M$

L	M	T/K	I.P.	ΔH°_0/kcal mol^{-1}			D°_0/ kcal mol^{-1} [g]	
		Range	eV	2nd Law	3rd Law	Ref.	MO	LO
Sc	Y	1760-2580	12	10.2	9.2	b	170	160.3
Sc	La	1810-2220	12	29.7	28.7	b	191	161.8
Sc	La	1880-2070	25	27.7	27.0	c	191	163.6
Y	La	1890-2270	12	16.5	19.3	b	191	173.1
Y	La	1880-2200	25	22.7	19.6	c	191	169.8
Y	La	1783-2184	11	21.4	19.6	e	191	170.5
La	Si	1877-2088	30	-	-1.0	d	189.9[f]	190.9
Ce	La	1698-2040	25	0.3	-0.6	a	191	191.1
Ce	La	1625-2150	30	2.1	-0.3	d	191	189.2
Pr	La	1749-2067	25	15.0	7.9	a	191	179.6
Pr	Nd	1729-2088	25	-6.8	-10.9	a	166	174.8
Pr	Tb	1870-2050	25	-3.5	-12.7	c	170	178.1
Sm	Y	2320-2500	25	26.5	28.0	c	170	142.8
Eu	Sm	2270-2390	25	-	13.0	c	141	128
Tb	La	1870-2050	25	17.6	21.9	c	191	171.2
Tb	Gd	1930-2180	25	0.2	1.5	c	169	168.2
Ho	Tb	-	25	-	16.4	c	170	153.6
Lu	La	2090-2320	25	24.1	25.2	c	191	166.4

[a] Walsh _et_. _al_. (1961).
[b] Smoes _et_. _al_. (1965).
[c] Ames _et_. _al_. (1967).
[d] Coppens _et_. _al_. (1967).
[e] Ackermann and Rauh (1971), ref. 2.

[f] Stull and Prophet (1971)

[g] Values for LO were calculated from selections for MO less the averaged 2nd and 3rd Law ΔH's.

VI. Recalculated Results

Using the weight-loss and ion-intensity data which are available in the literature, the $\underline{K}_p$ of reactions 3 and 25 are evaluated; and the corresponding dissociation energies are calculated from the auxiliary data which are given in Section III. Second Law and average Third Law values of the dissociation energies for the monoxides are reported in table 12. Selections of D_0° values listed in tables 11 and 12, are compiled in the last column of table 1. Comments on the results from each source follow below in the order that they appeared in the literature.

Chupka et al. (1956) had used mass-spectrometry in 4 experiments to measure the LaO^+/La^+ ion-intensity ratio, which is proportional to the LaO/La pressure ratio in equilibrium with La(ℓ) and La_2O_3(s). Instead of using their estimate of 0.5, the value of 1.6 deduced by Ames et al. was used in eq. 26 for the La^+/LaO^+ ratio of cross-sections. The resulting D_0° value is exceptionally close to that in table 11 for the isomolecular reaction involving Si.

Kulvarskaia and Maslovskaia (1960) had studied the vaporization of several sesquioxides by Knudsen effusion. The 3rd Law D_0° in table 12 are those from table 9 which were corrected for tantalum oxides. Second Law values of D_0° were obtained by using eqs. 20 and 21.

Goldstein et al. (1961) had used both Knudsen-effusion and mass-spectrometry to study the vaporization of La_2O_3 and Nd_2O_3. The Knudsen value of the dissociation energy for NdO was selected as the average of the extremes which are reported in table 8 and is strikingly close to the mass-spectrometric value which resulted, using eq. 27. The Knudsen value of D_0° for LaO is the result of assumption 3 described above for table 10. Similar to the NdO results the higher value of D_0° for LaO by mass-effusion than by mass-spectrometry corresponds to a possible presence of the dioxide which was not corrected.

Ackermann et al. (1964) had studied the vaporization of Y_2O_3 by Knudsen effusion. The corrections which correspond to assumptions 1, 2, and 3 in table 10 had negligible effect on calculating the dissociation energy for YO.

Semenov (1965) had used mass-spectrometry to measure the ScO^+ ion-intensity which corresponds to the vaporization of Sc_2O_3. The 2nd Law value of D_0° for ScO in table 12 was calculated, using eq. 27. The 3rd Law value of D_0° was calculated from the $\underline{K}_p$ of reaction 3, using Semenov's values of the pressures of ScO and O which he had calculated from his measurements of the effusion rate for Sc_2O_3 and which he had corrected with his estimate of 8 for the ScO/Sc pressure ratio.

Alcock and Peleg (1967) had measured rates of effusion for Gd_2O_3 and Y_2O_3 by torsion-effusion and Langmuir-torsion experiments. They had assumed that vaporization occurs as reaction 3 and had plotted log(P/atm) versus 1/T. Their "total pressure" was interpreted as the sum of the LO and O partial pressures so that the $\underline{K}_p$ of reaction 3 was evaluated by reading their small graph.

Table 12. Dissociation Energies Recalculated from Published Weight-Loss and Mass Spectrometric Data

Sample	T/K Range	Method	Source	$D_0^\circ(LO)$/kcal mol^{-1} 2nd Law	3rd Law
ScO					
Sc_2O_3 + W	2400-2570	Mass. Spect. (10 eV)	Semenov (1965)	172	-
	2551-2567	Effusion Rate (3 runs)		-	159.4
	2555-2693	Knudsen (5 runs)	Ames et. al. (1967)	160.4	160.9
YO					
Y_2O_3 + W	2509-2720	Knudsen (11 runs)	Ackermann et. al. (1964)	185	167.2
	2250-2390	Langmuir-torsion, Knudsen	Alcock et. al. (1967)	173	162
	2492-2697	Knudsen (14 runs)	Ames et. al. (1967)	181	170.5
	2220-2620	Mass-Spect. (11 eV)	Ackermann et. al. (1973)	171	-
LaO					
La + La_2O_3 + Ta	1650-1900	Mass Spect. (40 eV)	Chupka et. al. (1956)	-	191.1
La_2O_3 + Ta	1980-2220	Knudsen	Kulvarskaia et. al. (1960)	259	197
La_2O_3 + W	2234-2441	Knudsen (22 runs)	Goldstein et. al. (1961)	200	192.7
	2015-2280	Mass Spect. (25 eV)		187	-
	1490-2190	Mass Spect.	Bushkovich et. al. (1967)	181	-
La_2O_3	2150-2560	Transpiration	Benezech et. al. (1969)	194	199
La_2O_3 + Re	2258-2427	Knudsen (5 runs)	Ackermann et. al. (1971)[b]	-	192.1
	1778-2308	Mass-Spect. (11 eV)		189.3	-
PrO					
Pr_2O_3 + Ta	2060-2400	Knudsen	Kulvarskaia et. al. (1960)	214	180
NdO					
Nd_2O_3 + Ta	2080-2670	Knudsen	Kulvarskaia et. al. (1960)	205	169
Nd_2O_3 + W	2255-2434	Knudsen (30 runs)	Goldstein et. al. (1961)	-	166
	2095-2520	Mass Spect. (25 eV)		166	-
Nd_2O_3	2210-2560	Transpiration	Benezech et. al. (1969)	168	178
SmO					
Sm_2O_3 + Ta	2120-2350	Knudsen	Kulvarskaia et. al. (1960)	179	143
Sm_2O_3 + W	2333-2499	Knudsen (9 runs)	Ames. et. al. (1967)	138.9	138.1
Sm_2O_3	2410-2670	Transpiration	Benezech et. al. (1969)	130	133
EuO					
Eu_2O_3 + Ta	2050-2300	Knudsen	Kulvarskaia et. al. (1960)	139	125
Eu_2O_3 + W	1984-2188	Knudsen (9 runs)	Ames et. al. (1967)	94	131.6
	2192	Knudsen	Petzel et. al. (1971)	-	131[a]
GdO					
Gd_2O_3 + Ta	2080-2380	Knudsen	Kulvarskaia et. al. (1960)	222	177
Gd_2O_3 + W	2160-2390	Langmuir-torsion	Alcock et. al. (1967)	114	157
	2408-2546	Knudsen (9 runs)	Ames et. al. (1967)	183	169.2
	2350-2590	Knudsen (18 runs)	Messier (1967)	171.4	165.8
Gd_2O_3	2380-2670	Transpiration	Benezech et. al. (1969)	169	172
DyO					
Dy_2O_3 + Ta	2260-2460	Knudsen	Kulvarskaia et. al. (1960)	16	155
Dy_2O_3 + W	2432-2637	Knudsen (16 runs)	Ames et. al. (1967)	158	148.1
HoO					
Ho_2O_3 + Ta	2230-2490	Knudsen	Kulvarskaia et. al. (1960)	131	156
Ho_2O_3 + W	2487-2711	Knudsen (13 runs)	Ames et. al. (1967)	48	153.1
ErO					
Er_2O_3 + Ta	2270-2490	Knudsen	Kulvarskaia et. al. (1960)	154	157
Er_2O_3 + W	2492-2687	Knudsen (16 runs)	Ames et. al. (1967)	170	151.4
TmO					
Tm_2O_3 + W	2450-2641	Knudsen (11 runs)	Ames et. al. (1967)	163	134.8
YbO					
Yb_2O_3 + Ta	2060-2400	Knudsen	Kulvarskaia et. al. (1960)	144	123
Yb_2O_3 + W	2371-2626	Knudsen (12 runs)	Ames et. al. (1967)	127	93
LuO					
Lu_2O_3 + Ta	2120-2400	Knudsen	Kulvarakaia et. al. (1960)	84	183
Lu_2O_3 + W	2615-2700	Knudsen (9 runs)	Ames et. al. (1967)	128	157.2

[a] As reported by source.

[b] Reference 2.

Ames et al. (1967) had measured the rates of effusion for several sesquioxides. Except for YbO the values of D_0° in table 12 are the results of assumption 3 described for table 10. In the case of YbO, assumption 5 described for table 10 was used.

Bushkovich et al. (1967) had tested their mass-spectrometer by subliming La_2O_3. They had measured the LaO^+ ion-intensity as a function of temperature and deduced a ΔH_T° to be 435 kcal mol^{-1}, presumedly for reaction 3.

Messier (1967) had measured rates of effusion for Gd_2O_3 in a tungsten cell with 0.47 cm radius for which the Clausing factor was estimated to be 0.53. This cell was fitted with either of two lids with orifices which had radii of 0.450 and 0.855 mm and Clausing factors of 0.356 and 0.507, respectively. Using the average rate of effusion through each orifice, simultaneous solution of eqs. 10 and 11 gives the vaporization coefficient α as 0.074 and the vapor saturation f for each cell as 0.96 and 0.82, respectively. The D_0° for GgO in table 12 was calculated by using assumption 3 described above for table 10.

Benezech and Foex (1969) had used the entrainment method and a rotating solar furnace to study the vaporization of sesquioxides which served as their own containers. They had assumed that vaporization occurs as reaction 3 and had calculated pressures of the monoxides of La, Nd, Sm, Dy, Tb, Gd, Er, and Ho, which they gave on a small graph. At this time no attempt was made to read the graph; however, the authors did report 2nd and 3rd Law values of the ΔH_0° of reaction 3, involving La, Nd, Sm, and Gd, although they gave no sources for the values of the Gibbs free energy functions they had used.

Petzel and Greis (1971) had used the Knudsen effusion method to study the influence of tungsten on the vaporization behavior of Eu_2O_3 at 2192 K. They had placed both W and Eu_2O_3 in an iriduim-lined cell to control solid-solid contact, had analysed the effusate for a Eu/W molar ratio of 3.7 to 3.8, and had calculated partial pressures of various tungsten oxides and the dissociation energy of EuO which is given in table 12.

Recently Ackermann and Rauh (refs. 2, 3, and 4) have used both Knudsen effusion and mass-spectrometry to study the vaporization of some sesquioxides both alone and in the presence of their metals. They had also studied several isomolecular oxygen exchange reactions. The values of D_0° for LaO in table 12 were calculated from their rate of effusion and ion-intensity data which corresponds to the La_2O_3 vaporized in a Re cell. Only corrections for the metal atom and diatomic oxygen were made. A review of ref. 3 was not completed in time for inclusion here. In ref. 4 Ackermann and Rauh had used only mass-spectrometry to study the vaporization of Y_2O_3. Their YO^+ ion-intensity data was used to calculate from eq. 27 the 2nd Law value of D_0° for YO in table 12.

VII. References

1. R. J. Ackermann, E. G. Rauh, and R. J. Thorn, J. Chem. Phys., 40, 883 (1964).

2. R. J. Ackermann and E. G. Rauh, J. Chem. Thermodynamics, 3, 445 (1971).

3. R. J. Ackermann and E. G. Rauh, J. Chem. Thermodynamics, 3, 609 (1971).

4. R. J. Ackermann and E. G. Rauh, J. Chem. Thermodynamics, 5, 331 (1973).

5. C. B. Alcock and M. Peleg, Trans. Brit. Ceramic Soc., 66, 217 (1967).

6. L. L. Ames, P. N. Walsh, and D. White, J. Phys. Chem. 71, 2707 (1967).

7. F. B. Baker and C. E. Holley Jr., J. Chem. Eng. Data, 13, 405 (1968).

8. F. B. Baker, G. C. Fitzgibbon, D. Pavone, and C. E. Holley Jr., J. Chem. Thermodynamics, 4, 621 (1972).

9. G. Benezech and M. Foex, C. R. Acad. Sci., Paris, C268, 2315 (1969).

10. L. Brewer and G. M. Rosenblatt in "Advances in High Temperature Chemistry," Vol. 2, Leroy Eyring, Editor, Academic Press, New York, 1969, pp. 1-83.

11. S. N. Bushkovich, A. A. Ganichev, G. N. Petrov, and Yu. S. Rutgaizer, Industrial Lab. (USSR), 33, 441 (1967); Zavod. Lab., 33, 376 (1967).

12. K. D. Carlson, E. Ludena, and C. Moser, J. Chem. Phys. 43, 2408 (1965).

13. W. A. Chupka, M. G. Inghram, and R. F. Porter, Jr., J. Chem. Phys. 24, 792 (1956).

14. P. Coppens, S. Smoes, and J. Drowart, Trans. Faraday Soc., 63, 2140 (1967).

15. R. L. DeKock and W. Weltner, Jr., J. Phys. Chem., 75, 514 (1971).

16. R. C. Feber and C. C. Herrick, Atomic Energy Commission Report LA-3184, Los Alamos, N. M. (1965).

17. R. C. Feber and C. C. Herrick, J. Chem. Eng. Data, 12, 85 (1967).

18. G. C. Fitzgibbon, E. J. Huber, Jr., and C. E. Holley, Jr., J. Chem. Thermodynamics, 4, 349 (1972).

19. G. C. Fitzgibbon, E. J. Huber, Jr., and C. E. Holley, Jr., Rev. Chim. Min., 10, 29 (1973).

20. A. G. Gaydon, "Dissociation Energies and Spectra of Diatomic Molecules," Chapman and Hall Ltd., London (1968).

21. B. C. Gerstein, F. J. Jelinek, J. R. Mullaly, W. D. Shickell, and F. H. Spedding, J. Chem. Phys., 47, 5194 (1967).

22. H. W. Goldstein, P. N. Walsh, and D. White, J. Phys. Chem., 64, 1087 (1960).

23. H. W. Goldstein, P. N. Walsh, and D. White, J. Phys. Chem., 65, 1400 (1961).

24. D. W. Green, J. Phys. Chem., 75, 3103 (1971).

25. C. E. Holley, Jr., E. J. Huber, Jr., and F. B. Baker in "Progress in the Science and Technology of the Rare Earths," Vol. 3, Leroy Eyring, Editor, Pergamon Press, Oxford, 1968, p. 343-433.

26. E. J. Huber, Jr., and C. E. Holley, Jr., J. Amer. Chem. Soc., 77, 1444 (1955).

27. E. J. Huber, Jr., G. C. Fitzgibbon, and C. E. Holley, Jr., J. Chem. Thermodynamics, 3, 643 (1971).

28. R. Hultgren, P. D. Desai, D. T. Hawkins, M. Gleiser, K. K. Kelley, and D. D. Wagman, "Selected Values of the Thermodynamic Properties of the Elements," American Society for Metals, Metals Park, Ohio (1973).

29. M. G. Inghram, W. A. Chupka, and J. Berkowitz, Mem. Soc. Roy. Sci. Liege, 18, 513 (1957).

30. B. H. Justice, E. F. Westrum, Jr., E. Chang, and R. Radebaugh, J. Phys. Chem., 73, 333 (1969).

31. P. H. Kasai and W. Weltner, Jr., J. Chem. Phys., 43, 2553 (1965).

32. B. S. Kulvarskaia and R. S. Maslovskaia, Radio Eng. and Elect. (USSR), 5, 89 (1960); Radiotekh. i Elektron., 5, 1254 (1960).

33. D. R. Messier, J. Amer. Ceramic Soc., 50, 665 (1967).

34. M. B. Panish, J. Chem. Phys. 34, 1079 (1961); J. Chem. Phys., 34, 2197 (1961).

35. R. C. Paule and J. L. Margrave in "The Characterization of High Temperature Vapors," J. L. Margrave, Editor, John Wiley & Sons, Inc., New York, 1967, pp. 130-151.

36. T. Petzel and O. Greis, Rev. Int. Hautes Temp. Refract., 8, 269 (1971).

37. C. Pupp and K. A. Gingerich, J. Chem. Phys. 54, 3380 (1971).

38. B. Rosen, "Spectroscopic Data Relative to Diatomic Molecules," Pergamon Press, Oxford, 1970.

39. H. L. Schick, "Thermodynamics of Certain Refractory Compounds," Vols. 1 and 2, Academic Press, New York, 1966.

40. R. H. Schumm, D. D. Wagman, S. Bailey, W. H. Evans, and V. B. Parker, National Bureau of Standards Technical Note 270-7, U. S. Government Printing Office, Washington, D. C. 1973.

41. G. A. Semenov, Russian J. Inorg. Chem., 10, 1300 (1965).

42. S. A. Shchukarev and G. A. Semenov, Dokl. Akad. Nauk USSR, 141, 652 (1961).

43. S. Smoes, J. Drowart, and G. Verhaegen, J. Chem. Phys., 43, 732 (1965).

44. H. G. Staley and J. H. Norman, Int. J. Mass. Spect. and Ion Phys., 2, 35 (1969).

45. D. R. Stull and H. Prophet, "JANAF Thermochemical Tables", 2nd Edition, NSRDS-NBS 37, U. S. Government Printing Office, Washington, D. C., 1971.

46. S. N. Suchard, "Spectroscopic Constants for Selected Heteronuclear Diatomic Molecules," Vols. I, II, and III, The Aerospace Corp., El Segundo, Calif., 1974.

47. D. D. Wagman, W. H. Evans, V. B. Parker, I. Halow, S. M. Bailey, R. H. Schumm, and K. L. Churney, "Selected Values of Chemical Thermodynamic Properties", National Bureau of Standards Technical Note 270-5, U. S. Government Printing Office, Washington, D. C., 1971.

48. P. N. Walsh, D. F. Dever, and D. White, J. Phys. Chem., 65, 1410 (1961).

49. E. F. Westrum, Jr. and F. Grønvold in "Thermodynamics of Nuclear Materials", International Atomic Energy Agency, Vienna, 1962, p. 20.

50. D. White, P. N. Walsh, L. L. Ames, and H. W. Goldstein in "Thermodynamics of Nuclear Materials," International Atomic Energy Agency, Vienna, 1962, pp. 417-443.

Acknowledgement

Thanks go to R. H. Schumm and other members of the Chemical Thermodynamic Data Center at the National Bureau of Standards for use of their indexed files of published papers which they have been collecting for several years. A search of the literature was made considerably easier.

Chapter 10

Bibliography on Spectroscopy of Fluorides and Oxides Belonging to Lanthanide Series

This bibliography lists papers on the spectroscopy of lanthanide fluorides and oxides in gas, liquid, or solid phases. It also includes some papers dealint with the chemiluminescence or quenching of these compounds in excited states.

The list is divided into fiftene sections:

I. Cerium

- a. Cerium fluorides
- b. Cerium oxides
- c. Cerium oxide fluorides

II. Dysprosium

- a. Dysprosium fluorides
- b. Dysprosium oxides
- c. Dysprosium oxide fluorides

III. Erbium

- a. Erbium fluorides
- b. Erbium oxides
- c. Erbium oxide fluorides

IV. Europium

- a. Europium fluorides
- b. Europium oxides
- c. Europium oxide fluorides

V. Gadolinium

- a. Gadolinium fluorides
- b. Gadolinium oxides
- c. Gadolinium oxide fluorides

VI. Holmium

- a. Holmium fluorides
- b. Holmium oxides
- c. Holmium oxide fluorides

VII. Lanthanum

- a. Lanthanum fluorides
- b. Lanthanum oxides
- c. Lanthanum oxide fluorides

VIII. Lutetium

- a. Lutetium fluorides
- b. Lutetium oxides

IX. Neodymium

- a. Neodymium fluorides
- b. Neodymium oxides
- c. Neodymium oxide fluorides

X. Promethium

- a. Promethium fluorides
- b. Promethium oxides

XI. Praseodymium

- a. Praseodymium fluorides
- b. Praseodymium oxides
- c. Praseodymium oxide fluorides

XII. Samarium

- a. Samarium fluorides
- b. Samarium oxides
- c. Samarium oxide fluorides

XIII. Terbium

- a. Terbium fluorides
- b. Terbium oxides
- c. Terbium oxide fluorides

XIV. Thulium

- a. Thulium fluorides
- b. Thulium oxides

XV. Ytterbium

a. Ytterbium fluorides
b. Ytterbium oxides

The list is based on the files of the Chemical Kinetics Information Center and an examination of Chemical Abstracts (1967–1974).

Suggestions, additions and corrections are welcome.

The Chemical Kinetics Information Center, Institute for Materials Research, National Bureau of Standards, Washington, D.C. 20234, is part of the National Standard Reference Data System. The Center prepares bibliographies for general distribution and also in answer to specific requests.

The Center does not, normally, distribute copies of published papers or reports, although it will assist in the location of obscure or hard-to-obtain material. Papers should be obtained locally or from the author or publisher. Government R & D reports that are available to the public may be purchased from the National Technical Information Service, Springfield, Virginia 22151.

The Center indexes and stores copies of published papers and reports of research on chemical kinetics, photochemistry and collision dynamics. Contributions to its collection are welcome.

I. Cerium

(a). Cerium fluorides

Batsanov, S. S., Derbeneva, S. S., and Batsanova, L. R., Electronic Spectra of Rare Earth Metal Fluorides, Oxyfluorides and Oxides, Zh. Prikl. Spektrosk. 10, 332 (1969) (Russ); Chem. Abstr. 70:101332k (1969)

Bauman, R. P., and Porto, S. P. S., Lattice Vibrations and Structure of Rare-Earth Fluorides, Phys. Rev. 161, 842 (1967); Chem. Abstr. 67:112549a (1967)

Claudel, J., Hadni, A., and Strimer, P., Low-Frequency Vibration of Lanthanide Fluoride Lattices, C. R. Acad. Sci., Ser. B 274, 943 (1972) (Fr); Chem. Abstr. 77:40868k (1972)

Hadni, A., Strimer, P., and Vermillard, F., Far Infrared Absorption Observation of the Low Frequency Lines of Praseodymium Fluoride and Other Rare-Earth Fluorides, C. R. Acad. Sci., Ser. B 29, 1113 (1969) (Fr); Chem. Abstr. 72:49216a (1970)

Ovsyannikova, I. A., and Nasonova, L. I., L_{III} X-Ray Absorption Spectra of Praseodymium and Cerium and Effective Coordination Charges, Zh. Strukt. Khim. 11, 548 (1970) (Russ); Chem. Abstr. 73:82137u (1970)

Wertheim, G. K., Cohen, R. L., and Rosencwaig, A., Multiplet Splitting and Two-Electron Excitation in the Trivalent Rare Earths, Electron Spectrosc., Proc. Int. Conf. 1971, p. 813 (1972), Shirley, D. A., Ed., Chem. Abstr. 77:158530x (1972)

(b). Cerium oxides

Batsanov, S. S., Derbeneva, S. S., and Batsanova, L. R., Electronic Spectra of Rare Earth Metal Fluorides, Oxyfluorides and Oxides, Zh. Prikl. Spektrosk. 10, 332 (1969) (Russ); Chem. Abstr. 70:101332k (1969)

Bloor, D., and Dean, J. R., Spectroscopy of Rare-Earth Oxide Systems. I. Far-Infrared Spectra of the Rare-Earth Sesquioxides, Cerium Dioxide, and Nonstoichiometric Praseodymium and Terbium Oxides, J. Phys. C 5, 1237 (1972); Chem. Abstr. 77:54303j (1972)

Bonnelle, C., and Karnatak, R. C., Distribution of f-States in Rare-Earth Metals and Oxides, J. Phys. (Paris), Colloq. 230 (1971) (Fr); Chem. Abstr. 77:26817m (1972)

Bonnelle, C., and Karnatak, R. C., Distribution of f States in Rare-Earth Metals and Oxides, Colloq. Int. Cent. Nat. Rech. Sci. 1971, No. 196, 230 (Fr); Chem. Abstr. 77:81451n (1972)

Davidson, F. D., and Wyckoff, R. W. G., L and M X-Ray Spectra in the Region 2-85 A, Advan. X-Ray Anal. 9, 344 (1966); Chem. Abstr. 66:99767c (1967)

Demekhin, V. F., Platkov, A. I., and Lyubivaya, M. V., Multiplet Structure of the L-Series Lines of Rare-Earth Elements, Zh. Eksp. Teor. Fiz. 62, 49 (1972) (Russ); Chem. Abstr. 76:106015t (1972)

Derbeneva, S. S., and Batsanov, S. S., The Width of the Forbidden Zone for Rare-Earth Metal Oxides, Dokl. Akad. Nauk SSSR 175, 1062 (1967) (Russ); Chem. Abstr. 68:73735g (1968)

Fischer, D. W., and Baun, W. L., Self-Absorption Effects in the Soft X-Ray M_α and M_β Emission Spectra of the Rare Earth Elements, J. Appl. Phys. 38, 4830 (1967); Chem. Abstr. 68:17303c (1968)

Goldsmith, J. A., and Ross, S. D., Factors Affecting the Infrared Spectra of Some Planar Anions with D_{3h} Symmetry. III. The Spectra of Rare Earth Carbonates and their Thermal Decomposition Products, Spectrochim. Acta, Part A 23, 1909 (1967); Chem. Abstr. 67:68968k (1967)

Haensel, R., Rabe, P., and Sonntag, B., Optical Absorption of Cerium, Cerium Oxide, Praseodymium, Praseodymium Oxide, Neodymium, Neodymium Oxide, and Samarium in the Extreme Ultraviolet, Solid State Commun. 8, 1845 (1970); Chem. Abstr. 74:58999b (1971)

Lowndes, R. P., Parrish, J. F., and Perry, C. H., Optical Phonons and Symmetry of Tysonite Lanthanide Fluorides, Phys. Rev. 182, 913 (1969); Chem. Abstr. 71:75840y (1969)

McCrary, J. H., Singman, L. V., Ziegler, L. H., Looney, L. D., Edmonds, C. M., and Harris, C. E., L Fluorescent X-Ray Relative-Intensity Measurements, Phys. Rev. A 5, 1587 (1972); Chem. Abstr. 76:133772u (1972)

Ovsyannikova, I. A., and Nasonova, L. I., L_{III} X-Ray Absorption Spectra of Praseodymium and Cerium and Effective Coordination Charges, Zh. Strukt. Khim. 11, 548 (1970) (Russ); Chem. Abstr. 73:82137u (1970)

Petru, F., and Muck, A., Chemistry of Rare Earth elements. XXXVII. Infrared Absorption Spectra of CeO_2, Pr_6O_{11}, Nd_2O_3 and Sm_2O_3, Z. Chem. 7, 27 (1967) (Ger); Chem. Abstr. 67:27441q (1967)

Petru, F., and Muck, A., Chemistry of Rare Earth Elements. XL. Infrared Absorption Spectra of Oxides of the Lanthanides Eu. . .Lu, Z. Chem. 7, 159 (1967) (Ger); Chem. Abstr. 67:27442r (1967)

Sumbaev, O. I., Smirnov, Yu. P., Petrovich, E. V., Zykov, V. S., Egorov, A. I., and Grushko, A. I., Chemical Shifts of X-Ray $K\alpha_1$ Lines During Oxidation of Rare Earth Metals. Role of f-Electrons, Rentgen. Spektry Elektron. Strukt. Veshchestva 2, 172 (1969) (Russ); Chem. Abstr. 74:117626c (1971)

Sumbaev, O. I., Smirnov, Yu. P., Petrovich, E. V., Zykov, V. S., Egorov, A. I., and Grushko, A. I., Chemical Shifts of the $K\alpha_1$ X-Ray Lines During Oxidation of Rare Earth Metals. Role of f-electrons, Zh. Eksp. Teor. Fiz. 56, 536 (1969) (Russ); Chem. Abstr. 71:7985z (1969)

Vainshtein, E. E., Blokhin, S. M., and Bertenev, V. M., X-Ray Spectrum Study of Some Cerium and Praseodymium Compounds, Izv. Sib. Otd. Akad. Nauk SSSR, Ser. Khim. Nauk, 59 (166) (Russ); Chem. Abstr. 66:41906f (1967)

Weltner, W., Jr., and DeKock, R. L., Spectroscopy of Rare Earth Oxide Molecules in Inert Matrices at 4°K, J. Phys. Chem. 75, 514 (1971); Chem. Abstr. 74:105048c (1971)

(c). Cerium oxide fluorides

Batsanov, S. S., Derbeneva, S. S., and Batsanova, L. R., Electronic Spectra of Rare Earth Metal Fluorides, Oxyfluorides and Oxides, Zh. Prikl. Spektrosk. 10, 332 (1969) (Russ); Chem. Abstr. 70:101332k (1969)

II. Dysprosium

(a). Dysprosium fluorides

Batsanov, S. S., Derbeneva, S. S., and Batsanova, L. R., Electronic Spectra of Rare Earth Metal Fluorides, Oxyfluorides and Oxides, Zh. Prikl. Spektrosk. 10, 332 (1969) (Russ); Chem. Abstr. 70:101332k (1969)

Chase, E. W., Hepplewhite, R. T., Krupka, D. C., and Kahng, D., Electroluminescence of Zinc Sulfide Lumocen Devices Containing Rare-Earth and Transition-Metal Fluorides, J. Appl. Phys. 40, 2512 (1969); Chem. Abstr. 71:34384j (1969)

Chen, Y. S., DePaolis, M. V., Jr., and Kahng, S., Characteristics of Pulse-Excited Electroluminescence from Zinc Sulfide Films Containing Rare Earth Fluoride, Proc. IEEE 58, 184 (1970); Chem. Abstr. 72:115816z (1970)

Wertheim, G. K., Cohen, R. L., Rosencwaig, A., and Guggenheim, H. J., Multiplet Splitting and Two-Electron Excitation in the Trivalent Rare Earths, Electron. Spectrosc., Proc. Int. Conf. 1971, p. 813 Chem. Abstr. 77:158530x (1972)

Wertheim, G. K., Rosencwaig, S., Cohen, R. L., and Guggenheim, H. J., Exchange Splitting in the 4f Photoelectron Spectra of the Rare Earths, Phys. Rev. Lett. 27, 505 (1971); Chem. Abstr.75:103444a (1971)

(b). Dysprosium oxides

Batsanov, S. S., Derbeneva, S. S., and Batsanova, L. R., Electronic Spectra of Rare Earth Metal Fluorides, Oxyfluorides and Oxides, Zh. Prikl. Spektrosk. 10, 332 (1969) (Russ); Chem. Abstr. 70:101332k (1969)

Bloor, D., and Dean, J. R., Spectroscopy of Rare-Earth Oxide Systems. I. Far-infrared Spectra of the Rare-Earth Sesquioxides, Cerium Dioxide, and Nonstoichiometric Praseodymium and Terbium Oxides, J. Phys. C 5, 1237 (1972); Chem. Abstr. 77:54303j (1972)

Bonnelle, C., and Karnatak, R. C., Distribution of f States in Rare Earth Metals and Oxides, Colloq. Int. Cent. Nat. Rech. Sci. No 196, 230 (1971); Chem. Abstr. 77:31451n (1972)

Bonnelle, C., and Karnatak, R. C., Distribution of f-States in Rare-Earth Metals and Oxides, J. Phys. (Paris), Colloq., p. 230 (1971); Chem. Abstr. 77:26817m (1972)

Chen, Y. S., DePaolis, M. V., Jr., and Kahng, D., Characteristics of Pulse-Excited Electroluminescence from Zinc Sulfide Films Containing Rare Earth Fluoride, Proc. IEEE 58, 184 (1970); Chem. Abstr. 72:115816z (1970)

Davidson, F. D., and Wyckoff, R. W. G., L and M X-Ray Spectra in the Region 2-85 A, Advan. X-Ray Anal 9, 344 (1966); Chem. Abstr. 66:99767c (1967)

Demekhin, V. F., Platkov, A. I., Lyubivaya, M. V., Multiplet Structure of the L-Series Lines of Rare-Earth Elements, Zh. Eksp. Teor. Fiz. 62, 49 (1972) (Russ); Chem. Abstr. 76:106015t (1972)

Dentai, A. G., Fluorescent High Alumina Ceramic Substrates, Amer. Ceram. Soc., Bull. 51, 681 (1972); Chem. Abstr. 77:143291w (1972)

Derbeneva, S. S., and Batsanov, S. S., The Width of the Forbidden Zone for Rare-Earth Metal Oxides, Dokl. Akad. Nauk SSSR 175, 1062 (1967); Chem. Abstr. 68:73735g (1968)

Fischer, D. W., and Baun, W. L., Self-Absorption Effects in the Soft X-Ray Mα and Mβ Emission Spectra of the Rare Earth Elements, J. Appl. Phys. 38, 4830 (1967); Chem. Abstr. 68:17303c (1968)

Goldsmith, J. A., and Ross., S. D., Factors Affecting the Infrared Spectra of Some Planar Anions with D_{3h} Symmetry. II. The Spectra of Rare Earth Carbonates and Their Thermal Decomposition Products, Spectrochim. Acta, Part A 23, 1909 (1967); Chem. Abstr. 67:68968k (1967)

Petru, F., and Muck A., Chemistry of Rare Earth Elements. XL. Infrared Absorption Spectra of Oxides of the Lanthanides Eu...Lu, Z. Chem. 7, 159 (1967); Chem. Abstr. 67:27442r (1967)

Ratinen, H., X-Ray Excited Optical Fluorescence of Nine Rare Earth Ions in Yttrium Oxide, Gadolinium Oxide, and Lanthanum Oxide, Acta Polytechn. Scand., Chem. Incl. Met. Ser. No. 107 (1971); Chem. Abstr. 76:106021s (1972)

Sumbaev, O. I., Smirnov, Yu. P., Petrovich, E. V., Zykov, V. S., Egorov, A. I., and Grushko, A. I., Chemical Shifts of X-Ray $K\alpha_1$ Lines During Oxidation of Rare Earth Metals. Role of f-Electrons, Rentgen. Spektry Elektron. Strukt. Veshchestva 2, 172 (1969); Chem. Abstr. 74:117626c (1971)

Sumbaev, O. I., Smirnov, Yu. P., Petrovich, E. V., Zykov, V. S., Egorov, A. I., Grushko, A. I., Chemical Shifts of the $K_{\alpha 1}$ X-Ray Lines During Oxidation of Rare Earth Metals. Role of f-Electrons, Zh. Eksp. Teor. Fiz. 56, 536 (1969) (Russ); Chem. Abstr. 71:7985z (1969)

Weltner, W., Jr., and DeKock, R. L., Spectroscopy of Rare Earth Oxide Molecules in Inert Matrices at 4°K, J. Phys. Chem. 75, 514 (1971); Chem. Abstr. 74:105048c (1971)

White, W. B., Diffuse-Reflectance Spectra of Rare Earth Oxides, Appl. Spectrosc. 21, 167 (1967); Chem. Abstr. 67:69158h (1967)

(c). Dysprosium oxide fluorides

Batsanov, S. S., Derbeneva, S. S., and Batsanova, L. R., Electronic Spectra of Rare Earth Metal Fluorides, Oxyfluorides and Oxides, Zh. Prikl. Spektrosk. 10, 332 (1969) (Russ); Chem. Abstr. 70:101332k (1969)

III. Erbium

(a). Erbium fluorides

Batsanov, S. S., Derbeneva, S. S., and Batsanova, L. R., Electronic Spectra of Rare Earth Metal Fluorides, Oxyfluorides and Oxides, Zh. Prikl. Spektrosk. 10, 332 (1969) (Russ); Chem. Abstr. 70:101332k (1969)

Chase, E. W., Hepplewhite, R. T., Krupka, D. C., and Kahng, D., Electroluminescence of Zinc Sulfide Lumocen Devices Containing Rare-Earth and Transition-Metal Fluorides, J. Appl. Phys. 40, 2512 (1969); Chem. Abstr. 71:34384j (1969)

Chen, Y. S., DePaolis, M. V., Jr., and Kahng, D., Characteristics of Pulse-Excited Electroluminescence from Zinc Sulfide Films Containing Rare Earth Fluoride, Proc. IEEE 58, 184 (1970); Chem. Abstr. 72:115816z (1970)

Hadni, A., Morlot, G., and Strimer, P., Far-Infrared Electronic Transitions in Solids, J. Quantum Electron. 3, 111 (1967); Chem. Abstr. 67:86235y (1967)

Joergensen, C. K., and Berthou, H., Measurements of Photoelectron Spectra and Charging Effects in Fluorides, Iodates, and Oxides, J. Fluorine Chem. 2, 425 (1973); Chem. Abstr. 78:130353u (1973)

Taylor, M. D., Cheung, T. T., and Hussein, M. A., Variations of the Infrared Spectra with the Nature and Structure of the Rare Earth Metal Halides, J. Inorg. Nucl. Chem. 34, 3073 (1972); Chem. Abstr. 77:132692b (1972)

Vakhidov, Sh. A., Kaipov, B., and Tavshunskii, G. A., Luminescence of CaF_2-LnF_3 Crystals in a Cobalt-60 γ-Ray Field, Opt. Spektrosk. 28, 949 (1970) (Russ); Chem. Abstr. 73:82314z (1970)

Wertheim, G. K., Cohen, R. L., Rosencwaig, A., and Guggenheim, H. J., Multiplet Splitting and Two-electron Excitation in the Trivalent Rare Earths, Electron Spectrosc., Proc. Int. Conf. 1971, p. 813 Chem. Abstr. 77:153530x (1972)

(b). Erbium oxides

Batsanov, S. S., Derbeneva, S. S., and Batsanova, L. R., Electronic Spectra of Rare Earth Metal Fluorides, Oxyfluorides and Oxides, Zh. Prikl. Spektrosk. 10, 332 (1969) (Russ); Chem. Abstr. 70:101332k (1969)

Bloor, D., and Dean, J. R., Spectroscopy of Rare-Earth Oxide Systems. I. Far-infrared Spectra of the Rare-Earth Sesquioxides, Cerium Dioxide, and Nonstoichiometric Praseodymium and Terbium Oxides, J. Phys. C 5, 1237 (1972); Chem. Abstr. 77:54303j (1972)

Davidson, F. D., and Wyckoff, R. W. G., L and M X-Ray Spectra in the Region 2-85 A, Advan. X-Ray Anal. 9, 344 (1966); Chem. Abstr. 66:99767c (1967)

Demekhin, V. F., Platkov, A. I., and Lyubivaya, M. V., Multiplet Structure of the L-Series Lines of Rare-Earth Elements, Zh. Eksp. Teor. Fiz. 62, 49 (1972); Chem. Abstr. 76:106015t (1972)

Derbeneva, S. S., and Batsanov, S. S., The Width of the Forbidden Zone for Rare-Earth Metal Oxides, Dokl. Akad. Nauk SSSR 175, 1062 (1967) (Russ); Chem. Abstr. 68:73735g (1968)

Fischer, D. W., and Baun, W. L., Self-Absorption Effects in the Soft X-Ray Mα and Mβ Emission Spectra of the Rare Earth Elements, J. Appl. Phys. 38, 4830 (1967); Chem. Abstr. 68:17303c (1968)

Goldsmith, J. A., and Ross, S. D., Factors Affecting the Infrared Spectra of Some Planar Anions with D_{3h} Symmetry. III. The Spectra of Rare Earth Carbonates and Their Thermal Decomposition Products, Spectrochim. Acta, Part A 23, 1909 (1967); Chem. Abstr. 67:68968k (1967)

Gruber, J. B., Two Photon Spectroscopy. Rare Earth and Actinide Ions in Single Crystals, Proc. Rare Earth Res. Conf., 9th 1971, 2, p. 466 Chem. Abstr. 77:11898q (1972)

Gruss, L. L., Electronic Spectra of Solid Solutions of Erbium and Ytterbium Oxides, Diss. Abstr. Int. B 31, 5902 (1971); Chem. Abstr. 76:8365n (1972)

Guazzoni, G. E., and Shapiro, S. J., Spectral Emittance of Neodymium, Samarium, Erbium, and Ytterbium Oxides at High Temperatures, Nat. Tech. Inform. Serv., AD 708547 (1970); Chem. Abstr. 74:36594p (1971)

Hoskins, R. H., and Soffer, B. H., Energy Transfer and CW Laser Action in $HO^{2+}:Er_2O_2$, IEEE(Inst. Elec. Electron. Eng.), J. Quantum Electron. 2, 253 (1966); Chem. Abstr. 66:60594u (1967)

Joergensen, C. K., and Berthou, H., Measurements of Photoelectron Spectra and Charging Effects in Fluorides, Iodates, and Oxides, J. Fluorine Chem. 2, 425 (1973); Chem. Abstr. 78:130358u (1973)

McMahon, W. R., Hemispherical Spectral Emittance of Selected Rare Earth Oxides, U.S. At. Energy Comm., IS-T-182 (1967); Chem. Abstr. 69:6796k (1968)

Matsubara, T., Mixed Rare Earth Phosphors, Japan Kokai 73 26, 685 (Cl.13(9)-C112, 7 Apr 73, Appl. 71 61,170, 11 Aug 71; Chem. Abstr. 79:25573h (1973)

Petru, F., and Muck, A., Chemistry of Rare Earth Elements. XL. Infrared Absorption Spectra of Oxides of the Lanthanides Eu. . .Lu, Z. Chem. 7, 159 (1967) (Ger); Chem. Abstr. 67:27442r (1967)

Satybaev, N. M., and Ganichenko, L. G., Photoluminescence of Some Rare Earth Oxides, Dokl. Nauch.-Tekh. Konf. Itogam Nauch.-Issled Rab. 1966-1967 gg. Mosk. Energ. Inst. Sekts. Elektron. Tekh. Podsekts. Poluprov. Proborov. p 150 (1967) (Russ); Chem. Abstr. 69:72576q (1968)

Sumbaev, O. I., Smirnov, Yu. P., Petrovich, E. V., Zykov, V. S., Egorov, A. I., and Grushko, A. I., Chemical Shifts of X-Ray $K\alpha_1$ Lines During Oxidation of Rare Earth Metals, Rentgen. Spektry Elektron. Strukt. Veshchestva 2, 172 (1969); Chem. Abstr. 74:117626c (1971)

Sumbaev, O. I., Smirnov, Yu. P., Petrovich, E. V., Zykov, V. S., Egorov, A. I., and Grushko, A. I., Chemical Shifts of the $K\alpha_1$ X-Ray Lines During Oxidation of Rare Earth Metals. Role of f-Electrons, Zh. Eksp. Teor. Fiz. 56, 536 (1969) (Russ); Chem. Abstr. 71:7985z (1969)

Weltner, W. Jr., and De Kock, R. L., Spectroscopy of Rare Earth Oxide Molecules in Inert Matrices at 4°K, J. Phys. Chem. 75, 514 (1971); Chem. Abstr. 74:105048c (1971)

White, W. B., Diffuse-Reflectance Spectra of Rare Earth Oxides, Appl. Spectrosc. 21, 167 (1967); Chem. Abstr. 67:69158h (1967)

(c). Erbium oxide fluorides

Batsanov, S. S., Derbeneva, S. S., and Batsanova, L. R., Electronic Spectra of Rare Earth Metal Fluorides, Oxyfluorides and Oxides, Zh. Prikl. Spektrosk. 10, 332 (1969) (Russ); Chem. Abstr. 70:101332k (1969)

IV. Europium

(a). Europium fluorides

Batsanov, S. S., Derbeneva, S. S., and Batsanova, L. R., Electronic Spectra of Rare Earth Metal Fluorides, Oxyfluorides and Oxides, Zh. Prikl. Spektrosk. 10, 332 (1969) (Russ); Chem. Abstr. 70:101332k (1969)

Caspers, H. H., Rast, H. E., and Fry, J. L., Optical Absorption and Fluorescence Spectra of Europium Trifluoride, J. Chem. Phys 47, 4505 (1967); Chem. Abstr. 68:55153m (1968)

Chase, E. W., Hepplewhite, R. T., Krupka, D. C., and Kahng, D., Electroluminescence of Zinc Sulfide Lumocen Devices Containing Rare-Earth and Transition-Metal Fluorides, J. Appl. Phys. 40, 2512 (1969); Chem. Abstr. 71:34384j (1969)

DeKock, C. W., Wesley, R. D., and Radtke, D. D., Infrared Spectra and Geometries of Rare Earth Dihalides. Samarium(II) Fluoride, Samarium(II) Chloride, Europium(II) Fluoride, Europium(II) Chloride, Ytterbium(II) Fluoride, and Ytterbium(II) Chloride, High Temp. Sci. 4, 41 (1972); Chem. Abstr. 76:119428e (1972)

Freiser, M. J., Holtzberg, F., Methfessel, S. I., and Pettit, G. D., Shafer, M. W., and Suits, J. C., Magnetic Red Shift in Europium Chalcogenides, Helv. Phys. Acta 41, 832 (1968); Chem. Abstr. 70:32997s (1969)

Joergensen, C. K., and Berthou, H., Measurements of Photoelectron Spectra and Charging Effects in Fluorides, Iodates, and Oxides, J. Fluorine Chem. 2, 425 (1973); Chem. Abstr. 78:130358u (1973)

Petrovich, E. V., Smirnov, Yu. P., Zykov, V. S., Grushko, A. I., Sumbaev, O. I., Band I. M., and Trzhaskovskii, M. B., Chemical Shifts of the $K\alpha_{1,2}$ $K\beta_{1,3}$ and $K\beta_{2,4}$ X-Ray Lines in Heavy Elements due to s-, p-, d-, or f-Valency Electrons, Zh. Eksp. Teor. Fiz. 61, 1756 (1971) (Russ); Chem. Abstr. 76:65903k (1972)

Taylor, M. D., Cheung, T. T., and Hussein, M. A., Variations of the Infrared Spectra with the Nature and Structure of the Rare Earth Metal Halides, J. Inorg. Nucl. Chem. 34, 3073 (1972); Chem. Abstr. 77:132692b (1972)

Wertheim, G. K., Cohen, R. L., Rosencwaig, A., and Guggenheim H. J., Multiplet Splitting and Two-Electron Excitation in the Trivalent Rare Earths, Electron Spectrosc., Proc. Int. Conf. 1971, p. 813, (Pub. 1972), Shirley, D. A., Ed.; Chem. Abstr. 77:158530x (1972)

(b). Europium oxides

Batsanov, S. S., Derbeneva, S. S., and Batsanova, L. R., Electronic Spectra of Rare Earth Metal Fluorides, Oxyfluorides and Oxides, Zh. Prikl. Spektrosk. 10, 332 (1969) (Russ); Chem. Abstr. 70:101332k (1969)

Bloor, D., and Dean, J. R., Spectroscopy of Rare-Earth Oxide Systems. I. Far-Infrared Spectra of the Rare-Earth Sesquioxides, Cerium Dioxide, and Nonstoichiometric Praseodymium and Terbium Oxides, J. Phys. C 5, 1237 (1972); Chem. Abstr. 77:54303j (1972)

Bonnelle, C., and Karnatak, R. C., Distribution of f States in Rare-Earth Metals and Oxides, Colloq. Int. Cent. Nat. Rech. Sci. 1971, No. 196, 230 (Fr); Chem. Abstr. 77:81451n (1972)

Bonnelle, C., and Karnatak, R. C., Distribution of f-States in Rare-Earth Metals and Oxides, J. Phys. (Paris), Colloq. p. 230 (1971) (Fr); Chem. Abstr. 77:26817m (1972)

Busch, G., Guentherodt, G., and Wachter, P., Optical Transitions and the Energy Level Scheme of the Europium Chalcogenides, J. Phys. (Paris), Colloq. 1971, No. 1 Part 2, C1, 928; Chem. Abstr. 75:27774r (1971)

Demekhin, V. F., Platkov, A. I., and Lyubivaya, M. V., Multiplet Structure of the L-Series Lines of Rare-Earth Elements, Zh. Eksp. Teor. Fiz. 62, 49 (1972) (Russ); Chem. Abstr. 76:106015t (1972)

Dentai, A. G., Fluorescent High Alumina Ceramic Substrates, Amer. Ceram. Soc., Bull. 51, 681 (1972); Chem. Abstr. 77:143291w (1972)

Derbeneva, S. S., and Batsanov, S. S., The Width of the Forbidden Zone for Rare-Earth Metal Oxides, Dokl. Akad. Nauk SSSR 175, 1062 (1967) (Russ); Chem. Abstr. 68:73735g (1968)

Dimmock, J. O., Hanus, J., and Feinleib, J., Multiplet Structure in the Reflectance Spectra of Europium Chalcogenides, J. Appl. Phys. 41, 1088 (1970); Chem. Abstr. 73:20105y (1970)

Fischer, D. W., and Baun, W. L., Self-Absorption Effects in the Soft X-Ray Mα and Mβ Emission Spectra of the Rare Earth Elements, J. Appl. Phys. 38, 4830 (1967); Chem. Abstr. 68:17303c (1968)

Freiser, M. J., Holtzberg, F., Methfessel, S. I., Pettit, G. D., Shafer, M. W., and Suits, J. C., Magnetic Red Shift in Europium Chalcogenides, Helv. Phys. Acta 41, 832 (1968); Chem. Abstr. 70:32997s (1969)

Golding, B., Barmatz, M., Buehler, E., and Salamon, M. B., Critical Acoustic Relaxation in Europium(II) Oxide, Phys. Rev. Lett. 30, 968 (1973); Chem. Abstr. 80:74399k (1974)

Goldsmith, J. A., and Ross, S. D., Factors Affecting the Infrared Spectra of Some Planar Anions with D_{3h} Symmetry. III. The Spectra of Rare Earth Carbonates and Their Thermal Decomposition Products, Spectrochim. Acta, Part A 23, 1909 (1967); Chem. Abstr. 67:68968k (1967)

Guentherodt, G., Wachter, P., and Imboden, D. M., Energy Level Scheme and the Effect of Magnetic Order on the Optical Transitions in Europium Chalcogenides, Phys. Kondens. Mater. 12, 292 (1971); Chem. Abstr. 75:82049h (1971)

Hill, P., and Huefner, S., Lineshift and Linewidth in Optical Spectra of Europium Salts, Z. Phys. 240, 168 (1970); Chem. Abstr. 74:47651f (1971)

Hulin, D., Benoit a la Guillaume, C., and Hanus, J., Magnon Sidebands in the Luminescence Spectrum of Ferromagnetic Europium Oxide, AIP (Amer. Inst. Phys.) Conf. Proc. 1972, No. 5 (Pt. 2), p. 850; Chem. Abstr. 77:26858a (1972)

Hulin, D., Benoit a la Guillaume, C., and Hanus, J., Lateral Magnon Emission Bands in Ferromagnets, C. R. Acad. Sci., Ser. B 272, 1207 (1971); Chem. Abstr. 75:81792h (1971)

Joergensen, C. K., and Berthou, H., Measurements of Photoelectron Spectra and Charging Effects in Fluorides Iodates, and Oxides, J. Fluorine Chem. 2, 425 (1973); Chem. Abstr. 78:130358u (1973)

Petru, F., and Muck, A., Chemistry of Rare Earth Elements. XL. Infrared Absorption Spectra of oxides of the Lanthanides Eu. . .Lu, Z. Chem. 7, 159 (1967) (Ger); Chem. Abstr. 67:27442r (1967)

Ratinen, H., X-Ray Excited Optical Fluorescence of Nine Rare Earth Ions in Yttrium Oxide, Gadolinium Oxide, and Lanthanum Oxide, Acta Polytech. Scand., Chem. Incl. Met. Ser. No. 107 (1971); Chem. Abstr. 76:106021s (1972)

Ryl′nikov, A. S., Ivanov, G. A., Marushenko, V. I., Smirnov, A. I., and Sumbaev, O. I., Isotopic Effect of the Hyperfine Broadening of X-Ray Lines, Pis′ma Zh. Eksp. Teor. Fiz. 12, 128 (1970) (Russ); Chem. Abstr. 73:125179d (1970)

Sinha, S. P., Reflection Spectra of Europium(II), Europium(III), and Gadolinium(III) Oxides, Indian J. Chem. 5, 451 (1967); Chem. Abstr. 68:109780j (1968)

Sumbaev, O. I., Smirnov, Yu. P., Petrovich, E. F., Zykov, V. S., Egorov, A. I., and Grushko, A. I., Chemical Shifts of X-Ray $K\alpha_1$ Lines during Oxidation of Rare Earth Metals. Role of f-Electrons, Rentgen. Spektry Elektron. Strukt. Veshchestva 2, 172 (1969); Chem. Abstr. 74:117626c (1971)

Sumbaev, O. I., Smirnov, Yu. P., Petrovich, E. V., Zykov, V. S., Egorov, A. I., Grushko, A. I., Chemical Shifts of the $K\alpha_1$ X-Ray Lines during Oxidation of Rare Earth Metals. Role of f-Electrons, Zh. Eksp. Teor. Fiz. 56, 536 (1969) (Russ); Chem. Abstr. 71:7985z (1969)

Trond, S. S., Martin, J. S., Stranavage, J. P., and Smith, A. L., Properties of some Selected Europium-Activated Red Phosphors, J. Electrochem. Soc. 116, 1047 (1969); Chem. Abstr. 71:43407w (1969)

Tsu, R., and Esaki, L., Luminescence Spectra of Europium Chalcogenides: Europium Oxide, Europium Sulfide, and Europium Selenide, Phys. Rev. Lett. 24, 455 (1970); Chem. Abstr. 72:126968b (1970)

White, W. B., Diffuse-Reflectance Spectra of Rare Earth Oxides, Appl. Spectrosc. 21, 167 (1967); Chem. Abstr. 67:69158h (1967)

(c). Europium oxide fluorides

Batsanov, S. S., Derbeneva, S. S., and Batsanova, L. R., Electronic Spectra of Rare Earth Metal Fluorides, Oxyfluorides and Oxides, Zh. Prikl. Spektrosk. 10, 332 (1969) (Russ); Chem. Abstr. 70:101332k (1969)

Briffaut, J. P., Spectral Study of Eu^{3+} in Rhombohedral EuOF, C. R. Acad. Sci., Ser. B 269, 1281 (169); Chem. Abstr. 72:84615b (1970)

V. Gadolinium

(a). Gadolinium fluorides

Batsanov, S. S., Derbeneva, S. S., and Batsanova, L. R., Electronic Spectra of Rare Earth Metal Fluorides, Oxyfluorides and Oxides, Zh. Prikl. Spektrosk. 10, 332 (1969) (Russ); Chem. Abstr. 70:101332k (1969)

Batsanov, S. S., and Kustova, G. N., Effect of Structural Defects on the Infrared Spectra of Rare-Earth Metal Oxides and Fluorides, Spektrosk. Tverd. Tela p. 249 (1969); Chem. Abstr 73:135527e (1970)

Gil'fanov, F. Z., and Stolov, A. L., Reflection Spectrum of Gd_2O_3 and GdF_3 Powders, Zh. Prikl. Spektrosk. 6, 511 (1967) (Russ); Chem. Abstr 67:77559e (1967)

Hewes, R. A., Multiphoton Excitation and Efficiency in the Yb^{3+}-Ho^{3+}, -Er^{3+}, -Tm^{3+} Systems, Proc. Int. Conf. Lumin. p 778 (1969); F. Williams, Ed., North-Holland Publ. Co., Amsterdam, Neth., (Publ. 1970); Chem. Abstr 74:17762a (1971)

Hewes, R. A., and Sarver, J. F., Infrared Excitation Processes for the Visible Luminescence of Erbium(III), Holmium(III), and Thulium(III) in Ytterbium(III) Sensitized Rare-Earth Trifluorides, Phys. Rev. 182, 427 (1969); Chem. Abstr 71:65731z (1969)

Joergensen, C. K., and Berthou, H., Measurements of Photoelectron Spectra and Charging Effects in Fluorides, Iodates, and Oxides, J. Fluorine Chem. 2, 425 (1973); Chem. Abstr. 78:130353u (1973)

Low, N. M., and Major, A. L., Effects of Preparation on the Anti-Stokes Luminescence of Erbium-Activated Rare-Earth Phosphors, J. Lumin. 4, 357 (1971); Chem. Abstr 76:133736k (1972)

Taylor, M. D., Cheung, T. T., and Hussein, M. A., Variations of the Infrared Spectra with the Nature and Structure of the Rare Earth Metal Halides, J. Inorg. Nucl. Chem. 34, 3073 (1972); Chem. Abstr. 77:132692b (1972)

Wertheim, G. K., Cohen, R. L., Rosencwaig, A., and Guggenheim, H. J., Multiplet Splitting and Two-Electron Excitation in the Trivalent Rare Earths, Electron. Spectrosc., Proc. Int. Conf. 1971, p. 813, (Pub. 1972), Shirley, D. A., Ed.; Chem. Abstr. 77:158530x (1972)

Wertheim, G. K., Rosencwaig, S., Cohen, R. L., and Guggenheim, H. J., Exchange Splitting in the 4f Photoelectron Spectra of the Rare Earths, Phys. Rev. Lett. 27, 505 (1971); Chem. Abstr 75:103444a (1971)

(b). Gadolinium oxides

Batsanov, S. S., Derbeneva, S. S., and Batsanova, L. R., Electronic Spectra of Rare Earth Metal Fluorides, Oxyfluorides and Oxides, Zh. Prikl. Spektrosk. 10, 332 (1969) (Russ); Chem. Abstr. 70:101332k (1969)

Bloor, D., and Dean, J. R., Spectroscopy of Rare-Earth Oxide Systems. I. Far-Infrared Spectra of the Rare-Earth Sesquioxides, Cerium Dioxide, and Nonstoichiometric Praseodymium and Terbium Oxides, J. Phys. C 5, 1237 (1972); Chem. Abstr. 77:54303j (1972)

Bonnelle, C., and Karnatak, R. C., Distribution of f States in Rare Earth Metals and Oxides, Collq. Int. Cent. Nat. Rech. Sci. 1971, No. 196, p. 230 (Fr); Chem. Abstr. 77:81451n (1972)

Bonnelle, C., and Karnatak, R. C., M Spectra [X-Ray] of Gadolinium in the Metal and the Oxide, C. R. Acad. Sci., Paris, Ser. A,B 268, 494 (1969) (Fr); Chem. Abstr 70:82492u (1969)

Bonnelle, C., and Karnatak, R. C., Distribution of f-States in Rare-Earth Metals and Oxides, J. Phys. (Paris), Colloq. p. 230 No. 4 (1971) (Fr); Chem. Abstr. 77:26817m (1972)

Boulon, G., Photoluminescence Processes in Bismuth Ion Activated Polycrystalline Rare Earth Oxides and Orthovanadates, J. Phys. (Paris) 32, 333 (1971) (Fr); Chem. Abstr 75:82137k (1971)

Datta, R, K., Luminescent Behavior of Bismuth in Rare Earth Oxides, Electrochem. Soc. 114, 1137 (1967); Chem. Abstr 68:64265b (1968)

Davidson, F. D., and Wyckoff, R. W. G., L and M X-Ray Spectra in the Region 2-85 A, Advan. X-Ray Anal. 9, 344 (1966); Chem. Abstr. 66:99767c (1967)

Demekhin, V. F., Platkov, A. I., and Lyubivaya, M. V., Multiplet Structure of the L-Series Lines of Rare-Earth Elements, Zh. Eksp. Teor. Fiz. 62, 49 (1972) (Russ); Chem. Abstr. 76:106015t (1972)

Derbeneva, S. S., and Batsanov, S. S., The Width of the Forbidden Zone for Rare-Earth Metal Oxides, Dokl. Akad. Nauk SSSR 175, 1062 (1967) (Russ); Chem. Abstr. 68:73735g (1968)

Fischer, D. W., and Baun, W. L., Self-Absorption Effects in the Soft X-Ray $M\alpha$ and $M\beta$ Emission Spectra of the Rare Earth Elements, J. Appl. Phys. 38, 4830 (1967); Chem. Abstr. 68:17303c (1968)

Gil'fanov, F. Z., and Stolov, A. L., Reflection Spectrum of Gd_2O_3 and GdF_3 Powders, Zh. Prikl. Spektrosk. 6, 511 (1967) (Russ); Chem. Abstr 67:77559e (1967)

Goldsmith, J. A., and Ross, S. D., Factors Affecting the Infrared Spectra of Some Planar Anions with D_{3h} Symmetry. III. The Spectra of Rare Earth Carbonates and Their Thermal Decomposition Products, Spectrochim. Acta, Part A 23, 1909 (1967); Chem. Abstr. 67:68968k (1967)

Joergensen, C. K., and Berthou, H., Measurements of Photoelectron Spectra and Charging Effects in Fluorides, Iodates, and Oxides, J. Fluorine Chem. 2, 425 (1973); Chem. Abstr. 78:130358u (1973)

Karyakin, A. V., Davitashvili, E. G., and Kublashvili, Zh. Sh., Infrared Absorption Spectra of Carbonates and Oxalates of some Rare Earth Group Metals, Soobschch. Akad. Nauk Gruz SSR 55, 297 (1969) (Russ); Chem. Abstr 71:117990e (1969)

Low, N. M., and Major, A. L., Effects of Preparation on the Anti-Stokes Luminescence of Erbium-Activated Rare-Earth Phosphors, J. Lumin. 4, 357 (1971); Chem. Abstr 76:133736k (1972)

McMahon, W. R., Hemispherical Spectral Emittance of Selected Rare Earth Oxides, U. S. At. Energy Comm., IS-T-182, (1967); Chem. Abstr. 69:6796k (1968)

Matsubara, T., Mixed Rare Earth Phosphors, Japan Kokai 73 26.685 (Cl. 13(9)-C112), 7 Apr. 1973, Appl. 71 61,170, 11 Aug 1971; 4 pp.; Chem. Abstr 79:25573h (1973)

Petru, F., and Muck, A., Chemistry of Rare Earth Elements. XL. Infrared Absorption Spectra of Oxides of the Lanthanides Eu. . .Lu, Z. Chem. 7, 159 (1967) (Ger); Chem. Abstr. 67:27442r (1967)

Ratinen, H., X-Ray Excited Optical Fluorescence of Nine Rare Earth Ions in Yttrium Oxide, Gadolinium Oxide, and Lanthanum Oxide, Acta Polytech. Scand., Chem. Incl. Met. Ser. No. 107, 19 pp. (1971); Chem. Abstr 76:106021s (1972)

Sinha, S. P., Reflection Spectra of Europium(II), Europium(III), and Gadolinium(III) Oxides, Indian J. Chem. 5, 451 (1967); Chem. Abstr 68:109780j (1968)

Sumbaev, O. I., Smirnov, Yu. P., Petrovich, E. V., Zykov, V. S., Egorov, A. I., and Grushko, A. I., Chemical Shifts of X-Ray $K\alpha_1$ Lines during Oxidation of Rare Earth Metals. Role of f-Electrons, Rentgen. Spektry Elektron. Strukt. Veshchestva 2, 172 (1969); Chem. Abstr. 74:117626c (1971)

Sumbaev, O. I., Smirnov, Yu. P., Petrovich, E. V., Zykov, V. S., Egorov, A. I., Grushko, A. I., Chemical Shifts of the $K\alpha_1$ X-Ray Lines during Oxidation of Rare Earth Metals. Role of f-Electrons, Zh. Eksp. Teor. Fiz. 56, 536 (1969) (Russ); Chem. Abstr. 71:7985z (1969)

Suarez, C. B., and Grinfeld, R., The Gadolinium Oxide Band Spectrum, J. Chem. Phys. 53, 1110 (1970); Chem. Abstr. 73:60782y (1970)

Sweet, J. R., and White, W. B., Flame Excited Luminescence in Terbium and Europium Doped Rare Earth Oxides, Proc. Rare Earth Res. Conf., 9th 1971, 2, 452; P. E. Field, Ed.; Chem. Abstr 76:133834r (1972)

Trond, S. S., Martin, J. S., Stranavage, J. P., and Smith, A. L., Properties of Some Selected Europium-Activated Red Phosphors, J. Electrochem. Soc. 116, 1047 (1969); Chem. Abstr. 71:43407w (1969)

Weltner, W., Jr., and DeKock, R. L., Spectroscopy of Rare Earth Oxide Molecules in Inert Matrices at 4°K, J. Phys. Chem. 75, 514 (1971); Chem. Abstr. 74:105048c (1971)

White, W. B., Diffuse-Reflectance Spectra of Rare Earth Oxides, Appl. Spectrosc. 21, 167 (1967); Chem. Abstr. 67:69158h (1967)

Wittke, J. P., Ladany, I., and Yocom, P. N., Erbium-Ytterbium Double Doped Yttrium Oxide, J. Appl. Phys. 43, 595 (1972); Chem. Abstr 76:78978p (1972)

(c). Gadolinium oxide fluorides

Batsanov, S. S., Derbeneva, S. S., and Batsanova, L. R., Electronic Spectra of Rare Earth Metal Fluorides, Oxyfluorides and Oxides, Zh. Prikl. Spektrosk. 10, 332 (1969) (Russ); Chem. Abstr. 70:101332k (1969)

VI. Holmium

(a). Holmium fluorides

Batsanov, S. S., Derbeneva, S. S., and Batsanova, L. R., Electronic Spectra of Rare Earth Metal Fluorides, Oxyfluorides and Oxides, Zh. Prikl. Spektrosk. 10, 332 (1969) (Russ); Chem. Abstr. 70:101332k (1969)

Chase, E. W., Hepplewhite, R. T., Krupka, D. C., and Kahng, D., Electroluminescence of Zinc Sulfide Lumocen Devices Containing Rare-Earth and Transition-Metal Fluorides, J. Appl. Phys. 40, 2512 (1969); Chem. Abstr. 71:34384j (1969)

Vakhidov, Sh. A., Kaipov, B., and Tavshunskii, G. A., Luminescence of CaF_2-LnF_3 Crystals in a Cobalt-60 γ-Ray Field, Opt. Spektrosk. 28, 949 (1972), Shirley, D. A., Ed.; Chem. Abstr. 77:158530x (1972)

Wertheim, G. K., Cohen, R. L., Rosencwaig, A., and Guggenheim, H. J., Multiplet Splitting and Two-Electron Excitation in the Trivalent Rare Earths, Electron Spectrosc., Proc. Int. Conf. 1971, p. 813 (Publ. 1972), Shirley D. A., Ed.; Chem. Abst. 77:158530x (1972)

(b). Holmium oxides

Batsanov, S. S., Derbeneva, S. S., and Batsanova, L. R., Electronic Spectra of Rare Earth Metal Fluorides, Oxyfluorides and Oxides, Zh. Prikl. Spektrosk. 10, 332 (1969) (Russ); Chem. Abstr. 70:101332k (1969)

Bloor, D., and Dean, J. R., Spectroscopy of Rare-Earth Oxide Systems. I. Far-Infrared Spectra of the Rare-Earth Sesquioxides, Cerium Dioxide, and Nonstoichiometric Praseodymium and Terbium Oxides, J. Phys. C 5, 1237 (1972); Chem. Abstr. 77:54303j (1972)

Davidson, F. D., and Wyckoff, R. W. G., L and M X-Ray Spectra in the Region 2-85 A, Advan. X-Ray Anal. 9, 344 (1966); Chem. Abstr. 66:99767c (1967)

Demekhin, V. F., Platkov, A. I., and Lyubivaya, M. V., Multiplet Structure of the L-Series Lines of Rare-Earth Elements, Zh. Eksp. Teor. Fiz. 62, 49 (1972) (Russ); Chem. Abstr. 76:106015t (1972)

Derbeneva, S. S., and Batsanov, S. S., The Width of the Forbidden Zone for Rare-Earth Metal Oxides, Dokl. Akad. Nauk SSSR 175, 1062 (1967) (Russ); Chem. Abstr. 68:73735g (1968)

Fischer, D. W., and Baun, W. L., Self-Absorption Effects in the Soft X-Ray $M\alpha$ and $M\beta$ Emission Spectra of the Rare Earth Elements, J. Appl. Phys. 38, 4830 (1967); Chem. Abstr. 68:17303c (1968)

Goldsmith, J. A., and Ross, S. D., Factors Affecting the Infrared Spectra of Some Planar Anions with D_{3h} Symmetry. III. The Spectra of Rare Earth Carbonates and Their Thermal Decomposition Products, Spectrochim. Acta, Part A 23, 1909 (1967); Chem. Abstr. 67:68968k (1967)

Petru, F., and Muck, A., Chemistry of Rare Earth Elements. XL. Infrared Absorption Spectra of Oxides of the Lanthanides Eu. . .Lu, Z. Chem. 7, 159 (1967) (Ger); Chem. Abstr. 67:27442r (1967)

Satybaev, N. M., and Ganichenko, L. G., Photoluminescence of Some Rare Earth Oxides, Dokl. Nauch.-Tekh. Konf. Itogam Nauch.-Issled. Rab. 166-1967 gg. Mosk. Energ. Inst. Sekts. Elektron. Tekh. Podsekts. Poluprov Proborov, p. 150 (1967) (Russ); Chem. Abstr. 69:72576q (1968)

Sumbaev, O. I., Smirnov, Yu. P., Petrovich, E. V., Zykov, V. S., Egorov, A. I., and Grushko, A. I., Chemical Shifts of X-Ray $K\alpha_1$ Lines during Oxidation of Rare Earth Metals. Role of f-Electrons, Rentgen. Spektry Elektron. Strukt. Veshchestva 2, 172 (1969); Chem. Abstr. 74:117626c (1971)

Weltner, W., Jr., and DeKock, R. L., Spectroscopy of Rare Earth Oxide Molecules in Inert Matrices at 4°K, J. Phys. Chem. 75, 514 (1971); Chem. Abstr. 74:105048c (1971)

White, W. B., Diffuse-Reflectance Spectra of Rare Earth Oxides, Appl. Spectrosc. 21, 167 (1967); Chem. Abstr. 67:69158h (1967)

(c). Holmium oxide fluorides

Batsanov, S. S., Derbeneva, S. S., and Batsanova, L. R., Electronic Spectra of Rare Earth Metal Fluorides, Oxyfluorides and Oxides, Zh. Prikl. Spektrosk. 10, 332 (1969) (Russ); Chem. Abstr. 70:101332k (1969)

VII. Lanthanum

(a). Lanthanum fluorides

Azarov, V. V., and Skorobogatov, B. S., Photo- and X-Ray Luminescence of Rare Earth Metal-Activated LaF_3 Single Crystals, Ukr. Fiz. Zh. (Russ. Ed.) 14, 690 (1969); Chem. Abstr. 71:107260c (1969)

Batsanov, S. S., Derbeneva, S. S., and Batsanova, L. R., Electronic Spectra of Rare Earth Metal Fluorides, Oxyfluorides and Oxides, Zh. Prikl. Spektrosk. 10, 332 (1969) (Russ); Chem. Abstr. 70:101332k (1969)

Batsanov, S. S., and Kustova, G. N., Effect of Structural Defects on the Infrared Spectra of Rare-Earth Metal Oxides and Fluorides, Spektrosk. Tverd. Tela, p. 249 (1969) (Russ); Chem. Abstr. 73:135527e (170)

Bauman, R. P., and Porto, S. P. S., Lattice Vibrations and Structure of Rare-Earth Fluorides, Phys. Rev. 161, 842 (1967); Chem. Abstr. 67:112549a (1967)

Claudel, J., Hadni, A., and Strimer, P., Low-Frequency Vibration of Lanthanide Fluoride Lattices, C. R. Acad. Sci., Ser. B 274, 943 (1972) (Fr); Chem. Abstr. 77:40868k (1972)

Hadni, A., Strimer, P., and Vermillard, F., Far Infrared Absorption Observation of the Low Frequency Lines of Praseodymium Fluoride and Other Rare-Earth Fluorides, C. R. Acad. Sci., Ser. B 29, 1113 (1969) (Fr); Chem. Abstr. 72:49216a (1970)

Hewes, R. A., Multiphoton Excitation and Efficiency in the Yb^{3+}-Ho^{3+}, -Er^{3+}, -Tm^{3+} Systems, Proc. Int. Conf. Lumin., p. 778 (1969); Chem. Abstr. 74:17762a (1971)

Hewes, R. A., and Sarver, J. F., Infrared Excitation Processes for the Visible Luminescence of Erbium(III), Holmium(III), and Thulium(III) in Ytterbium(III) Sensitized Rare-Earth Trifluorides, Phys. Rev. 182, 427 (1969); Chem. Abstr. 71:65731z (1969)

Joergensen, C. K., and Berthou, H., Measurements of Photoelectron Spectra and Charging Effects in Fluorides, Iodates, and Oxides, J. Fluorine Chem. 2, 425 (1973); Chem. Abstr. 78:130358u (1973)

Krupke, W. F., Transition Intensities between Excited States of Rare Earth Ions in Crystals, IEEE (Inst. Elec. Electron. Eng.) J. Quant. Electron. 2, 693 (1966); Chem. Abstr. 66:100077m (1967)

Lowndes, R. P., Parrish, J. F., and Perry, C. H., Optical Phonons and Symmetry of Tysonite Lanthanide Fluorides, Phys. Rev. 182, 913 (1969); Chem. Abstr. 71:75840y (1969)

Rast, H. E., Caspers, H. H., and Miller, S. A., Infrared Dispersion and Lattice Vibrations of Lanthanum Fluoride, Phys. Rev. 171, 1051 (1968); Chem. Abstr. 69:47830k (1968)

Shenyavskaya, E. A., Gurvich, L. V., and Mal´tsev, A. A., One Band System in the Discharge Spectrum in Lanthanum Trifluoride Vapors, Opt. Spektrosk. 24, 1025 (1968) (Russ); Chem. Abstr. 69:56070q (1968)

Sychugov, V. A., and Shipulo, G. P., Relaxation Rate from the Lower Laser Level, Zh. Eksp. Teor. Fiz. 58, 817 (1970) (Russ); Chem. Abstr. 72:127157y (1970)

Taylor, M. D., Cheung, T. T., and Hussein, M. A., Variations of the Infrared Spectra with the Nature and Structure of the Rare Earth Metal Halides, J. Inorg. Nucl. Chem. 34, 3073 (1972); Chem. Abstr. 77:132692b (1972)

Wertheim, G. K., Cohen, R. L., Rosencwaig, A., and Guggenheim, H. J., Multiplet Splitting and Two-Electron Excitation in the Trivalent Rare Earths, Electron Spectrosc., Proc. Int. Conf. 1971, p. 813 (Publ. 1972), Shirley, D. A., Ed.; Chem. Abstr. 77:158530x (1972)

(b). Lanthanum oxides

Bacis, R., High Resolution Molecular Spectra Obtained with a Fabry-Perot-photoelectric Spectrometer and a Hollow-Cathode Tube Made up of an Alloy; Lanthanum Oxide, C. R. Acad. Sci., Paris, Ser. A,B 266, 1071 (1968) (Fr); Chem. Abstr. 69:6523u (1968)

Batsanov, S. S., Derbeneva, S. S., and Batsanova, L. R., Electronic Spectra of Rare Earth Metal Fluorides, Oxyfluorides and Oxides, Zh. Prikl. Spektrosk. 10, 332 (1969) (Russ); Chem. Abstr. 70:101332k (1969)

Batsanov, S. S., and Kustova, G. N., Effect of Structural Defects on the Infrared Spectra of Rare-Earth Metal Oxides and Fluorides, Spektrosk. Tverd. Tela, 249 (1969) (Russ); Chem. Abstr. 73:135527e (1970)

Bloor, D., and Dean, J. R., Spectroscopy of Rare-Earth Oxide Systems. I. Far-Infrared Spectra of the Rare-Earth Sesquioxides, Cerium Dioxide, and Nonstoichiometric Praseodymium and Terbium Oxides, J. Phys. C 5, 1237 (1972); Chem. Abstr. 77:54303j (1972)

Boulon, G., Photoluminescence Processes in Bismuth Ion Activated Polycrystalline Rare Earth Oxides and Orthovanadates, J. Phys. (Paris) 32, 333 (1971) (Fr); Chem. Abstr. 75:82137k (1971)

Boulon, G., and Gaume-Mahn, F., Luminescence Properties of Lanthanum Oxide Activated by Bismuth, C. R. Acad. Sci., Paris, Ser. A,B 264B, 1511 (1967) (Fr); Chem. Abstr. 67:77215q (1967)

Carette, P., and Blondeau, J. M., Analysis of the Rotation of the Indigo System in the Emission Spectrum of the Lanthanum(II) Oxide Molecule, C. R. Acad. Sci., Ser. B 268, 1743 (1969) (Fr); Chem. Abstr. 71:75909c (1969)

Carette, P., and Houdart, R., High Resolution Study of the Vibration Structure of the Ultraviolet System of the LaO Molecule Emission Spectrum, C. R. Acad. Sci., Ser. B 271, 110 (1970); Chem. Abstr. 73:103901f (1970)

Carette, P., and Houdart, R., Rotational analysis of the D and F Ultraviolet Systems of the Emission Spectrum of the Lanthanum(II) Oxide Molecule, C. R. Acad. Sci., Ser. B 272, 595 (1971) Chem. Abstr. 74:148613a (1971)

Chun, H. U., and Hendel, D., X-Ray Spectroscopic Study of Chemical Bonds in Oxides, Z. Naturforsch. A 22, 1401 (1967) (Ger); Chem. Abstr. 68:63941g (1968)

Datta, R. K., Luminescent Behavior of Bismuth in Rare Earth Oxides, J. Electrochem. Soc. 114, 1137 (1967); Chem. Abstr. 68:64265b (1968)

Davidson, F. D., and Wyckoff, R. W. G., L and M X-Ray Spectra in the Region 2-85 A, Advan. X-Ray Anal. 9, 344 (1966); Chem. Abstr. 66:99767c (1967)

Derbeneva, S. S., and Batsanov, S. S., The Width of the Forbidden Zone for Rare-Earth Metal Oxides, Dokl. Akad. Nauk SSSR 175, 1062 (1967) (Russ); Chem. Abstr. 68:73735g (1968)

Fischer, D. W., and Baun, W. L., Self-Absorption Effects in the Soft X-Ray $M\alpha$ and $M\beta$ Emission Spectra of the Rare Earth Elements, J. Appl. Phys. 38, 4830 (1967); Chem. Abstr. 68:17303c (1968)

Goldsmith, J. A., and Ross, S. D., Factors Affecting the Infrared Spectra of Some Planar anions with D_{3h} Symmetry. III. The Spectra of Rare Earth Carbonates and Their Thermal Decomposition Products, Spectrochim. Acta, Part A 23, 1909 (1967); Chem. Abstr. 67:68968k (1967)

Green, D. W., Rotational Analysis of the $C^2\Pi_r \rightarrow X^2\Sigma^+$ Electronic Transition of Lanthanum Oxide, Can. J. Phys. 49, 2552 (1971); Chem. Abstr. 75:156462m (1971)

Green, D. W., Rotational Analysis of the $C^2\Pi_r \rightarrow A^2\Delta_r$ Electronic Transition in Lanthanum Oxide, J. Mol. Spectrosc. 38, 155 (1971); Chem. Abstr. 74:117814n (1971)

Joergensen, C. K., and Berthou, H., Measurements of Photoelectron Spectra and Charging Effects in Fluorides, Iodates, and Oxides, J. Fluorine Chem. 2, 425 (1973); Chem. Abstr. 78:130358u (1973)

Matsubara, T., Mixed Rare Earth Phosphors, Japan Kokai 73 26,685 (Cl. 13(9)-C112), 7 Apr 1973, Appl. 71 61,170, 11 Aug (1971); Chem. Abstr. 79:25573h (1973)

Murthy, N. S., and Murthy, B. N., Integrated Intensities of the Green-Yellow System of Lanthanum Monoxide Bands, Nature 223, 181 (1969); Chem. Abstr. 71:55132r (1969)

Petru, F., and Muck, A., Chemistry of Rare Earth Elements. XXIX. Infrared Absorption Spectra of Sc_2O_3, Y_2O_3, and La_2O_3, Z. Chem. 6, 386 (1966) (Ger); Chem. Abstr. 66:89813a (1967)

Ratinen, H., X-Ray Excited Optical Fluorescence of Nine Rare Earth Ions in Yttrium Oxide, Gadolinium Oxide, and Lanthanum oxide, Acta Polytech. Scand., Chem. Incl. Met. Ser., No. 107, 19 pp. (1971); Chem. Abstr. 76:106021s (1972)

Satybaev, N. M., and Ganichenko, L. G., Photoluminescence of Some Rare Earth Oxides, Dokl. Nauch.-Tekh. Konf. Itogam Nauch.-Issled. Rab. 1966-1967 gg. Mosk. Energ. Inst. Sekts. Elektron. Tekh. Podsekts. Poluprov. Proborov, p. 150 (167) (Russ); Chem. Abstr. 69:72576q (1968)

Suarez, C. B., Rotational Constants of the B-X System of Lanthanum Oxide-^{18}O Band Spectrum, Chem. Phys. Lett. 16, 515 (1972); Chem. Abstr. 77:170753e (1972)

Suarez, C. B., Vibrational Analysis of the Green-Yellow System of $La^{18}O$, J. Phys. B 3, 729 (1970); Chem. Abstr. 73:50397n (1970)

Sumbaev, O. I., Smirnov, Yu. P., Petrovich, E. V., Zykov, V. S., Egorov, A. I., and Grushko, A. I., Chemical Shifts of X-Ray $K\alpha_1$ Lines during Oxidation of Rare Earth Metals. Role of f-Electrons, Rentgen. Spektry Elektron. Strukt. Veshchestva 2, 172 (1969); Chem. Abstr. 74:117626c (1971)

Sumbaev, O. I., Smirnov, Yu. P., Petrovich, E. V., Zykov, V. S., Egorov, A. I., Grushko, A. I., Chemical Shifts of the $K\alpha_1$ X-Ray lines during Oxidation of Rare Earth Metals. Role of f-Electrons, Zh. Eksp. Teor. Fiz. 56, 536 (1969) (Russ); Chem. Abstr. 71:7985z (1969)

Sweet, J. R., and White, W. B., Flame Excited Luminescence in Terbium and Europium Doped Rare Earth Oxides, Proc. Rare Earth Res. Conf., 9th 1971, 2, 452, Field, P. E, Ed.; Chem. Abstr. 76:133834r (1972)

Matsubara, T., Mixed Rare Earth Phosphors, Japan. Kokai 73 26,685 (Cl. 13(9)-C112), 7 Apr 1973, Appl. 71 61,170, 11 Aug 1971; Chem. Abstr. 79:25573h (1973)

Weltner, W., Jr., and DeKock, R. L., Spectroscopy of Rare Earth Oxide Molecules in Inert Matrices at 4°K, J. Phys. Chem. 75, 514 (1971); Chem. Abstr. 74:105048c (1971)

IX. Neodymium

(a). Neodymium fluorides

Batsanov, S. S., Derbeneva, S. S., and Batsanova, L. R., Electronic Spectra of Rare Earth Metal Fluorides, Oxyfluorides and Oxides, Zh. Prikl. Spektrosk. 10, 332 (1969) (Russ); Chem. Abstr. 70:101332k (1969)

Batsanov, S. S., and Kustova, G. N., Effect of Structural Defects on the Infrared Spectra of Rare-Earth Metal Oxides and Fluorides, Spektrosk. Tverd. Tela, p. 249 (1969) (Russ); Chem. Abstr. 73:135527e (1970)

Bauman, R. P., and Porto, S. P. S., Lattice Vibrations and Structure of Rare-Earth Fluorides, Phys. Rev. 161, 842 (1967); Chem. Abstr. 67:112549a (1967)

Chase, E. W., Hepplewhite, R. T., Krupka, D. C., and Kahng, D., Electroluminescence of Zinc Sulfide Lumocen Devices Containing Rare-Earth and Transition-Metal Fluorides, J. Appl. Phys. 40, 2512 (1969); Chem. Abstr. 71:34384j (1969)

Chen, Y. S., DePaolis, M. V., Jr., and Kahng, D., Characteristics of Pulse-Excited Electroluminescence from Zinc Sulfide Films Containing Rare Earth Fluoride, Proc. IEEE 58, 184 (1970); Chem. Abstr. 72:115816z (1970)

Claudel, J., and Hadni, A., Low-Frequency Vibration of Lanthanide Fluoride Lattices, C. R. Acad. Sci., Ser. B 274, 943 (1972) (Fr); Chem. Abstr. 77:40868k (1972)

Hadni, A., Strimer, P., and Vermillard, F., Far Infrared Absorption Observation of the Low Frequency Lines of Praseodymium Fluoride and Other Rare-Earth Fluorides, C. R. Acad. Sci., Ser. B 29, 1113 (1969) (Fr); Chem. Abstr. 72:49216a (1970)

Lowndes, R. P., Parrish, J. F., and Perry, C. H., Optical Phonons and Symmetry of Tysonite Lanthanide Fluorides, Phys. Rev. 182, 913 (1969); Chem. Abstr. 71:75340y (1969)

Sumbaev, O. I., Petrovich, E. V., Zykov, V. S., Ryl'nikov, A. S., and Grushko, A. I., Isotopic Shifts of the $K\alpha_1$ Lines in the Intermediate Region between Spherical and Deformed Nuclei, Yad. Fiz 5, 544 (1967) (Russ); Chem. Abstr. 67:68844s (1967)

Taylor, M. D., Cheung, T. T., and Hussein, M. A., Variations of the Infrared Spectra with the Nature and Structure of the Rare Earth Metal Halides, J. Inorg. Nucl. Chem. 34, 3073 (1972); Chem. Abstr. 77:132692b (1972)

Wertheim, G. K., Cohen, R. L., Rosencwaig, A., and Guggenheim, H. J., Multiplet Splitting and Two-Electron Excitation in the Trivalent Rare Earths, Electron Spectrosc., Proc. Int. Conf. 1971, p. 813 (Pub. 1972), Shirley, D. A., Ed.; Chem. Abstr. 77:158530x (1972)

(b). Neodymium oxides

Amosov, A. V., Zakharov, V. K., Petrovskii, G., T., Prokhorova, T. I., and Yudin, D. M., Optical Spectrum of Quartz-glass Containing Neodymium, Zh. Prikl. Spektrosk. 11, 742 (1969) (Russ); Chem. Abstr. 72:24101w (1970)

Batsanov, S. S., Derbeneva, S. S., and Batsanova, L. R., Electronic Spectra of Rare Earth Metal Fluorides, Oxyfluorides and Oxides, Zh. Prikl. Spektrosk. 10, 332 (1969) (Russ); Chem. Abstr. 70:101332k (1969)

Bloor, D., and Dean, J. R., Spectroscopy of Rare-Earth Oxide Systems. I. Far-Infrared Spectra of the Rare-Earth Sesquioxides, Cerium Dioxide, and Nonstoichiometric Praseodymium and Terbium Oxides, J. Phys. C 5, 1237 (1972); Chem. Abstr. 77:54303j (1972)

Davidson, F. D., and Wyckoff, R. W. G., L and M X-Ray Spectra in the Region 2-85 A, Advan. X-Ray Anal. 9, 344 (1966); Chem. Abstr. 66:99767c (1967)

Demekhin, V. F., Platkov, A. I., and Lyubivaya, M. V., Multiplet Structure of the L-Series Lines of Rare-Earth Elements, Zh. Eksp. Teor. Fiz. 62, 49 (1972) (Russ); Chem. Abstr. 76:106015t (1972)

Derbeneva, S. S., and Batsanov, S. S., The Width of the Forbidden Zone for Rare-Earth Metal Oxides, Dokl. Akad. Nauk SSSR 175, 1062 (1967) (Russ); Chem. Abstr. 68:73735g (1968)

Fischer, D. W., and Baun, W. L., Self-Absorption Effects in the Soft X-Ray $M\alpha$ and $M\beta$ Emission Spectra of the Rare Earth Elements, J. Appl. Phys. 38, 4830 (1967); Chem. Abstr. 68:17303c (1968)

Goldsmith, J. A., and Ross, S. D., Factors Affecting the Infrared Spectra of Some Planar Anions with D_{3h} Symmetry. III. The Spectra of Rare Earth Carbonates and Their Thermal Decomposition Products, Spectrochim. Acta, Part A 23, 1909 (1967); Chem. Abstr. 67:68968k (1967)

Guazzoni, G. E., and Shapiro, S. J., Spectral Emittance of Neodymium, Samarium, Erbium, and Ytterbium Oxides at High Temperatures, Natl. Techn. Inform. Serv., AD 708547 (1970); Chem. Abstr. 74:36594p (1971)

Haensel, R., Rabe, P., and Sonntag, B., Optical Absorption of Cerium, Cerium Oxide, Praseodymium, Praseodymium Oxide, Neodymium, Neodymium Oxide, and Samarium in the Extreme Ultraviolet, Solid State Commun. 8, 1845 (1970); Chem. Abstr. 74:58999b (1971)

Karyakin, A. V., Davitashvili, E. G., and Kublashvili, Zh. Sh., Infrared Absorption Spectra of Carbonates and Oxalates of Some Rare Earth Group Metals, Soobschch. Akad. Nauk Gruz. SSR 55, 297 (1969) (Russ); Chem. Abstr. 71:117990e (1969)

Mak, A. A., Mikhailov, Yu. N., Stepanov, A. I., and Yastrebova, L. S., Effect of the Microrelief of the Lateral Face of the Active Element of a Solid-State Laser on its Thermal Stability, Opt.-Mekh. Prom. 36, 73 (1969) (Russ); Chem. Abstr. 72:116667p (1970)

Petru, F., and Muck, A., Chemistry of Rare Earth Elements. XXXVII. Infrared Absorption Spectra of CeO_2, Pr_6O_{11}, Nd_2O_3, and Sm_2O_3, Z. Chem. 7, 27 (1967) (Ger); Chem. Abstr. 67:27441q (1967)

Satybaev, N. M., and Ganichenko, L. G., Photoluminescence of some Rare Earth Oxides, Dokl. Nauch.-Tekh. Konf. Itogam Nauch.-Issled. Rab. 1966-1967 gg. Mosk. Energ. Inst. Sekts. elektron. Tekh. Podsekts. Poluprov, p. 150 (1967) (Russ); Chem. Abstr. 69:72576q (1968)

Sumbaev, O. I., Smirnov, Yu. P., Petrovich, E. V., Zykov, V. S., Egorov, A. I., and Grushko, A. I., Chemical Shifts of X-Ray $K\alpha_1$ Lines during Oxidation of Rare Earth Metals. Role of f-Electrons, Rentgen. Spektry Elektron. Strukt. Veshchestva 2, 172 (1969); Chem. Abstr. 74:117626c (1971)

Sumbaev, O. I., Smirnov, Yu. P., Petrovich, E. V., Zykov, V. S., Egorov, A. I., Grushko, A. I., Chemical Shifts of the $K\alpha_1$ X-Ray Lines during Oxidation of Rare Earth Metals. Role of f-Electrons, Zh. Eksp. Teor. Fiz. 56, 536 (1969) (Russ); Chem. Abstr. 71:7985z (1969)

Weichselgartner, H., Preparation of Laser-Active Liquids with High Fluorescence Lifetime, Z. Naturforsch. A 24, 1665 (1969) (Ger); Chem. Abstr. 72:26955b (1970)

Weltner, W., Jr., and DeKock, R. L., Spectroscopy of Rare Earth Oxide Molecules in Inert Matrices at 4^0K, J. Phys. Chem. 75, 514 (1971); Chem. Abstr. 74:105048c (1971)

White, W. B., Diffuse-Reflectance Spectra of Rare Earth Oxides, Appl. Spectrosc. 21, 167 (1967); Chem. Abstr. 67:69158h (1967)

(c). Neodymium oxide fluorides

Batsanov, S. S., Derbeneva, S. S., and Batsanova, L. R., Electronic Spectra of Rare Earth Metal Fluorides, Oxyfluorides and Oxides, Zh. Prikl. Spektrosk. 10, 332 (1969) (Russ); Chem. Abstr. 70:101332k (1969)

X. Promethium

(a). Promethium fluorides

Wertheim, G. K., Cohen, R. L., Rosencwaig, A., and Guggenheim, H. J. Multiplet Splitting and Two-Electron Excitation in the Trivalent Rare Earths, Electron Spectrosc., Proc. Int. Conf. 1971, p. 813, (Pub. 1972), Shirley, D. A., Ed.; Chem. Abstr. 77:158530x (1972)

(b). Promethium oxides

Bloor, D., and Dean, J. R., Spectroscopy of Rare-Earth Oxide Systems. I. Far-Infrared Spectra of the Rare-Earth Sesquioxides, Cerium Dioxide, and Nonstoichiometric Praseodymium and Terbium Oxides, J. Phys. C 5, 1237 (1972); Chem. Abstr. 77:54303j (1972)

Fischer, D. W., And Baun, W. L., Self-Absorption Effects in the Soft X-Ray $M\alpha$ and $M\beta$ Emission Spectra of the Rare Earth Elements, J. Appl. Phys. 38, 4830 (1967); Chem. Abstr. 68:17303c (1968)

Sumbaev, O. I., Smirnov, Yu. P., Petrovich, E. V., Zykov, V. S., Egorov, A. I., and Grushko, A. I., Chemical Shifts of X-Ray $K\alpha_1$ Lines during Oxidation of Rare Earth Metals. Role of f-Electrons, Rentgen. Spektry Elektron. Strukt. Veshchestva 2, 172 (1969); Chem. Abstr. 74:117626c (1971)

XI. Praseodymium

(a). Praseodymium fluorides

Batsanov, S. S., Derbeneva, S. S., and Batsanova, L. R., Electronic Spectra of Rare Earth Metal Fluorides, Oxyfluorides and Oxides, Zh. Prikl. Spektrosk. 10, 332 (1969) (Russ); Chem. Abstr. 70:101332k (1969)

Bauman, R. P., and Porto, S. P. S., Lattice Vibrations and Structure of Rare-Earth Fluorides, Phys. Rev. 161, 842 (1967); Chem. Abstr. 67:112549a (1967)

Chase, E. W., Hepplewhite, R. T., Krupka, D. C., and Kahng, D., Electroluminescence of Zinc Sulfide Lumocen Devices Containing Rare-Earth and Transition-Metal Fluorides, J. Appl. Phys. 40, 2512 (1969); Chem. Abstr. 71:34384j (1969)

Chen, Y. S., DePaolis, M. V., Jr., and Kahng, D., Characteristics of Pulse-Excited Electroluminescence from Zinc Sulfide Films Containing Rare Earth Fluoride, Proc. IEEE 58, 184 (1970); Chem. Abstr. 72:115816z (1970)

Claudel, J., Hadni, A., and Strimer, P., Low-Frequency Vibration of Lanthanide Fluoride Lattices, C. R. Acad. Sci., Ser. B 274, 943 (1972); Chem. Abstr. 77:40868k (1972)

Hadni, A., and Strimer, P., Low-Temperature Absorption and Dichroism in the Far Infrared of a Praseodymium Fluoride Single Crystal, C. R. Acad. Sci., Paris, Ser. A,B 265B, 811 (1967) (Fr); Chem. Abstr. 68:109641q (1968)

Hadni, A., and Strimer, P., Far Infrared Absorption Observation of the Low Frequency Lines of Praseodymium Fluoride and Other Rare-Earth Fluorides, C. R. Acad. Sci., Ser B 29, 1113 (1969) (Fr); Chem. Abstr. 72:49216a (1970)

Lee, P. L., Seltzer, E. C., and Boehm, F., Energy Shifts of K X-Ray Lines from Tri- and Tetravalent Praseodymium, Phys. Lett. A 38, 29 (1972); Chem. Abstr. 76:92301u (1972)

Lowndes, R. P., Parrish, J. F., and Perry, C. H., Optical Phonons and Symmetry of Tysonite Lanthanide Fluorides, Phys. Rev. 182, 913 (1969); Chem. Abstr. 71:75840y (1969)

Ovsyannikova, I. A., and Nasonova, L. I., L$_{III}$ X-Ray Absorption Spectra of Praseodymium and Cerium and Effective Coordination Charges, Zh. Strukt. Khim. 11, 548 (1970) (Russ); Chem. Abstr. 73:82137u (1970)

Wertheim, G. K., Cohen, R. L., Rosencwaig, A., and Guggenheim, H. J., Multiplet Splitting and Two Electron Excitation in the Trivalent Rare Earths, Electron Spectrosc., Proc. Int. Conf. 1971, p. 813, (Pub. 1972), Shirley, D. A., Ed.; Chem. Abstr. 77:158530x (1972)

Wertheim, G. K., Rosencwaig, S., Cohen, R. L., and Guggenheim, H. J., Exchange Splitting in the 4f Photoelectron Spectra of the Rare Earths, Phys. Rev. Lett. 27, 505 (1971); Chem. Abstr. 75:103444a (1971)

(b). Praseodymium oxides

Bloor, D., and Dean, J. R., Spectroscopy of Rare-Earth Oxide Systems. I. Far-Infrared Spectra of the Rare-Earth Sesquioxides, Cerium Dioxide, and Nonstoichiometric Praseodymium and Terbium Oxides, J. Phys. C 5, 1237 (1972); Chem. Abstr. 77:54303j (1972)

Davidson, F. D., and Wyckoff, R. W. G., L and M X-Ray Spectra in the Region 2-85 A, Advan. X-Ray Anal. 9, 344 (1966); Chem. Abstr. 66:99767c (1967)

Demekhin, V. F., Platkov, A. I., and Lyubivaya, M. V., Multiplet Structure of the L-Series Lines of Rare-Earth Elements, Zh. Eksp. Teor. Fiz. 62, 49 (1972) (Russ); Chem. Abstr. 76:106015t (1972)

Derbeneva, S. S., and Batsanov, S. S., The Width of the Forbidden Zone for Rare-Earth Metal Oxides, Dokl. Akad. Nauk SSSR 175, 1062 (1967) (Russ); Chem. Abstr. 68:73735g (1968)

Fischer, D. W., and Baun, W. L., Self-Absorption Effects in the Soft X-Ray Mα and Mβ Emission Spectra of the Rare Earth Elements, J. Appl. Phys. 38, 4830 (1967); Chem. Abstr. 68:17303c (1968)

Goldsmith, J. A., and Ross, S. D., Factors Affecting the Infrared Spectra of Some Planar Anions with D_{3h} Symmetry. III. The Spectra of Rare Earth Carbonates and Their Thermal Decomposition Products, Spectrochim. Acta, Part A 23, 1909 (1967); Chem. Abstr. 67:63963k (1967)

Haensel, R., Rabe, P., and Sonntag, B., Optical Absorption of Cerium, Cerium Oxide, Praseodymium, Praseodymium Oxide, Neodymium, Neodymium Oxide, and Samarium in the Extreme Ultraviolet, Solid State Commun. 8, 1845 (1970); Chem. Abstr. 74:58999b 81971)

Kapfhammer, W., Maurer, W., Wagner, F. E., and Kienle, P., Isomer Shifts and Hyperfine Splitting of the 145 keV Moessbauer Line of Praseodymium-141, Hyperfine Interactions Excited Nucl., Proc. Conf. 1970, 3, 839 (Pub. 1971), Goldring, G., ed.; Chem. Abstr. 77:68259m (1972)

Karyakin, A. V., Davitashvili, E. G., and Kublashvili, Zh. Sh., Infrared Absorption Spectra of Carbonates and Oxalates of Some Rare Earth Group Metals, Soobschch. Akad. Nauk Gruz. SSR 55, 297 (1969) (Russ); Chem. Abstr. 71:117990e (1969)

Lee, P. L., Seltzer, E. C., and Boehm, F., Energy Shifts of K X-Ray Lines from Tri- and Tetravalent Praseodymium, Phys. Lett. A 38, 29 (1972); Chem. Abstr. 76:92301u (1972)

Ovsyannikova, I. A., Nasonova, L. I., L_{III} X-Ray Absorption Spectra of Praseodymium and Cerium and Effective Coordination Charges, Zh. Strukt. Khim. 11, 548 (1970) (Russ); Chem. Abstr. 73:82137u (1970)

Petru, F., and Muck, A., Chemistry of Rare Earth Elements. XXXVII. Infrared Absorption Spectra of CeO_2, Pr_6O_{11}, Nd_2O_3, and Sm_2O_3, (1967)

Shenyavskaya, E. A., Egorova, I. V., and Lupanov, V. N., Electronic Spectrum of Praseodymium Monoxide, J. Mol. Spectrosc. 47, 355 (1973); Chem. Abstr. 79:98743y (1973)

Sumbaev, O. I., Smirnov, Yu. P., Petrovich, E. V., Zykov, V. S., Egorov, A. I., and Grushko, A. I., Chemical Shifts of X-Ray $K\alpha_1$ Lines during Oxidation of Rare Earth Metals. Role of f-Electrons, Rentgen. Spektry Elektron. Strukt. Veshchestva 2, 172 (1969); Chem. Abstr. 74:117626c (1971)

Vainshtein, E. E., Blokhin, S. M., and Bertenev, V. M., X-Ray Spectrum of Some Cerium and Praseodymium Compounds, Izv. Sib. Otd. Akad. Nauk SSSR, Ser. Khim. Nauk p. 59 (1966) (Russ); Chem. Abstr. 66:41906f (1967)

Venkitachalam, T. V., Krishnamurty, G., and Narasimham, N. A., Emission Spectrum of Praseodymium Monoxide, Proc. Indian Acad. Sci., Sect. A 76, 113 (1972); Chem. Abstr. 78:64845x (1973)

Warmkessel, J. M., Lin, S.-H., and Eyring, L., Optical Absorption Spectra of the Ordered Phases in the Praseodymium Oxide-Oxygen System, Inorg. Chem. 8, 875 (1969); Chem. Abstr. 70:119822e (1969)

White, W. B., Diffuse-Reflectance Spectra of Rare Earth Oxides, Appl. Spectrosc. 21, 167 (1967); Chem. Abstr. 67:69158h (1967)

Weltner, W., Jr., and DeKock, R. L., Spectroscopy of Rare Earth Oxide Molecules in Inert Matrices at 4°K, J. Phys. Chem. 75, 514 (1971); Chem. Abstr. 74:105048c (1971)

(c). Praseodymium oxide fluorides

Ovsyannikova, I. A., and Nasonova, L. I., L_{III} X-Ray Absorption Spectra of Praseodymium and Cerium and Effective Coordination Charges, Zh. Strukt. Khim. 11, 548 (1970) (Russ); Chem. Abstr. 73:82137u (1970)

XII. Samarium

(a). Samarium fluorides

Batsanov, S. S., Derbeneva, S. S., and Batsanova, L. R., Electronic Spectra of Rare Earth Metal Fluorides, Oxyfluorides and Oxides, Zh. Prikl. Spektrosk. 10, 332 (1969) (Russ); Chem. Abstr. 70:101332k (1969)

Chase, E. W., Hepplewhite, R. T., Krupka, D. C., and Kahng, D., Electroluminescence of Zinc Sulfide Lumocen Devices Containing Rare-Earth and Transition-Metal Fluorides, J. Appl. Phys. 40, 2512 (1969); Chem. Abstr. 71:34384j (1969)

Chen, Y. S., DePaolis, M. V., Jr., and Kahng, D., Characteristics of Pulse-Excited Electroluminescence from Zinc Sulfide Films Containing Rare Earth Fluoride, Proc. IEEE 58, 184 (1970); Chem. Abstr. 72:115816z (1970)

DeKock, C. W., Wesley, R. D., and Radtke, D. D., Infrared Spectra and Geometries of Rare Earth Dihalides. Samarium(II) Fluoride, Samarium(II) Chloride, Europium(II) Fluoride, Europium(II) Chloride, Ytterbium(II) Fluoride, and Ytterbium(II) Chloride, High Temp. Sci. 4, 41 (1972); Chem. Abstr. 76:119428e (1972)

Hadni, A., Morlot, G., and Strimer, P., Far-Infrared Electronic Transitions in Solids, IEEE (Inst. Elec. Electron. Eng.) J. Quant. Electron. 3, 111 (1967); Chem. Abstr. 67:86235y (1967)

Joergensen, C. K., and Berthou, H., Measurements of Photoelectron Spectra and Charging Effects in Fluorides, Iodates, and Oxides, J. Fluorine Chem. 2, 425 (1973); Chem. Abstr. 78:130358u (1973)

Petrovich, E. V., Smirnov, Yu. P., Zykov, V. S., Grushko, A. I., Sumbaev, O. I., Band, I. M., and Trzhaskovskii, M. B., Chemical Shifts of the $K_{\alpha 1,2}$ $K_{\beta 1,3}$ and $K_{\beta 2,4}$ X-Ray Lines in Heavy Elements Due to s-, p-, d-, or f-Valency Electrons, Zh. Eksp. Teor. Fiz. 61, 1756 (1971); Chem. Abstr. 76:65903k (1972)

Sumbaev, O. I., Petrovich, E. V., Zykov, V. S., Ryl'nikov, A. S., and Grushko, A. I., Isotropic Shifts of the $K\alpha_1$ Lines in the Intermediate Region between Spherical and Deformed Nuclei, Yad. Fiz. 5, 544 (1967) (Russ); Chem. Abstr. 67:68844s (1967)

Taylor, M. D., Cheung, T. T., and Hussein, M. A., Variations of the Infrared Spectra with the Nature and Structure of the Rare Earth Metal Halides, J. Inorg. Nucl. Chem. 34, 3073 (1972); Chem. Abstr. 77:132692b (1972)

Wertheim, G. K., Cohen, R. L., Rosencwaig, A., and Guggenheim, H. J., Multiplet Splitting and Two Electron Excitation in the Trivalent Rare Earths, Electron Spectrosc., Proc. Int. Conf. 1971, p. 813, (Pub. 1972), Shirley, D. A., Ed.; Chem. Abstr. 77:158530x (1972)

(b). Samarium oxides

Batsanov, S. S., Derbeneva, S. S., and Batsanova, L. R., Electronic Spectra of Rare Earth Metal Fluorides, Oxyfluorides and Oxides, Zh. Prikl. Spektrosk. 10, 332 (1969) (Russ); Chem. Abstr. 70:101332k (1969)

Bloor, D., and Dean, J. R., Spectroscopy of Rare-Earth Oxide Systems. I. Far-Infrared Spectra of the Rare-Earth Sesquioxides, Cerium Dioxide, and Nonstoichiometric Praseodymium and Terbium Oxides, J. Phys. C 5, 1237 (1972); Chem. Abstr. 77:54303j (1972)

Chun, H. U., and Hendel, D., X-Ray Spectroscopic Study of Chemical Bonds in Oxides, Z. Naturforsch. A 22, 1401 (1968) (Ger); Chem. Abstr. 68:63941g (1968)

Davidson, F. D., and Wyckoff, R. W. G., L and M X-Ray Spectra in the Region 2-85 A, Advan. X-Ray Anal. 9, 344 (1966); Chem. Abstr. 66:99767c (1967)

Demekhin, V. F., Platkov, A. I., and Lyubivaya, M. V., Multiplet Structure of the L-Series Lines of Rare-Earth Elements, Zh. Eksp. Teor. Fiz. 62, 49 (1972) (Russ); Chem. Abstr. 76:106015t (172)

Dentai, A. G., Fluorescent High Alumina Ceramic Substrates, Amer. Ceram. Soc., Bull. 51, 681 (1972); Chem. Abstr. 77:143291w (1972)

Derbeneva, S. S., and Batsanov, S. S., The Width of the Forbidden Zone for Rare-Earth Metal Oxides, Dokl. Akad. Nauk SSSR 175, 1062 (1967) (Russ); Chem. Abstr. 68:73735g (1968)

Fischer, D. W., and Baun, W. L., Self-Absorption Effects in the Soft X-Ray Mα and Mβ Emission Spectra of the Rare Earth Elements, J. Appl. Phys. 38, 4830 (1967); Chem. Abstr. 68:17303c (1968)

Goldsmith, J. A., and Ross, S. D., Factors Affecting the Infrared Spectra of Some Planar Anions with D_{3h} Symmetry. III. The Spectra of Rare Earth Carbonates and Their Thermal Decomposition Products, Spectrochim. Acta, Part A 23, 1909 (1967); Chem. Abstr. 67:68968k (1967)

Guazzoni, G. E., and Shapiro, S. J., Spectral Emittance of Neodymium, Samarium, Erbium, and Ytterbium Oxides at High Temperatures, Nat. Techn. Inform. Serv., AD 708547 (1970); Chem. Abstr. 74:36594p (1971)

Kublashvili, Zh. Sh., Karyakin, A. V., and Davitashvili, E. G., Infrared Spectra of some Samarium Compounds, Soobshch. Akad. Nauk Gruz. SSR 52, 363 (1968) (Russ); Chem. Abstr. 70:119756m (1969)

McMahon, W. R., Hemispherical Spectral Emittance of Selected Rare Earth Oxides, U.S. At. Energy Comm. 1967, IS-T-182, Nat. Techn. Inform. Ser.; Chem. Abstr. 69:67966k (1968)

Petru, F., and Muck, A., Chemistry of Rare Earth Elements. XXXVII. Infrared Absorption Spectra of CeO_2, Pr_6O_{11}, Nd_2O_3, and Sm_2O_3, Z. Chem. 7, 27 (1967) (Ger); Chem. Abstr. 67:27441q (1967)

Satybaev, N. M., and Ganichenko, L. G., Photoluminescence of Some Rare Earth Oxides, Dokl. Nauch.-Tekh. Konf. Itogam Nauch.-Issled. Rab. 1966-1967 gg. Mosk. Energ. Inst. Sekts. Elektron. Tekh. Podsekts. Poluprov. Proborov p. 150 (1967) (Russ); Chem. Abstr. 69:72576q (1968)

Sumbaev, O. I., Smirnov, Yu. P., Petrovich, E. V., Zykov, V. S., Egorov, A. I., and Grushko, A. I., Chemical Shifts of X-Ray $K\alpha_1$ Lines during Oxidation of Rare Earth Metals. Role of f-Electrons, Rentgen. Spektry Elektron. Strukt. Veshchestva 2, 172 (1969); Chem. Abstr. 74:117526c (1971)

Sumbaev, O. I., Smirnov, Yu. P., Petrovich, E. V., Zykov, V. S., Egorov, A. I., Grushko, A. I., Chemical Shifts of the $K\alpha_1$ X-Rays Lines during Oxidation of Rare Earth Metals. Role of f-Electrons, Zh. Eksp. Teor. Fiz. 56, 536 (1969) (Russ); Chem. Abstr. 71:7985z (1969)

Weltner, W., Jr., and DeKock, R. L., Spectroscopy of Rare Earth Oxide Molecules in Inert Matrices at 4°K, J. Phys. Chem. 75, 514 (1971); Chem. Abstr. 74:105048c (1971)

White, W. B., Diffuse-Reflectance Spectra of Rare Earth Oxides, Appl. Spectrosc. 21, 167 (1967); Chem. Abstr. 67:69153h (1967)

(c). Samarium oxide fluorides

Batsanov, S. S., Derbeneva, S. S., and Batsanova, L. R., Electronic Spectra of Rare Earth Metal Fluorides, Oxyfluorides and Oxides, Zh. Prikl. Spektrosk. 10, 332 (1969) (Russ); Chem. Abstr. 70:101332k (1969)

XIII. Terbium

(a). Terbium fluorides

Batsanov, S. S., Derbeneva, S. S., and Batsanova, L. R., Electronic Spectra of Rare Earth Metal Fluorides, Oxyfluorides and Oxides, Zh. Prikl. Spektrosk. 10, 332 (1969) (Russ); Chem. Abstr. 70:101332k (1969)

Benoit, J., and Benalloul, P., ${}^5D_3 \rightarrow {}^7F_j$ Transition in the Cathodoluminescence of Terbium Trifluoride, Zinc Sulfide-Terbium Trifluoride, and Terbium-(3+)-Doped Zinc Sulfide Thin Films, Phys. Status Solidi A 15, 67 (1973) (Fr); Chem. Abstr. 78:90615s (1973)

Chase, E. W., Hepplewhite, R. T., Krupka, D. C., and Kahng, D., Electroluminescence of Zinc Sulfide Lumocen Devices Containing Rare-Earth and Transition-Metal Fluorides, J. Appl. Phys. 40, 2512 (1969); Chem. Abstr. 71:34384j (1969)

Chen, Y. S., DePaolis, M. V., Jr., and Kahng, D., Characteristics of Pulse-Excited Electroluminescence from Zinc Sulfide Films Containing Rare Earth Fluoride, Proc. IEEE 58, 184 (1970); Chem. Abstr. 72:115816z (1970)

Chun, H. U., and Hendel, D., X-Ray Spectroscopic Study of Chemical Bonds in Oxides, Z. Naturforsch. A 22, 1401 (1967) (Ger); Chem. Abstr. 68:63941g (1968)

Krupka, D. C., and Guggenheim, H. J., Optical Absorption and Fluorescence Spectra of Single-Crystal Terbium Trifluoride, J. Chem. Phys. 51, 4006 (1969); Chem. Abstr. 72:7665r (1970)

Krupka, D. C., and Rochkind, M. M., Infrared Spectroscopic Study on Terbium Fluoride in Solid Nitrogen and on Electroluminescent Thin Films of Terbium Fluoride-Doped Zinc Sulfide, J. Appl. Phys. 43, 194 (1972); Chem. Abstr. 76:52239y (1972)

Wertheim, G. K., Cohen, R. L., Rosencwaig, A., and Guggenheim, H. J., Multiplet Splitting and Two Electron Excitation in the Trivalent Rare Earths, Electron Spectrosc., Proc. Int. Conf. 1971, p. 813, (Pub. 1972), Shirley, D. A., Ed.; Chem. Abstr. 77:158530x (1972)

Wertheim, G. K., Rosencwaig, S., Cohen, R. L., and Guggenheim, H. J., Exchange Splitting in the 4f Photoelectron Spectra of the Rare Earths, Phys. Rev. Lett. 27, 505 (1971); Chem. Abstr. 75:103444a (1971)

(b). Terbium oxides

Bloor, D., and Dean, J. R., Spectroscopy of Rare-Earth Oxide Systems. I. Far-Infrared Spectra of the Rare-Earth Sesquioxides, Cerium Dioxide, and Nonstoichiometric Praseodymium and Terbium Oxides, J. Phys. C 5, 1237 (1972); Chem. Abstr. 77:54303j (1972)

Davidson, F. D., and Wyckoff, R. W. G., L and M X-Ray Spectra in the Region 2-85 A, Advan. X-Ray Anal. 9, 344 (1966); Chem. Abstr. 66:99767c (1967)

Demekhin, V. F., Platkov, A. I., and Lyubivaya, M. V., Multiplet Structure of the L-Series Lines of Rare-Earth Elements, Zh. Eksp. Teor. Fiz. 62, 49 (1972) (Russ); Chem. Abstr. 76:106015t (1972)

Dentai, A. G., Fluorescent High Alumina Ceramic Substrates, Amer. Ceram. Soc., Bull. 51, 681 (1972); Chem. Abstr. 77:143291w (1972)

Derbeneva, S. S., and Batsanov, S. S., The Width of the Forbidden Zone for Rare-Earth Metal Oxides, Dokl. Akad. Nauk SSSR 175, 1062 (1967) (Russ); Chem. Abstr. 68:73735g (1968)

Fischer, D. W., and Baun, W. L., Self-Absorption Effects in the Soft X-Ray $M\alpha$ and $M\beta$ Emission Spectra of the Rare Earth Elements, J. Appl. Phys. 38, 4830 (1967); Chem. Abstr. 68:17303c (1968)

Goldsmith, J. A., and Ross, S. D., Factors Affecting the Infrared Spectra of Some Planar Anions with D_{3h} Symmetry. III. The Spectra of Rare Earth Carbonates and Their Thermal Decomposition Products, Spectrochim. Acta, Part A 23, 1909 (1967); Chem. Abstr. 67:68968k (1967)

Nigam, A. N., and Garg, K. B., New Lines in the L-Spectrum of Terbium, Naturwissenschaften 54, 641 (1967); Chem. Abstr. 68:55047e (1968)

Petru, F., and Muck, A., Chemistry of Rare Earth Elements. XL. Infrared Absorption Spectra of Oxides of the Lanthanides Eu. . .Lu, Z. Chem. 7, 159 (1967) (Ger); Chem. Abstr. 67:27442r (1967)

Sumbaev, O. I., Smirnov, Yu. P., Petrovich, E. V., Zykov, V. S., Egorov, A. I., and Grushko, A. I., Chemical Shifts of X-Ray $K\alpha_1$ Lines during Oxidation of Rare Earth Metals. Role of f-Electrons, Rentgen. Spektry Elektron. Strukt. Veshchestva 2, 172 (1969); Chem. Abstr. 74:117626c (1971)

Weltner, W., Jr., and DeKock, R. L., Spectroscopy of Rare Earth Oxide Molecules in Inert Matrices at 4°K, J. Phys. Chem. 75, 514 (1971); Chem. Abstr. 74:105048c (1971)

White, W. B., Diffuse-Reflectance Spectra of Rare Earth Oxides, Appl. Spectrosc. 21, 167 (1967); Chem. Abstr. 67:69158h (1967)

(c). Terbium oxide fluorides

Batsanov, S. S., Derbeneva, S. S., and Batsanova, L. R., Electronic Spectra of Rare Earth Metal Fluorides, Oxyfluorides and Oxides, Zh. Prikl. Spektrosk. 10, 332 (1969) (Russ); Chem. Abstr. 70:101332k (1969)

XIV. Thulium

(a). Thulium fluorides

Batsanov, S. S., Derbeneva, S. S., and Batsanova, L. R., Electronic Spectra of Rare Earth Metal Fluorides, Oxyfluorides and Oxides, Zh. Prikl. Spektrosk. 10, 332 (1969) (Russ); Chem. Abstr. 70:101332k (1969)

Chase, E. W., Hepplewhite, R. T., Krupka, D. C., and Kahng, D., Electroluminescence of Zinc Sulfide Lumocen Devices Containing Rare-Earth and Transition-Metal Fluorides, J. Appl. Phys. 40, 2512 (1969); Chem. Abstr. 71:34384j (1969)

Chen. Y. S., DePaolis, M. V., Jr., and Kahng, D., Characteristics of Pulse-Excited Electroluminescence from Zinc Sulfide Films Containing Rare Earth Fluoride, Proc. IEEE 58, 184 (1970); Chem. Abstr. 72:115816z (1970)

Wertheim, G. K., Cohen, R. L., Rosencwaig, A., and Guggenheim, H. J., Multiplet Splitting and Two-Electron Excitation in the Trivalent Rare Earths, Electron Spectrosc., Proc. Int. Conf. 1971, p. 813, (Pub. 1972), Shirley, D. A., Ed.; Chem. Abstr. 77:158530x (1972)

Wertheim, G. K., Rosencwaig, S., Cohen, R. L., and Guggenheim, H. J., Exchange Splitting in the 4f Photoelectron Spectra of the Rare Earths, Phys. Rev. Lett. 27, 505 (1971); Chem. Abstr. 75:103444a (1971)

(b). Thulium oxides

Bloor, D., and Dean, J. R., Spectroscopy of Rare-Earth Oxide Systems. I. Far-Infrared Spectra of the Rare-Earth Sesquioxides, Cerium Dioxide, and Nonstoichiometric Praseodymium and Terbium Oxides, J. Phys. C 5, 1237 (1972); Chem. Abstr. 77:54303j (1972)

Demekhin, V. F., Platkov, A. I., and Lyubivaya, M. V., Multiplet Structure of the L-Series Lines of Rare-Earth Elements, Zh. Eksp. Teor. Fiz. 62, 49 (1972) (Russ); Chem. Abstr. 76:106015t (1972)

Derbeneva, S. S., and Batsanov, S. S., The Width of the Forbidden Zone for Rare-Earth Metal Oxides, Dokl. Akad. Nauk SSSR 175, 1062 (1967) (Russ); Chem. Abstr. 68:73735g (1968)

Fischer, D. W., and Baun, W. L., Self-Absorption Effects in the Soft X-Ray $M\alpha$ and $M\beta$ Emission Spectra of the Rare Earth Elements, J. Appl. Phys. 38, 4830 (1967); Chem. Abstr. 68:17303c (1968)

Goldsmith, J. A., and Ross, S. D., Factors Affecting the Infrared Spectra of Some Planar Anions with D_{3h} Symmetry. III. The Spectra of Rare Earth Carbonates and Their Thermal Decomposition Products, Spectrochim. Acta, Part A 23, 1909 (1967); Chem. Abstr. 67:68968k (1967)

McMahon, W. R., Hemispherical Spectral Emittance of Selected Rare Earth Oxides, U.S. At. Energy Comm. 1967, IS-T-182, Nat. Techn. Inform. Ser.; Chem. Abstr. 69:6796k (1968)

Petru, F., and Muck, A., Chemistry of Rare Earth Elements. XL. Infrared Absorption Spectra of Oxides of the Lanthanides Eu. . .Lu, Z. Chem. 7, 159 (1967) (Ger); Chem. Abstr. 67:27442r (1967)

Sumbaev, O. I., Smirnov, Yu. P., Petrovich, E. V., Zykov, V. S., Egorov, A. I., and Grushko, A. I., Chemical Shifts of X-Ray $K\alpha_1$ Lines during Oxidation of Rare Earth Metals. Role of f-Electrons, Rentgen. Spektry Elektron. Strukt. Veshchestva 2, 172 (1969); Chem. Abstr. 74:117626c (1971)

Sumbaev, O. I., Smirnov, Yu. P., Petrovich, E. V., Zykov, V. S., Egorov, A. I., Grushko, A. I., Chemical Shifts of the $K\alpha_1$ X-Ray Lines during Oxidation of Rare Earth Metals. Role of f-Electrons, Zh. Eksp. Teor. Fiz. 56, 536 (1969) (Russ); Chem. Abstr. 71:7985z (1969)

Weltner, W., Jr., and DeKock, R. L., Spectroscopy of Rare Earth Oxide Molecules in Inert Matrices at 4°K, J. Phys. Chem. 75, 514 (1971); Chem. Abstr. 74:105048c (1971)

White, W. B., Diffuse-Reflectance Spectra of Rare Earth Oxides, Appl. Spectrosc. 21, 167 (1967); Chem. Abstr. 67:69152h (1967)

XV. Ytterbium

(a). Ytterbium fluorides

Batsanov, S. S., Derbeneva, S. S., and Batsanova, L. R., Electronic Spectra of Rare Earth Metal Fluorides, Oxyfluorides and Oxides, Zh. Prikl. Spektrosk. 10, 332 (1969) (Russ); Chem. Abstr. 70:101332k (1969)

Chase, E. W., Hepplewhite, R. T., Krupka, D. C., and Kahng, D., Electroluminescence of Zinc Sulfide Lumocen Devices Containing Rare-Earth and Transition-Metal Fluorides, J. Appl. Phys. 40, 2512 (1969); Chem. Abstr. 71:34384j (1969)

Combley, F. H., Stewardson, E. A., and Wilson, J. E., The M X-Ray Absorption of Ytterbium, Proc. Phys. Soc. 1, 120 (1968); Chem. Abstr. 68:44307p (1968)

DeKock, C. W., Wesley, R. D., and Radtke, D. D., Infrared Spectra and Geometries of Rare Earth Dihalides. Samarium(II) Fluoride, Samarium(II) Chloride, Europium(II) Fluoride, Europium(II) Chloride, Ytterbium(II) Fluoride and Ytterbium(II) Chloride, High Temp. Sci. 4, 41 (1972); Chem. Abstr. 76:119428e (1972)

Hewes, R. A., Multiphoton Excitation and Efficiency in the Yb^{3+}-Ho^{3+}, -Er^{3+}, -Tm^{3+} Systems, Proc. Int. Conf. Lumin. 1969, p. 778 (Pub. 1970), Williams, F., Ed.; Chem. Abstr. 74:17762a (1971)

Hewes, R. A., and Sarver, J. F., Infrared Excitation Processes for the Visible Luminescence of Erbium(III), Holmium(III), and Thulium(III) in Ytterbium(III) Sensitized Rare-Earth Trifluorides, Phys. Rev. 182, 427 (1969); Chem. Abstr. 71:65731z (1969)

Joergensen, C. K., and Berthou, H., Measurements of Photoelectron Spectra and Charging Effects in Fluorides, Iodates, and Oxides, J. Fluorine Chem. 2, 425 (1973); Chem. Abstr. 78:130358u (1973)

Taylor, M. D., Cheung, T. T., and Hussein, M. A., Variations of the Infrared Spectra with the Nature and Structure of the Rare Earth Metal Halides, J. Inorg. Nucl. Chem. 34, 3073 (1972); Chem. Abstr. 77:132692b (1972)

Wertheim, G. K., Cohen, R. L., Rosencwaig, A., and Guggenheim, H. J., Multiplet Splitting and Two Electron Excitation in the Trivalent Rare Earths, Electron Spectrosc., Proc. Int. Conf. 1971, p. 813, (Pub. 1972), Shirley, D. A., Ed.; Chem. Abstr. 77:158530x (1972)

(b). Ytterbium oxides

Batsanov, S. S., Derbeneva, S. S., and Batsanova, L. R., Electronic Spectra of Rare Earth Metal Fluorides, Oxyfluorides and Oxides, Zh. Prikl. Spektrosk. 10, 332 (1969) (Russ); Chem. Abstr. 70:101332k (1969)

Bloor, D., and Dean, J. R., Spectroscopy of Rare-Earth Oxide Systems. I. Far-Infrared Spectra of the Rare-Earth Sesquioxides, Cerium Dioxide, and Nonstoichiometric Praseodymium and Terbium Oxides, J. Phys. C 5, 1237 (1972); Chem. Abstr. 77:54303j (1972)

Chun, H. U., and Hendel, D., X-Ray Spectroscopic Study of Chemical Bonds in Oxides, Z. Naturforsch. A 22, 1401 (1967) (Ger); Chem. Abstr. 68:63941g (1968)

Combley, F. H., Stewardson, E. A., and Wilson, J. E., The M X-Ray Absorption of Ytterbium, Proc. Phys. Soc. 1, 120 (1968); Chem. Abstr. 68:44307p (1968)

Davidson, F. D., and Wyckoff, R. W. G., L and M X-Ray Spectra in the Region 2-85 A, Advan. X-Ray Anal. 9, 344 (1966); Chem. Abstr. 66:99767c (1967)

Demekhin, V. F., Platkov, A. I., and Lyubivaya, M. V., Multiplet Structure of the L-Series Lines of Rare-Earth Elements, Zh. Eksp. Teor. Fiz. 62, 49 (1972) (Russ); Chem. Abstr. 76:106015t (1972)

Derbeneva, S. S., and Batsanov, S. S., The Width of the Forbidden Zone for Rare-Earth Metal Oxides, Dokl. Akad. Nauk SSSR 175, 1062 (1967) (Russ); Chem. Abstr. 68:73735g (1968)

Fischer, D. W., and Baun, W. L., Self-Absorption Effects in the Soft X-Ray $M\alpha$ and $M\beta$ Emission Spectra of the Rare Earth Elements, J. Appl. Phys. 38, 4830 (1967); Chem. Abstr. 68:17303c (1968)

Goldsmith, J. A., and Ross, S. D., Factors Affecting the Infrared Spectra of Some Planar Anions with D_{3h} Symmetry. III. The Spectra of Rare Earth Carbonates and Their Thermal Decomposition Products, Spectrochim. Acta, Part A 23, 1909 (1967); Chem. Abstr. 67:68968k (1967)

Gruss, L. L., Electronic Spectra of Solid Solutions of Erbium and Ytterbium Oxides, Diss. Abstr. Int. B 31, 5902 (1971); Chem. Abstr. 76:8365n (1972)

Guazzoni, G. E., and Shapiro, S. J., Spectral Emittance of Neodymium, Samarium, Erbium, and Ytterbium Oxides at High Temperatures, Nat. Techn. Inform. Serv. AD 708547 (1970); Chem. Abstr. 74:36594p (1971)

Joergensen, C. K., and Berthou, H., Measurements of Photoelectron Spectra and Charging Effects in Fluorides, Iodates, and Oxides, J. Fluorine Chem. 2, 425 (1973); Chem. Abstr. 78:130358u (1973)

McMahon, W. R., Hemispherical Spectral Emittance of Selected Rare Earth Oxides, U.S. At. Energy Comm. 1967, IS-T-182, Nat. Techn. Inform. Ser.; Chem. Abstr. 69:6796k (1968)

Matsubara, T., Mixed Rare Earth Phosphors, Japan. Kokai 73 26,685 (Cl. 13(9)-C112), 7 Apr 1973, Appl. 71 61,170, 11 Aug 1971; Chem. Abstr. 69:25573h (1973)

Petru, F., and Muck, A., Chemistry of Rare Earth Elements. XL. Infrared Absorption Spectra of Oxides of the Lanthanides Eu. . .Lu, Z. Chem. 7, 159 (1967) (Ger); Chem. Abstr. 67:27442r (1967)

Sumbaev, O. I., Smirnov, Yu. P., Petrovich, E. V., Zykov, V. S., Egorov, A. I., and Grushko, A. I., Chemical Shifts of X-Ray $K\alpha_1$ Lines during Oxidation of Rare Earth Metals. Role of f-Electrons, Rentgen. Spektry Elektron. Strukt. Veshchestva 2, 172 (1969); Chem. Abstr. 74:117626c (1971)

Sumbaev, O. I., Smirnov, Yu. P., Petrovich, E. V., Zykov, V. S., Egorov, A. I., Grushko, A. I., Chemical Shifts of the $K\alpha_1$ X-Ray Lines during Oxidation of Rare Earth Metals. Role of f-Electrons, Zh. Eksp. Teor. Fiz. 56, 536 (1969) (Russ); Chem. Abstr. 71:7985z (1969)

White, W. B., Diffuse-Reflectance Spectra of Rare Earth Oxides, Appl. Spectrosc. 21, 167 (1967); Chem. Abstr. 67:69158h (1967)

Chemical Kinetics Information Center
Institute for Materials Research

Prepared by: Francis Westley, October 1974

Taylor, M. D., Cheung, T. T., and Hussein, M. A., Variations of the Infrared Spectra with the Nature and Structure of the Rare Earth Metal Halides, J. Inorg. Nucl. Chem. 34, 3073 (1972); Chem. Abstr. 77:132692b (1972)

Wertheim, G. K., Cohen, R. L., Rosencwaig, A., and Guggenheim, H. J., Multiplet Splitting and Two Electron Excitation in the Trivalent Rare Earths, Electron Spectrosc., Proc. Int. Conf. 1971, p. 813, (Pub. 1972), Shirley, D. A., Ed.; Chem. Abstr. 77:158530x (1972)

(b). Ytterbium oxides

Batsanov, S. S., Derbeneva, S. S., and Batsanova, L. R., Electronic Spectra of Rare Earth Metal Fluorides, Oxyfluorides and Oxides, Zh. Prikl. Spektrosk. 10, 332 (1969) (Russ); Chem. Abstr. 70:101332k (1969)

Bloor, D., and Dean, J. R., Spectroscopy of Rare-Earth Oxide Systems. I. Far-Infrared Spectra of the Rare-Earth Sesquioxides, Cerium Dioxide, and Nonstoichiometric Praseodymium and Terbium Oxides, J. Phys. C 5, 1237 (1972); Chem. Abstr. 77:54303j (1972)

Chun, H. U., and Hendel, D., X-Ray Spectroscopic Study of Chemical Bonds in Oxides, Z. Naturforsch. A 22, 1401 (1967) (Ger); Chem. Abstr. 68:63941g (1968)

Combley, F. H., Stewardson, E. A., and Wilson, J. E., The M X-Ray Absorption of Ytterbium, Proc. Phys. Soc. 1, 120 (1968); Chem. Abstr. 68:44307p (1968)

Davidson, F. D., and Wyckoff, R. W. G., L and M X-Ray Spectra in the Region 2-85 A, Advan. X-Ray Anal. 9, 344 (1966); Chem. Abstr. 66:99767c (1967)

Demekhin, V. F., Platkov, A. I., and Lyubivaya, M. V., Multiplet Structure of the L-Series Lines of Rare-Earth Elements, Zh. Eksp. Teor. Fiz. 62, 49 (1972) (Russ); Chem. Abstr. 76:106015t (1972)

Derbeneva, S. S., and Batsanov, S. S., The Width of the Forbidden Zone for Rare-Earth Metal Oxides, Dokl. Akad. Nauk SSSR 175, 1062 (1967) (Russ); Chem. Abstr. 68:73735g (1968)

Fischer, D. W., and Baun, W. L., Self-Absorption Effects in the Soft X-Ray Mα and Mβ Emission Spectra of the Rare Earth Elements, J. Appl. Phys. 38, 4830 (1967); Chem. Abstr. 68:17303c (1968)

Goldsmith, J. A., and Ross, S. D., Factors Affecting the Infrared Spectra of Some Planar Anions with D_{3h} Symmetry. III. The Spectra of Rare Earth Carbonates and Their Thermal Decomposition Products, Spectrochim. Acta, Part A 23, 1909 (1967); Chem. Abstr. 67:68968k (1967)

Gruss, L. L., Electronic Spectra of Solid Solutions of Erbium and Ytterbium Oxides, Diss. Abstr. Int. B 31, 5902 (1971); Chem. Abstr. 76:8365n (1972)

Guazzoni, G. E., and Shapiro, S. J., Spectral Emittance of Neodymium, Samarium, Erbium, and Ytterbium Oxides at High Temperatures, Nat. Techn. Inform. Serv. AD 708547 (1970); Chem. Abstr. 74:36594p (1971)

Joergensen, C. K., and Berthou, H., Measurements of Photoelectron Spectra and Charging Effects in Fluorides, Iodates, and Oxides, J. Fluorine Chem. 2, 425 (1973); Chem. Abstr. 78:130358u (1973)

McMahon, W. R., Hemispherical Spectral Emittance of Selected Rare Earth Oxides, U.S. At. Energy Comm. 1967, IS-T-182, Nat. Techn. Inform. Ser.; Chem. Abstr. 69:6796k (1968)

Matsubara, T., Mixed Rare Earth Phosphors, Japan. Kokai 73 26,685 (Cl. 13(9)-C112), 7 Apr 1973, Appl. 71 61,170, 11 Aug 1971; Chem. Abstr. 69:25573h (1973)

Petru, F., and Muck, A., Chemistry of Rare Earth Elements. XL. Infrared Absorption Spectra of Oxides of the Lanthanides Eu. . .Lu, Z. Chem. 7, 159 (1967) (Ger); Chem. Abstr. 67:27442r (1967)

Sumbaev, O. I., Smirnov, Yu. P., Petrovich, E. V., Zykov, V. S., Egorov, A. I., and Grushko, A. I., Chemical Shifts of X-Ray $K\alpha_1$ Lines during Oxidation of Rare Earth Metals. Role of f-Electrons, Rentgen. Spektry Elektron. Strukt. Veshchestva 2, 172 (1969); Chem. Abstr. 74:117626c (1971)

Sumbaev, O. I., Smirnov, Yu. P., Petrovich, E. V., Zykov, V. S., Egorov, A. I., Grushko, A. I., Chemical Shifts of the $K\alpha_1$ X-Ray Lines during Oxidation of Rare Earth Metals. Role of f-Electrons, Zh. Eksp. Teor. Fiz. 56, 536 (1969) (Russ); Chem. Abstr. 71:7985z (1969)

White, W. B., Diffuse-Reflectance Spectra of Rare Earth Oxides, Appl. Spectrosc. 21, 167 (1967); Chem. Abstr. 67:69158h (1967)

Chemical Kinetics Information Center
Institute for Materials Research

Prepared by: Francis Westley, October 1974

USCOMM-NBS-DC